Universitat Autònoma de Barcelona

Development, and modelling a hydrogen peroxide technology as a decontamination process within the Pharmaceutical, Healthcare and Food industries

Ignacio Cantera García

Universitat Autònoma de Barcelona

Development, and modelling a hydrogen peroxide technology as a decontamination process within the Pharmaceutical, Healthcare and Food industries

Ignacio Cantera García

Universitat Autònoma de Barcelona

Universitat Autònoma de Barcelona

Veterinary Faculty

Department of Animal and Food Science

PhD in Food Science, Cleaning and Disinfection

THESIS

Development and modelling of a hydrogen peroxide technology as a decontamination process within the Pharmaceutical, Healthcare and Food industries

Ignacio Cantera García

Bellaterra, February 2022

Universitat Autònoma de Barcelona

PhD THESIS

Development, and modelling a hydrogen peroxide technology as a decontamination process within the Pharmaceutical, Healthcare and Food industries

Ignacio Cantera García

Directors

Dra. Manuela Hernández Herrero

Titular Professor of the Animal and Food Science Department, Veterinary Faculty, UAB

Dr. Artur Xavier Roig Sagués

Titular Professor of the Animal and Food Science Department, Veterinary Faculty, UAB

Tutor

Dra. Marta Capellas Puig

Titular Professor of the Animal and Food Science Department, Veterinary Faculty, UAB

Phd in Food Science

Department of Animal and Food Science, Veterinary Faculty,
Universitat Autònoma de Barcelona

Bellaterra, February 2022

This work was funded by a collaboration in between the Generalitat de Catalunya throughout the programme of Doctorats Industrials, and Azbil Telstar Technologies SLU. The author received the grant DI-2017-18 from AGAUR and started the project considering both entities proposal.

ACKNOWLEDGMENTS

It has been a long way.

A long and rewarding path that started back in 2013 when I decided to resume my academical career. Since then, and after many changes (a MEng. in Chemical Processes for Sustainable development, a new professional challenge, a relocation, etc.), in 2017, I decided to start over again, and apply for an Industrial Phd.

During this time, I did not only learn about microbiological or pharmaceutical concepts, but overall, I learnt that collaboration is the only way to get a truly innovative, and disruptive progress. No matter the research field, collaboration will multiply the final results.

During this thesis development, the collaboration started from my family. Julie did collaborate in many forms, but the most important one was the faith she showed in me during every step of the path. Even when our new family project started, and our two beloved daughters were coming into our lives, she still believed in the project, and pushed me to carry on. Also, my mother and sister, always encouraging and supporting me from the distance, are also part of this collaborative process.

Then, Azbil Telstar Technologies, and specially Jordi Serrat and Mónica Mañas, allowing me to start this new way of collaboration in between the Industry and the University. Surely, this cooperation will not end with the results of this thesis but will serve as the base for further collaborative projects. Within Telstar, I would like also to highlight the importance of the whole R&D Pharma team, and particularly two people, that without them, an important part of this thesis would have not been possible, Mireia Capella and Guillem Martinez. Both of them always supportive and working with me hand by hand, even during the difficult times that we faced.

This collaboration would have not made sense, without Manuela Hernandez and Artur Xavier Roig. They accepted the challenge, seeing a potential project where others understood that the proposed subject was out of their scope. Furthermore, they did not just accept, but guided me, and helped me in technical and academical matters, providing resources during the whole successful cooperation. I still believe that this collaboration should not end with this research but last longer to carry on enlightening a subject that still have many uncertainties, the decontamination processes. As part of the academical group, but also a very close friend, I'd like to mention the support I always got from Carlos Laorden, always there, and always believing in my capability to coordinate all to reach the final goal.

Finally, I'd like to cite Oliver Wendell when he mentioned that "Many ideas grow better when transplanted into another mind than the one where they sprang up". It is the base of the collaboration, to be humble enough to understand that one alone cannot reach full potential of a particular project. Believe in your peer, team, or family, all of them can increase your potential.

ABSTRACT

Decontamination methods have commonly relied on thermal or chemical non-automated processes that ensured a minimum microbial reduction. However, in the last decade, the evolution of the pharmaceutical drugs towards biological active compounds, advanced thermolabile containers or thermal sensitive materials in the production area, has reduced the number of applications where thermal processes can be applied. Analogously, the food and healthcare industries have suffered a technological and regulatory evolution that required an alternative to the traditional non-automated methods. As published by the FDA, 48 million people got sick each year from foodborne diseases as consequence of poor sanitization programs, and more than 50% of the hospital surfaces remain untouched by the traditional decontamination methods.

It is, in this scenario, where automated decontamination methods, and particularly hydrogen peroxide-based technologies are starting to show interesting results in the battle against the biocontamination. These results are not only related to a lowered biological risk during production, but also to a more efficient application of the biocides. Many hydrogen peroxide technologies have appeared in the last years, and their differences are focused on the promotion of one or the other thermodynamic status of the hydrogen peroxide solution, gas, or liquid. Nevertheless, few fundamental (and independent) research is focused on understanding how each phase can vary the inactivation mechanism of different representative bioburden. Concerns related to the validation, integration, and method of appliance of this type of technology, are starting to be raised by the scientific community in the pharmaceutical and food sectors.

Along this research, an automated hydrogen peroxide technology, based on atomization, was developed, and modelled. Representative bioburden such as *Listeria monocytogenes*, methicillin-resistant *Staphylococcus aureus* (MRSA), *G. stearothermophilus* and *B. atropheaus* were selected as the most representative contamination for each of the targeted industries, Pharmaceutical, Food and Healthcare industries. These contaminants inactivation models were studied and compared at different environmental conditions, different hydrogen peroxide distribution points and even different microorganism preparation methods.

Significant differences were found not only in the microorganism resistance against the biocide, but also in between the different temperature or distribution levels where the inactivation kinetic models were studied. The comparison in between microorganisms showed that the *B. atropheaus* was the one with higher resistance against the developed method. In addition, while minor temperature differences (2-4ºC) led to a decreased resistance of this spore, it had almost null impact in the *G. stearothermophilus*. On the other hand, while the MRSA showed a significant resistance, with a 4D value of 18.97 min, the *Listeria monocytogenes* demonstrated the lowest opposition against this process, with less than 10 min to achieve complete lethality from a starting population higher than 10^6.

Furthermore, unexpectedly, a good distribution did not directly show a much faster inactivation of the *G. stearothermophilus* spore, demonstrating how, even in a liquid phase technology, the vapor in equilibrium could play an important role in the decontamination. The preparation method or the wettability of one or the other

microorganisms appeared to be variables with higher importance than expected. Microorganisms of the same strain showed more than 100% higher resistance when prepared following a sporulation process different than the proposed by the ISO11138.

During the current attempt of achieving a complete model of the process, it was obvious that considering the number of variables that have influence in the final outcome, and that not all of them can be controlled or automated, it is key to assess each particular scenario and understand the risks associated to them. The most important uncertainties were focused on the temperature and distribution impact over the inactivation model of a particular bioburden.

RESUMEN

Los métodos de descontaminación se han basado históricamente en procesos térmicos o químicos no automatizados que garantizaban una mínima reducción microbiana. Sin embargo, en la última década, la evolución de los fármacos hacia compuestos biológicos, envases termolábiles avanzados o materiales sensibles al calor en el área de producción ha reducido el número de aplicaciones en las que se pueden aplicar procesos térmicos de descontaminación. De la misma manera, las industrias, alimentaria y sanitaria, han sufrido una evolución tecnológica y normativa que requiere una alternativa a los métodos tradicionales no automatizados. Tal y como publicó la FDA, 48 millones de personas enferman cada año por enfermedades transmitidas por los alimentos como consecuencia de programas de desinfección deficientes, y más del 50% de las superficies de los hospitales permanecen sin tratar por los métodos tradicionales de descontaminación.

Es, en este escenario, donde los métodos de descontaminación automatizados, y en particular las tecnologías basadas en peróxido de hidrógeno, están empezando a mostrar resultados interesantes en la batalla contra la bio-contaminación. Estos resultados no sólo están relacionados con la disminución del riesgo de contaminación biológica durante la producción, sino también con una aplicación más eficaz de los biocidas. En los últimos años han aparecido una gran variedad de tecnologías basadas en el peróxido de hidrógeno como sustancia activa, siendo sus diferencias principales basadas en la promoción de uno u otro estado termodinámico de la solución de peróxido de hidrógeno, gas o líquido. Sin embargo, pocas investigaciones fundamentales (e independientes) se centran en modelar y entender los mecanismos de desactivació y cómo cada fase puede impactar sobre el proceso de inactivación de las diferentes cargas biológicas. Además, tanto el sector farmacéutico como el alimentario, están plantean serias dudas relacionadas con la validación, la integración y el propio método de aplicación de este tipo de tecnología.

A lo largo de esta investigación, una tecnología automatizada de peróxido de hidrógeno, basada en la atomización, ha sido desarrollada y modelizada. Para esta modelización, se seleccionaron cargas microbianas representativas de cada una de las industrias que fueron objeto de estudio, Industria farmacéutica, alimentaria y sanitaria. *Listeria monocytogenes, Staphylococcus aureus* resistente a la meticilina (SARM), *G. stearothemophilus* y *B. atropheaus* fueron los microorganismos de estudio, y a través de las cuales se llevó a cabo la modelización. Estos modelos de inactivación se compararon en diferentes condiciones ambientales, diferentes puntos de distribución de peróxido de hidrógeno e incluso diferentes métodos de preparación de los microorganismos.

Se encontraron diferencias significativas no sólo en las diferentes resistencias de los microorganismos contra el biocida, sino también entre los diferentes niveles de temperatura o distribución en los que se estudiaron los modelos cinéticos de inactivación. La comparación entre microorganismos mostró que la espora *B. atropheaus* opuso la mayor resistencia frente al método desarrollado. Además, mientras que pequeñas diferencias de temperatura (2-4ºC) condujeron a una disminución de la resistencia de esta espora, esta mínima diferencia tuvo un impacto casi nulo en la espora *G. stearothemophilus*. Por otra parte, mientras que la SARM mostró una

resistencia significativa, con un valor de 4D de 18,97 min, la *Listeria monocytogenes* demostró la menor oposición contra este proceso, con menos de 10 min para alcanzar la letalidad completa desde una población siempre superior a 10^6.

Además, sorprendentemente, una buena distribución del biocida no mostró directamente una inactivación más rápida de la espora de *G. stearothemophilus*. Este hecho demuestra cómo, incluso en una tecnología basada en la fase líquida (atomización), el vapor en equilibrio puede desempeñar un papel importante en la descontaminación. El método de preparación o la humectabilidad de uno u otro microorganismo han mostrado ser variables con mayor importancia de la esperada. Microorganismos de una misma cepa mostraron una resistencia superior al 100% cuando se prepararon siguiendo un proceso de esporulación diferente al propuesto por la ISO11138.

Durante el presente intento de conseguir un modelo completo del proceso de descontaminación por peróxido de hidrógeno, fue evidente que, teniendo en cuenta el número de variables que influyen en el resultado final, es clave evaluar cada escenario y entender los riesgos asociados a cada uno de ellos. Las principales incertidumbres se centraron en el impacto de la temperatura y la distribución sobre el modelo de inactivación de una determinada carga biológica.

INDEX

INDEX OF FIGURES

INDEX OF TABLES

INDEX OF EQUATIONS

ABBREVIATIONS

ANOVA	Analysis of Variance
ATCC	American Type Culture Collection
BI	Bioindicator
BPR	Biocidal Product Regulation
CAS	Chemical Abstract Service
CECT	Colección Española de Cultivos Tipo
CFD	Computational Fluid Dynamics
CFU	Colony Forming Unit
cGMP	current Good Manufacturing Processes
CI	Chemical Indicator
CPU	Central Processing Unit
DENB	Dey-Engley Neutralizing Broth
DNA	Desoxyribonucleic Acid
ECHA	European Chemical Agency
EMA	European Medicinal Agency
EN	European Norm
EPA	Environmental Protection Agency
EtO	Ethylene Oxide
EU	European Union
FDA	Food and Drug Administration
GFL	General Food Law
HACCP	Hazard Analysis and Critical Control Points
HEPA	High Efficiency Particulate Air
HPV	Hydrogen Peroxide Vapor
IONHP	Ionized Hydrogen Peroxide
ISO	International Standard Organization
LR	Logarithmic Reduction
MPN	Most Probable Number
MRSA	Meticillin-resistant *Staphylococcus aureus*
OHSA	Occupational Health and Safety Assessment
P&Id	Piping and Instrumentation diagram
PAA	Peracetic Acid
PBS	Phosphate Buffer Solution
PID	Proportional Integral Derivative
PLC	Programmable Logic Controller
PPE	Personal Protective Equipment
REACH	Registration, Evaluation, Authorization and Restriction of Chemicals
RH	Relative Humidity
RMSE	Root Mean Squared Error
RNA	Ribonucleic Acid
ROS	Reactive Oxygen Species
SA	Sociedad Anónima
SAL	Sterility Assurance Level
SAS	Safety Access System
SCV	Small Colony Variant

SD	Standard Deviation
SE	Standard Error
STEL	Short Term Exposure Level
STI	Sterility Test Isolator
TOC	Total Organic Carbon
TSA	Tryptone Soy Agar
TSB	Trypticase Soy Broth
TWA	Time Weighted Average
TYB	Tryptone Yeast Broth
UK	United Kingdom
US	United States
USP	United States Pharmacopeia
VHP	Vaporized Hydrogen Peroxide
VIF	Variance Inflation Factor

1 INTRODUCTION

Reduction of the microbial load has historically been considered the most important goal of several processes within the Pharmaceutical, Food and Healthcare industries (Doll et al., 2015; Kaer et al., 2012; Rutala and Weber, 2013). Until the pandemic era, the latter industries were the main customers of decontamination methods that aimed to reduce this bioburden population.

Decontamination methods have commonly relied on thermal or chemical non-automated processes that ensured a minimum microbial reduction. While the thermal methods were known as robust processes, that in addition, offered the possibility of decontaminating many products in one single operation (Sandle, 2013), the chemical non-automated processes were the “only” option in certain applications such as surfaces disinfection.

In the last decade, the evolution of the pharmaceutical drugs towards biological active compounds, advanced thermolabile containers or thermal sensitive materials in the production area, has reduced the number of applications where thermal processes can be applied (Agalloco and Akers, 2016). Table 1 shows the last 10 years total drug release by the FDA. More than 25% of all drugs approved in the last five years were biologics (de la Torre and Albericio, 2020).

Table 1 FDA approved chemical entities and biologics in the last decade (adapted from de la Torre and Albericio, 2020)

Year	Chemical entities	Biologics	% Biologics over Total
2009	19	6	24%
2010	15	6	29%
2011	24	6	20%
2012	33	6	15%
2013	25	2	7%
2014	30	11	27%
2015	33	12	27%
2016	15	7	32%
2017	22	12	35%
2018	42	17	29%
2019	38	10	21%

None of these biologics can be terminally sterilized following traditional thermal methods, therefore, aseptic processing manufacturing should be considered. Aseptic processing intends, by means of ensuring sterility of the parts, to manufacture a sterile final product (without a final treatment) (Agalloco and Akers, 2016).

Analogously, the food and healthcare industries have suffered a technological and regulatory evolution that requires an alternative to the traditional microbial reduction manual methods (Davies et al., 2011; Pottage et al., 2012). As published by the FDA, 48 million people got sick each year from foodborne diseases (FDA, 2018) as consequence of poor sanitization programs, and, as published by Doll et al., (2015) more than 50% of the hospital surfaces remain untouched by the manual decontamination methods.

On the other hand, and coming back to the non-automated methods of the food and healthcare industry, the automation appears to be one of the best ways to avoid the subjectivity of the operator when applying a decontaminating agent (Abreu et al., 2013).

It is in this type of scenarios where cold decontamination methods, especially the hydrogen peroxide automated technologies are becoming key players. The chemical automated decontamination technology throughout hydrogen peroxide has been in the market for more than 30 years now, and three main technologies should be considered.

In 1979, Steris Corp. (Mentor, US), former AMSCO, filed the first Vaporized Hydrogen Peroxide related patent, US 416912 (Moore and Perkinson, 1979). Steris was the pioneer in this technology and its method was extensively used. Vaporized mainly meant that the gas phase of the chemical was promoted and maintained to avoid any condensation over the surfaces. It was the molecule in the gas phase, the one to ensure the inactivation of the microbial load. They claimed a dry process that was gentle with the materials and that ensured a perfect distribution of the molecules of hydrogen peroxide.

Alternatively, in 1995, Bioquell (Andover, Hants, UK) decided to file a patent describing an alternative to the Steris system, GB 9523717 (Watling, 1995). They even changed the name from Vaporized Hydrogen Peroxide (VHP) to Hydrogen Peroxide Vapor (HPV), basing its main appeal in changing the main principle of the former technology, from dry to wet based inactivation process. Bioquell's technology was, in the first phase, still promoting the gas phase, but then, once injected into the volume to be decontaminated, condensation was promoted. In fact, micro-condensation was claimed modifying the environmental conditions to promote so.

Finally, and as a third type of technology, many manufacturers, such as Azbil Telstar S.L.U (Terrassa, Spain) among them, had explored a different manner of delivering the chemical agent into the volume or surface to be decontaminated. The atomization of the hydrogen peroxide as an automated delivery method allowed to maintain the gas phase distribution advantages while maintaining the liquid phase concentration (Hayrapetyan et al., 2020; Richter et al., 2018). The main principle relies in the generation of microparticles, usually below 10 µm diameter, that are evenly distributed and deposited over the surface to be decontaminated.

The differences in between technologies are focused on the promotion of one or the other thermodynamic status of the hydrogen peroxide solution, gas, or liquid, to reduce the microbial load in the most robust and efficient manner. While there are many authors confirming the "dry" process and modelling the inactivation kinetics in the gas phase (Chan et al., 2011; Chung et al., 2008; Falagas et al., 2011; Kaer et al., 2012; Kirchner et al., 2013; Sandle, 2013), there are many others that argue and intend to prove that the liquid phase is unavoidable, and, it is the main status of the hydrogen peroxide during the inactivation, with no matter the technology applied (Agalloco, James, Akers, 2013; Davies et al., 2011; Drinkwater et al., 2009; Fu et al., 2012; Holmdahl et al., 2011; Jildeh et al., 2020; Richter, 2016).

The few fundamental and independent research in between the gas or liquid phase dichotomy, makes that the hydrogen peroxide inactivation mechanisms are not clear, and that no consensus is reached among the scientific community. There are even concerns related to its validation, operational and method appliance within the pharmaceutical industry (Finnegan et al., 2010; Linley et al., 2012).

A study performed by Ito et al., (2016) showed that the hydrogen peroxide technology has other uncertainties than the gas or liquid phase status ones. The concentration in

every point to be decontaminated was proved not to be just dependent on the total injected volume, temperature, and humidity, but also in the type of material (stainless steel, resin, plywood, and glass were tested) to be decontaminated, surface temperature and humidity homogeneity. Furthermore, other parameters such as droplet size, decomposition rate or diffusion are variables that have been separately studied by other authors (Eschlbeck et al., 2018; McMurtrie and Keyes, 1948; Radl et al., 2011; Watling et al., 2002).

After all, every decontamination method should ensure robustness, and be validatable under each industry requirements. The validation process is usually carried out throughout the use of bioindicators of a known resistance (Castro et al., 2011; Sandle, 2016) and are specific of a particular technology. The resistance of the microorganism should be representative of the actual bioburden and its inactivation mechanisms characterized. Uncertainties related to the inactivation mechanisms and actual resistances appear when choosing the most suitable microorganism for the validation of the hydrogen peroxide technologies (Davies et al., 2011; Pottage et al., 2012). The defences against a biocide vary from one type of microorganism to another. Additionally, even when the same microorganism is used, if the biocide is received in one form or another (liquid or gas phase for instance), it might end showing a different resistance (Eschlbeck et al., 2018; Wiencek et al., 1990).

Bearing in mind the reported physic-chemical and microbiological uncertainties, the current research will be focused on the development of a hydrogen peroxide atomization technology, its characterization and modelling, to reduce as much as possible the mentioned uncertainties. To consider the Pharmaceutical, Food and Healthcare industry specific requirements will also be part of the research and incorporated into the development of the technology.

The main objectives can be summarized as follows:

1) Engineer an atomization hydrogen peroxide technology. To develop, dimension and characterize under different physical-chemical conditions the technology to be integrated into the Azbil Telstar products.
2) Simulation and prediction of the atomized hydrogen peroxide fluid dynamics. The automation of the decontamination system should ensure a homogeneous distribution of the generated micro-particles.
3) Microbiological modelling. Inactivation models of the most important biological contaminants. The variations of these inactivation models under different physical-chemical circumstances should aid in the clarification of the gas or liquid dichotomy.

It is the hypothesis of this author that hydrogen peroxide decontamination technologies can be engineered and modelled to ensure an automated and reliable fulfilment of the Pharmaceutical, Food and Healthcare industries requirements. This engineering and modelling activity will only fulfil the expectations, when the microbiological, physic-chemical, and technological aspects are considered as part of the same system.

2 REGULATORY REVIEW

Any chemical substance is firstly regulated by the European Chemicals Agency (ECHA) in Europe or by the Environmental Protection Agency (EPA) in the US. In addition, if the substance is a biocide, then, in Europe, the Biocidal Product Regulation (BPR) should be addressed. Moreover, and specifically as a decontaminating agent, it should follow, no matter the industry, a list of European Norms (EN) that intends to demonstrate the chemical substance efficacy against certain microorganisms. In this case, the UNE-EN13697 (UNE, 2015), UNE-EN13704 (UNE, 2019) and the AFNOR NF T 72-281:2014 (AFNOR, 2014) (currently EN17272) are the ones with more importance.

The hydrogen peroxide is already an ECHA approved active substance. Therefore, when applied for decontamination purposes, it is the specific formulation of the application the one that should comply with both the BPR and the EN Standards. Table 2 and 3 shows the most important physical-chemical data presented at the ECHA to describe the hydrogen peroxide as a biocide.

Table 2 Pure Hydrogen Peroxide Physic-chemical properties (European Chemicals Bureau European Union, 2003)

Property	Value	Reference
Melting point	-0.40 - 0.43°C	Budavari (1989)
Boiling point	150-152°C decomposition	Budavari (1989)
Density	1.4425 g/cm^3 (25°C)	Schumb et al. (1955)
Vapour pressure	3 hPa (25°C)	Weast and Melvin (1981)
Water solubility	miscible in all proportions	Weast and Melvin (1981)
pK_a	11.62 (25°C)	Weast and Melvin (1981)
Henry's law constant	$7.5 \cdot 10^{-4}$ Pa m^3/mol (20°C) measured	Hwang and Dasgupta (1985)

Table 3 Main Water Hydrogen Peroxide solutions Physic-chemical properties (European Chemicals Bureau European Union, 2003).

H_2O_2 %	35% w/w	50% w/w	70% w/w	90% w/w	Reference
Melting point	-33°C	-52°C	-40°C	-11°C	ECETOC (1993)
Boiling point	108°C	114°C	125°C	141°C	MCA (1969)
Density (25°C)	1.1282	1.1914	1.2839	1.3867	Goor et al. (1989)
Vapour pressure (partial)	0.48 hPa (30°C)	0.99 hPa (30°C)	2 hPa (30°C)		MCA (1969)
Vapour pressure (total)		24 hPa (30°C)	14.7 hPa (30)°C	6.7 hPa (30°C)	ECETOC (1993)
Saturated vapour concentration at 25 °C (mg/m^3)		787	1,685	3,049	HSDB database
Surface tension mN/m (20 °C)	74.6	75.7	77.3	79.2	Degussa AG (1993)
Viscosity ($1 \cdot 10^{-3}$ kg/ms)	1.11	1.17	1.24	1.26	Degussa AG (1993)

Particularly discussing about the pharmaceutical industry, both the European Medicines Agency (EMA) and Food and Drug Administration (FDA) are the most important regulators present in the industry. The FDA in the Guidance for Industry, Sterile Drug Products Produced by Aseptic Processing (FDA, 2004) and the EMA in the Annex I, Manufacture of Sterile Medicinal Products (EMA, 2017), delivers a series of recommendations to minimize the risk during the manufacturing of aseptically manufactured drugs. Aseptic manufacturing is the main process where the identification of critical areas, and its decontamination (mainly cold), is crucial. To do so, the critical areas tend to be reduced in volume, and the Isolator technology (Figure 1) is recommended to mitigate the risk. The design of those should avoid hidden spaces and should consider a decontamination program.

Figure 1 Sterility Test Isolator (STI) - Telstar

The hydrogen peroxide technology to be integrated in such a program should consider not only the functions as a decontaminating agent, but also ensure that the system is

validatable, included within the isolator (or other equipment or technologies) processes, and designed together with the volume or surface to de decontaminated.

Regarding the Food industry, the FDA, together with the European General Food Law-European Commission (GFL) (Figure 2) are the main entities when dealing with the food industry stakeholders. Throughout the “Hazard analysis and risk-based preventive controls for human food: guidance for industry” the FDA helps the Food industry to comply with the current Good Manufacturing Practices (cGMP) (FDA, 2018).

Figure 2 summarizes all Regulations within the European framework.

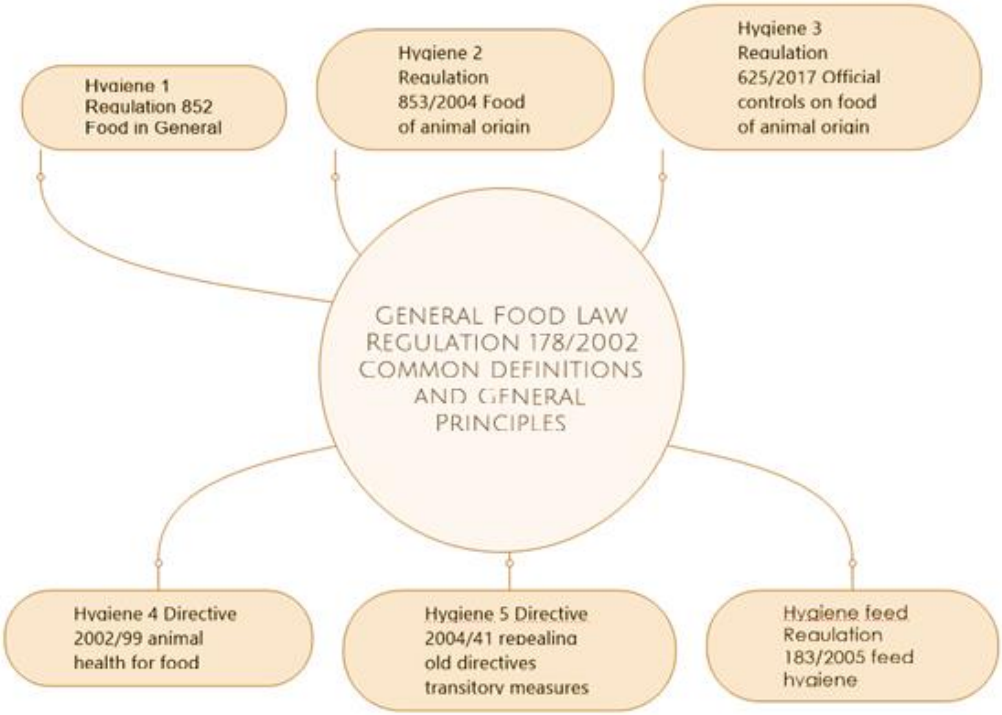

Figure 2 EU Safe Food Regulation overview (adapted from Van der Velde and Van der Meulen, 2011).

In general, all regulatory principles rely in that a correct sanitation program should consider the application of a proper decontaminant, an optimal equipment design, and the use of adequate cleaning processes. If one of the three factors is weaker, food safety might be compromised (Van der Velde and Van der Meulen, 2011). None of the mentioned regulations specifies a surface contamination threshold allowed within a manufacturing facility. All are related to the foodstuff.

To accomplish the main objectives of this research, it is important to know and effectively assess the biological hazards in the critical points of the food industries. Therefore, placing the decontamination step within the safety food program is important to ensure the expected effect. A proper integration could minimise the existence of the current food manufacturers' inadequate hygiene designs. It is clear that surfaces like those shown in Figure 3 are usual and might eventually be the source of foodborne outbreaks.

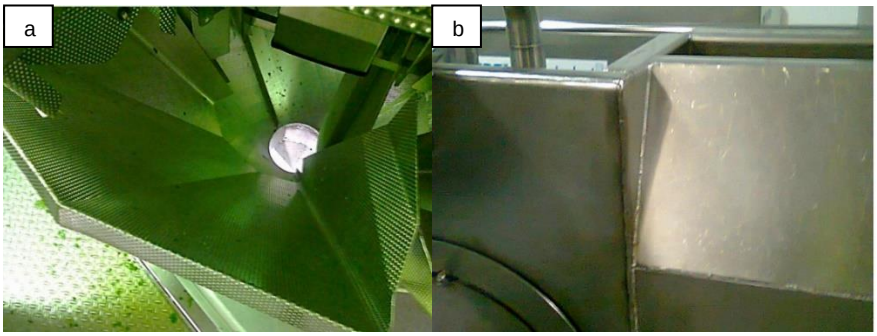

Figure 3 Examples of a poor hygienic cGMP design (Meireles and Simões, 2017)*. a) Sharp edges and high surface roughness; b) Sharp edges and "non-clean" welding process.*

3 COLD DECONTAMINATION

As discussed, cold decontamination technologies should be integrated within both the Pharmaceutical and Food industries decontamination programs (Healthcare industry is not explicitly commented as their specification are fulfilled with the compliance of the Pharmaceutical and Food industries requirements.

This chapter aims to overview the most important cold sterilization technologies, and the main processes and equipment where those would be integrated.

3.1 COLD DECONTAMINATION DEFINITION AND CONTEXT

Cold Sterilization methods are defined as processes where the temperature of the system, items or surfaces to be sterilized are maintained within certain level. There is not a clear consensus about this level, but values higher than 50-60 ºC should be already considered higher temperatures than expected when looking for a Cold Sterilization system (Gradini et al., 2019; Raguse et al., 2016).

The decontamination methods can be grouped in many classifications, but in this case, the division will be made considering its physic-chemical properties (Figure 4). The cold decontamination methods, according to the Figure 4, are all grouped within the chemical section as well as the radiation and filtration methods. As discussed during the introduction, even though hydrogen peroxide is placed within gas/vapour classification, the inactivation mechanisms are uncertain.

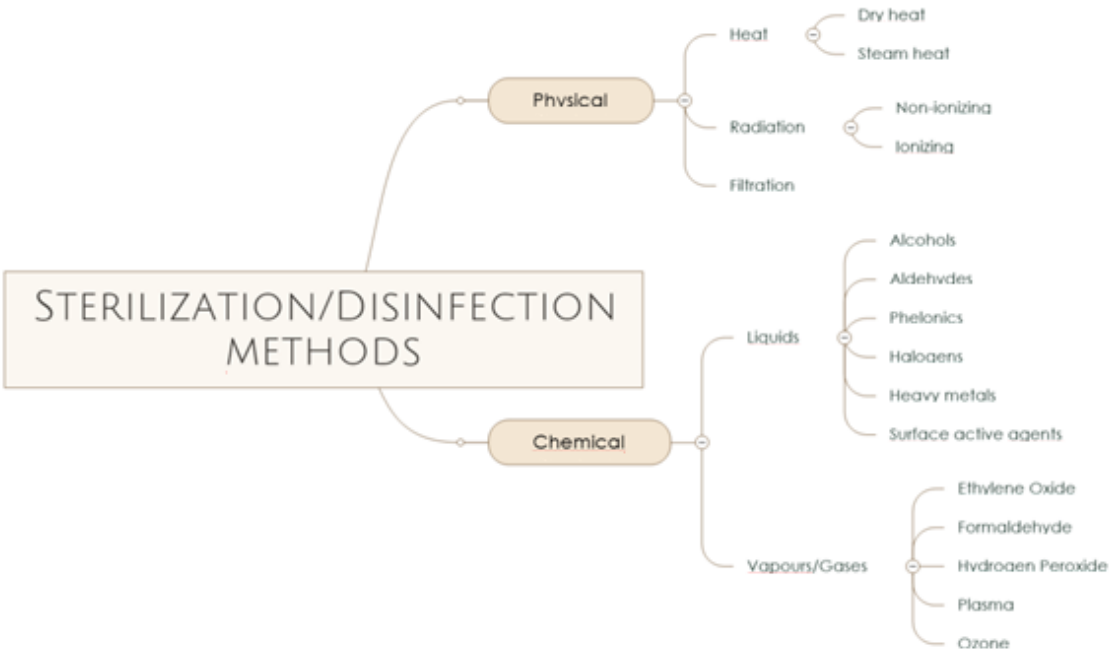

Figure 4 Sterilization / Disinfection methods

The EMA “Guideline on the sterilization of the medicinal product, active substance, excipient and primary container” (EMA, 2019) states throughout different decision trees the type of manufacturing and sterilization to be applied depending on the characteristics of both product and container (Figure 5).

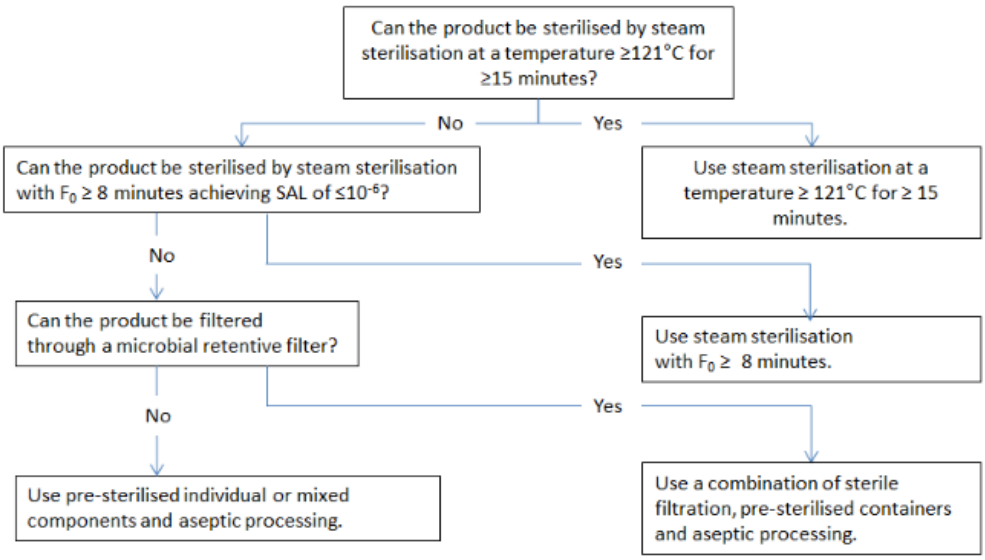

Figure 5 Example of one of the decision trees to choose the best technique to ensure sterility of the final product (EMA, 2019).

It is evident in Figure 5 that whenever possible, heat sterilization is recommended. But when it is not possible, a combination of different methods such as filtration or pre-sterilized containers together with aseptic processing should be applied. Aseptic processing intends, by means of ensuring sterility of the parts, a sterile final product (without a final treatment) (Agalloco and Akers, 2016; Akers et al., 1995). To ensure sterility of the parts, the main measures are to reduce the critical areas and automate their surface decontamination, throughout cold decontamination methods.

Nowadays, when the decision tree is followed, two main factors, thermolabile drug products and temperature sensitive containers, make the terminal sterilization not anymore possible. Thermolabile products can be of a very different nature, but biologics can be considered as the main drugs that cannot withstand high temperatures as their activity and structure would be highly affected. The biologics importance is increasing and consolidating in the pharmaceutical scenarios. More than 25% of all drugs approved in the last five years are Biologics (de la Torre and Albericio, 2020). Table 4 shows the last 20 years released drugs by the FDA, including the biologics.

Table 4 FDA approved chemical entities and biologics in the last two decades (adapted from de la Torre and Albericio, 2020).

Year	***Chemical entities***	***Biologics***	***% Biologics over Total***
2000	27	2	7%
2001	24	5	17%
2002	17	7	29%
2003	21	6	22%
2004	31	5	14%
2005	18	2	10%
2006	18	4	18%
2007	16	2	11%
2008	21	3	13%
2009	19	6	24%
2010	15	6	29%
2011	24	6	20%
2012	33	6	15%
2013	25	2	7%
2014	30	11	27%
2015	33	12	27%
2016	15	7	32%
2017	22	12	35%
2018	42	17	29%
2019	38	10	21%

The food industry, on the other hand, has increased the complexity in the logistics, automation, and quality fields, to eventually optimize the efficiency and production costs. The former decontamination non-automated methods bring not only inefficiencies to the production line, but also vulnerabilities in the biological risk management (Moerman and Mager, 2016). These vulnerabilities together with the Regulatory leading activities, make that the sanitation programs within the industry should evolve.

The cold decontamination automated methods do not have a specific niche within the food industry (as the aseptic processing manufacturing method in the pharmaceutical industry), but they can be engineered and designed to reduce biological contamination all along the production line.

3.2 MAIN COLD DECONTAMINATION TECHNOLOGIES

3.2.1 CHLORINE DIOXIDE

Chlorine dioxide (ClO_2) is listed under the Chemical Abstracts Service (CAS) number 10049-04-4 (EC/List no 233-162-8), and it is not registered yet under the Registration, Evaluation, Authorization and Restriction of Chemicals (REACH) regulation. The ECHA has not received any data about this substance. However, it is mentioned that it is being under evaluation to be used and approved by the BPR as a biocide. In the US, the EPA has already this chemical considered in its database as a disinfectant both in gas and aqueous forms.

This compound is a strong oxidant that functions by disrupting cell membranes and protein synthesis. Its effect on the microorganisms is not affecting the DNA (Ma et al., 2017). It can be used as an aqueous form but also as gas, and even though it does generate fewer by-products, chlorine and oxygen should be considered as their main decomposed compounds. It is important to reflect that its boiling point is way lower than hydrogen peroxide (11 ºC) and therefore, it is a gas at room temperature. It is very unstable and difficult to generate for storage and be ready to use at the point of injection. From the safety perspective, it is important to highlight that very low levels in air concentration can lead to acute effects over the human. The Occupational Safety and Health Administration (OHSA) in the USA states 0.1 ppm as the Time Weighted Average (TWA) and a Short Term Exposure Level (STEL) of 0.3 ppm (Gómez Lopez, 2014).

All published data that has been reviewed agree on the type of recipe to be used when applying gas phase (400-600 ppm) in a highly humid environment (> 65%), and the results showed in every case sporicidal capability. Specially, there is a publication of Pottage et al., (2012a) using the ClorDiSys (ClorDiSys Solution, Inc, New Jersey, US) system which is the main company promoting this technology in the pharmaceutical industry, where both *Geobacillus stearothermophilus* and *Bacillus atropheaus* are inactivated by Chlorine Dioxide and then compared with Hydrogen Peroxide.

The main results of the comparison concluded that chlorine dioxide required longer exposure times than hydrogen peroxide-based technology. The resistance of the different microorganisms tested is different for both technologies. Where the hydrogen peroxide-based technology finds *Geobacillus stearothermophilus* as the most resistant spore, Chlorine Dioxide is less efficient against the *Bacillus atropheaus* spore (Pottage et al., 2012a).

3.2.2 NITROGEN OXIDES (NOx)

Nitrogen oxides (NOx) include nitric oxide, nitrogen dioxide, dinitrogen tetroxide or additional oxide of nitrogen that can be found as a combination of both atomic elements. The use of these gas compounds as a sterilant is a proprietary technology patented by Noxilizer, Inc, US 8808622 (Doletski et al., 2014). None of the main regulation authorities, EPA or ECHA, have registered this compound as a biocide. However, recently the FDA has emitted a 501 (k) premarket notification of a medical device sterilized by this method. This fact, together with the inclusion of the Noxilizer technology as an alternative to the FDA challenge to replace Ethylene Oxide as the main Cold Sterilization technology in the medical device market, has made increase the interest in NOx as a sterilant. From the occupational safety point of view, the 8-hour TWA

recommended by the European Union Scientific Committee is 0.5 ppm and the STEL (15-min) is 1 ppm (Scientific Committee on Occupational Exposure Limits, 2014).

The technology is based on the *in-situ* generation of the sterilant, avoiding the manufacturing and transport implications (not just cost) of other liquid or gas sterilants. A typical cycle based on NOx is represented in the following Figure 6. The relative humidity when starting the cycle should be above 60 %RH and the NOx concentration reaches values of 12 ppm to then stabilize to 10 to 9 ppm during the exposure.

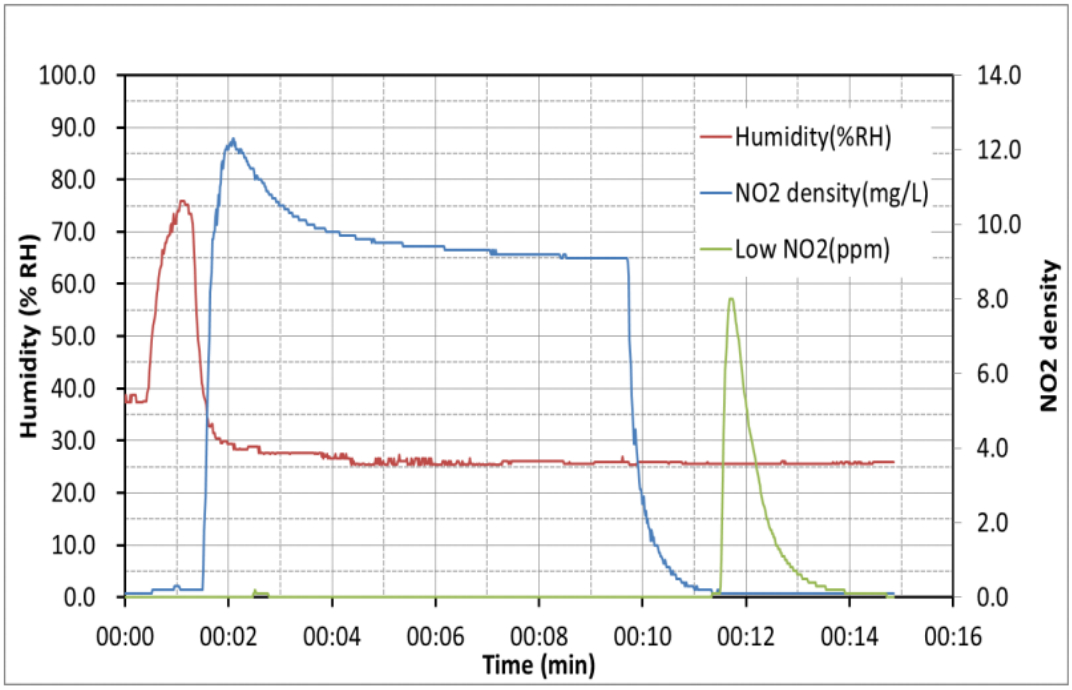

Figure 6 NOx decontamination cycle (Opie, D. 2018, Personal communication)

3.2.3 PERACETIC ACID

Peracetic acid ($C_2H_4O_3$) listed under the CAS 79-21-0 is also known as PAA. It is an oxidizer with higher disinfection activity than hydrogen peroxide. The decomposition reaction delivers non-hazardous by-products such as acetic acid and hydrogen peroxide that will eventually also decompose to water, oxygen, and carbon dioxide. From the Occupational Exposure levels of this compound, the OHSA set 15-min TWA in 0.4 ppm.

The compound has already shown inactivation effectiveness even in the sporicidal range. The PAA has been used in the wastewater disinfection application, and it is from this experience where new methods intend to apply this capacity to surface disinfection, among others (Gad, 2014).

The method to apply this chemical could be similar to the one used in hydrogen peroxide as the physical-chemical properties are similar. Richter et al., (2018) used the fogging method, and an evaluation of the PAA activity versus the hydrogen peroxide was done. The concentrations of PAA and hydrogen peroxide were 4.5% and up to 35% w/w, respectively. The results showed complete deactivation of 10^6 spores *Bacillus anthracis* for both technologies. There are other publications discussing this type of experiment but with higher PAA concentrations (Hayrapetyan et al., 2020; Kimura, 2012).

3.2.4 ETHYLENE OXIDE

The Ethylene Oxide (EtO, C_2H_4O) is listed under the CAS number 75-21-8. The 8 h TWA level set by the OHSA is 1 ppm while the STEL is fixed at 5 ppm. It is clearly the most common chemical used in the Cold Sterilization market. Its main user is the Medical Device industry, where all the components that cannot be subjected to high temperatures or that where steam cannot readily penetrate end up using this technology. Figure 7 shows Telstar's workshop, where one of the EtO autoclaves is under manufacturing.

The FDA states that up to 50% of all medical devices in the US are sterilized by the EtO technology (FDA, 2020a). As its use is so wide within a powerful market, there are standards not just to validate a certain cycle but even, to ensure that the aeration of the EtO from the final product has been done effectively (Handlos, 1980). One of those standards is ISO 11135:2014 (ISO, 2014).

EtO is an alkylating agent that acts as a poisonous compound to the microorganism, disrupting the cellular metabolism and reproductive processes. The sterilization process requires a very thorough control of the gas concentration, air concentration and inert gas injection, as when mixed with oxygen can create explosive environments (Freeman and Auer, 2012; Moerman and Mager, 2016).

Figure 7 EtO Chamber for Medical Device sterilization (red circle).

3.2.5 COATINGS

There are many coatings with disinfection capabilities. The mechanisms of deactivation are different depending on the coating to be applied. Titanium dioxide, copper or silver are some of the most important elements used when applying certain treatments to a surface to decrease the risk of receiving a risky bioburden (Rutala and Weber, 2019). While copper or silver are mainly based on the release of toxic metal ions that end up in the microorganism and affects its metabolism, titanium dioxide is based on photocatalysis. The disinfection capabilities of copper have been known during the last century, but still, recent articles are still studying the mechanisms and effective deactivation throughout the generation of reactive oxygen radicals that damage the nucleic acid and proteins (Boyce, 2016). Schmidt et al., (2016) reported how the

inanimate objects could hold reduced bioburden when copper-based materials are used (Figure 8).

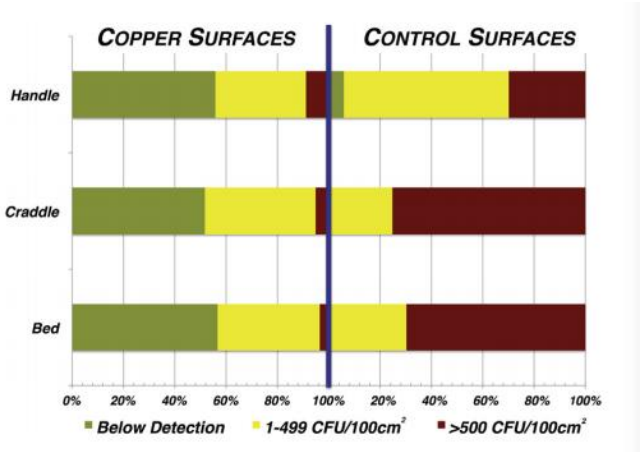

Figure 8 Copper surfaces bioburden comparison versus control surfaces. Right hand of the image shows more than 50% of the surfaces with bioburden below the level of detection (Schmidt et al., 2016)

In the case of silver surface treatments, recently, nanotechnology has been used to cover critical surfaces. Silver also acts as a poisonous material to the bacteria's cell, interacting with the sulphurous components of the cell membrane. Once inside the cell, the interaction of the released ions takes place with the phosphorous material of the DNA. Figure 9 shows that many mechanisms of deactivation are known, and all of them are dependent, among other variables, on an available specific surface, silver particle size or concentration of the applied coating (Deshmukh et al., 2019). As with any chemical reaction where a catalyst is present, the larger the specific surface or higher the concentration of the compound, the more deactivation effect would be achieved due to higher availability of toxic molecules per microorganism.

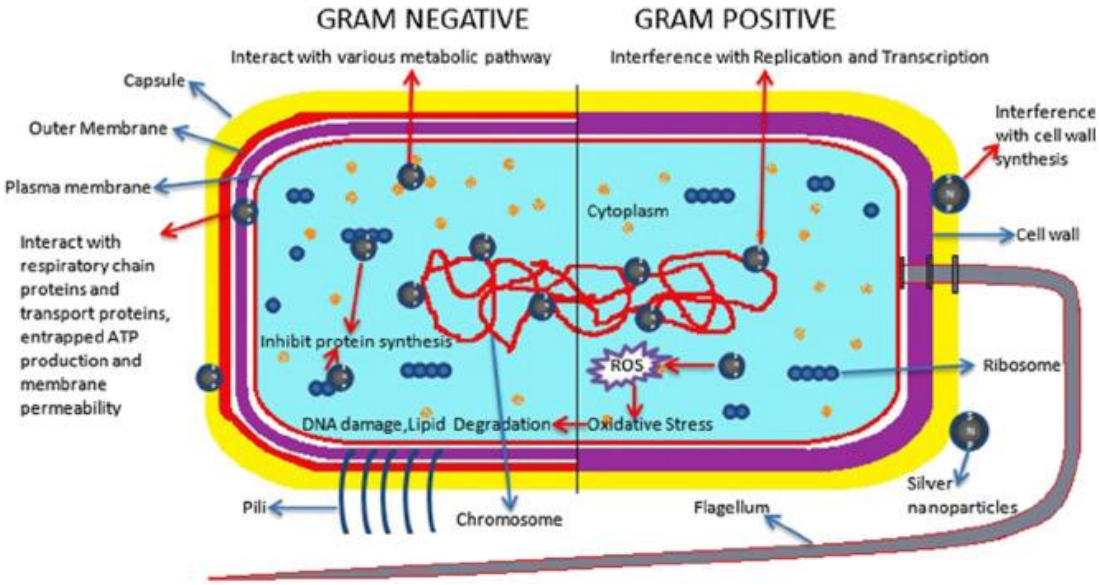

Figure 9 Silver deactivation mechanisms: interference with cell wall synthesis, replication and transcription and interaction with respiratory chain proteins and transport proteins. Also, Reactive Oxygen Species creation and consequent oxidative stress to the DNA and lipids (Deshmukh et al., 2019).

Finally, titanium dioxide, as mentioned, it is based on photocatalysis. Oxide semiconductors respond to light releasing electrons when exited with certain photoenergy, being oxidized (acting therefore as a reductor). In fact, this first reaction triggers a more important reaction of radical's generation when in contact with water or oxygen that will then act as antimicrobial agents or even decomposing organic material such Volatile Organic Compounds that are in contact (Liu et al., 2018).

Again, nanotechnology is raising the importance of such a coating as the available surface for the reaction is higher and the efficiency increases dramatically. Companies such as Pureti Inc. (Pureti Inc, New York, US) have patented US6107241 (Ogata and Matsui, 2000) as a way of depositing titanium dioxide so that even in low energy bands, the results of deactivation appear to be high.

3.3 COLD DECONTAMINATION APPLICATIONS

3.3.1 ISOLATOR TECHNOLOGY

Akers et al., (1995) defined an isolator as a device that provide total separation in between one environment and another. The isolator does not exchange air with the surrounding environment and all air must enter through High Efficiency Particulate Air (HEPA) filtration system. An isolator can either be protecting the environment and operators from highly potent or toxic products with negative pressure or using positive pressure protecting the product to be manufactured or treated within the enclosure. An example of this technology is shown in Figure 10.

In this system, the cold sterilization technologies integration is key. All volumes within the isolators, are considered critical areas, and those, require surface decontamination technologies to avoid contamination of the manufactured sterile product. In addition, these technologies have to be integrated within a larger program that includes cleaning, sanitization, environmental monitoring, disinfection and, in some cases, even sterilization.

Figure 10 Aseptic process of filling and loading unloading process to a freeze dryer. Facility manufactured by Azbil Telstar Technologies. A line of isolators together with an automatic loading and unloading system is introduced.

The Sterility Testing and Aseptic processing are the main applications of this technology into the pharmaceutical industry. The surface of the isolator as well as the load to be introduced for Sterility Testing should be decontaminated by automatic means (Akers et al., 1995). These means are, in most cases, automated systems that ensure repeatability over the process, and that use a chemical, that does not leave residues (as hydrogen peroxide decontamination technologies).

The level of decontamination does not require a full deactivation of all Bioindicators (BI) within the volume, since sterilization of surfaces is not required in such an environment (Agalloco et al., 2016). Total volumes to be decontaminated can range from <1 m^3 when dealing with Sterility Test Isolators, to up to 10-15 m^3 in a whole filling line (Castro et al., 2011).

Therefore, the application should be engineered project by project. The type of load and surface to be decontaminated does not differ much from one use case to another.

Usually, chemical reagents as well as glass containers can be introduced to perform the sterility test. When decontaminating the whole volume, usually, stainless steel surfaces are decontaminated together with process equipment that might be installed within the volume.

3.3.2 PASSTHROUGH BOX

The passthrough boxes are systems that ensure a safe transfer of material from one classified area to another classified area (usually more restrictive). A typical volume (1,3 m^3) and load to be decontaminated is shown in Figure 11.

This technology is basically a leak tight box that maintains the separation in between areas and that recently, counts with automated systems to decontaminate the material to be transferred (Sandle, 2013).

The surface decontamination should be performed by a chemical agent that acts during a certain time, being more and more important to ensure repeatability of the process by getting rid of the manual means.

In this case, the type of load might differ very much from one customer to another. Depending on the type of activity to be performed in the more restrictive area, the load will vary. Therefore, in this case, even though the design engineering is still relevant (as the volumes are usually < 5 m^3), the cycle development ensuring a proper distribution of the sterilant, becomes more important.

Figure 11 Passthrough box - BioSAS Telstar technology

3.3.3 CLEAN ROOMS

In most of the pharmaceutical processes, clean rooms are involved. The current trends tend to reduce the requirements for these rooms placing the critical production into the Barrier Systems Technology or even within the Isolating one (Rutala and Weber, 2013). However, the clean room will still be there, and even if less restrictive, the decontamination processes will occur.

The clean rooms in the food industry are also a frequent area that ensures a high-quality environment to be always in contact with critical food processing operations. The type of product that requires aseptic conditions is usually related to the beverage, meat (slices) or precooked food.

The main difference *versus* the pharmaceutical industry is the importance of proper cleaning prior to any decontamination activity. The load of organic material in some operations creates a “protective” layer for the microbial burden to be treated (Ling et al., 2015; Meireles and Simões, 2017). The food industry is still using manual cleaning and decontamination in most of these processes and the room for improvement in this field is high. However, in most applications, there is no sense to automate the disinfection without ensuring an automated Cleaning in Place system (CIP).

The automated cold decontamination methods are especially important in this case as both the Food and Healthcare industries are still relying in manual decontamination of larger areas. Many hidden spaces remain untouched, and the potential for contamination is still high (Doll et al., 2015). The integration of an automated system should consider that the load and geometrical distribution inside a clean room will significantly affect the decontamination result. Accordingly, a proper understanding of the physical-chemical, engineering, and microbiological processes is even more important.

3.3.4 PHARMACEUTICAL AND FOOD INDUSTRY: REQUIREMENTS

Even if all mentioned applications could be applied to both industries, it is worth describing the main requirements and differences in between them. Table 5 describes the main needs and differences in between the Food and Pharmaceutical industries.

Table 5 Food and Pharmaceutical industries main differences considering sanitation, disinfection, and sterilization processes

	Food industry	**Pharmaceutical industry**
Equipment	Very diverse and not following restrictive design guidelines. Hidden spaces or roughness are commonly found	Very specific and regulated design guidelines. Most of the design parameters, including the control system, are set
Operation cost	High importance. A very competitive market where the margins are low, and the operational cost is a key driver	Low importance. Quality of final product ensuring regulatory compliance is the main driver of the manufacturing process
Automation	Medium. As the operational cost is important, automation is becoming crucial in decreasing costs	Low. Most of the processes are still manual and as the regulatory bodies are restrictive, the industry is moving slowly in this direction
Facilities	Highly dependent on the type of food to be manufactured. The most restrictive one would the one without final treatments	Regulated and pre-defined the type of classification required depending on the type of manufacturing. Class A would be applied to sterile manufacturing.
Personnel	Medium qualified technicians.	Highly qualified technicians
Sanitation	Clear programmes are in place and audited by the authorities regularly, mainly focused on food safety. HACCP is the basis for a proper sanitation program setting	Clear programmes in place focused both on final product and facility. Risk Assessment following ISO14971 or ISO31010. HACCP is not specifically applied
Cleaning	High. The level of TOC is usually much higher	Medium. It is a must but lower generation of organic residues
Sterilization	The aim of sterilization is usually focused in the extension of the shelf life of the product. The potential contamination is addressed throughout cleaning-disinfection along the process	The aim of sterilization is to ensure a safe final administration of the product into the patient. The type of administration also plays a role in the level of decontamination.
Regulation	FDA and GFL as main regulatory bodies. Medium: long regulatory process for a new product into the market.	FDA and EMA as main regulatory bodies. Very long process to place a new product into the market. Any change in the process might alter the in place regulatory acceptance

3.3.5 COVID-19 PANDEMIA

3.3.5.1 INTRODUCTION

When this investigation was started in 2017, it was impossible to predict the huge importance of the results in our day-to-day lives. The importance of decontamination, and specifically airborne and surface disinfection, not just in the industry, but also now, 100% of the areas of the world, is now in the centre of most of our actions.

The COVID-19 disease is caused by a virus, so-called Severe Acute Respiratory Syndrome Coronavirus 2 (SARS-CoV-2). This virus is basically a nucleus of genetic material in a protein encapsuled structure (Figure 12). It is one of these complex proteins, named spike which can identify and make a close link with the human cells' receptor ACE2. Once in, the virus genetic material combines with the cell metabolism, generating thousands of replicates that first propagate within the cell and then disseminate along with the organism (Cui et al., 2019; Peiris et al., 2004; Shereen et al., 2020).

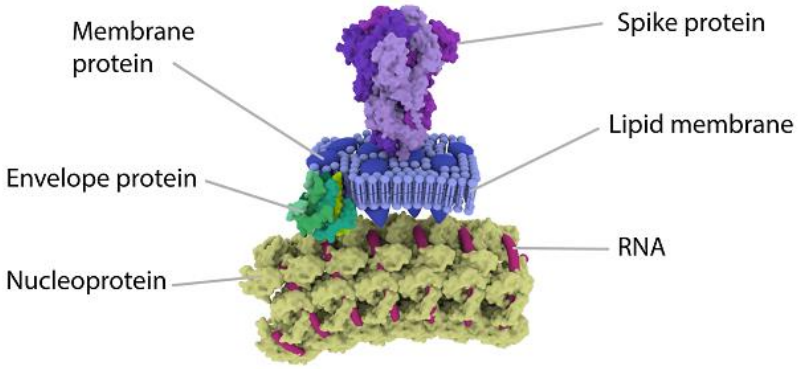

Figure 12 SARS-CoV-2 Basic Structure (Howard and McMeekin, 2020)

This virus, as well as most of the bacteria and viruses causing infections in the human being, travel from one host to others throughout aerosols formed by small droplets. These droplets, in the micrometre level, can stand suspended for even hours or days when the sizes are below 6 microns. Usually, these droplets when in contact with others would create larger droplets that would end up in surfaces (Figure 13) (Atkinson et al., 2009).

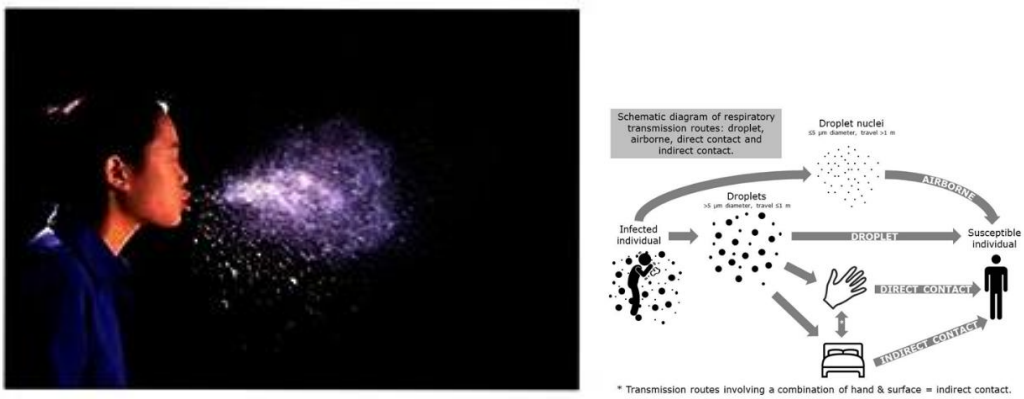

Figure 13 Virus distribution mechanisms (Atkinson et al., 2009)

Discussing the different mechanisms to stop the virus spread, the breakage of the airborne and surface related transmission paths looks to be the more critical ones. Others, such as gaining immunity throughout vaccines or stop the fluid transmission, are complementary measures to minimize the virus impact in our society.

To break that transmission mechanism, the options are (Shereen et al., 2020):

1) Isolating the current host
2) Protecting the future host
3) Dilute the virus concentration
4) Eliminate the virus from the aerosol stream
5) Eliminate the virus from the surface

The technology that is under investigation does have an effect over the last two options. The hydrogen peroxide that is generated can either reach the surface to be decontaminated or recombine with aerosolized virus particles and deactivate them. In next chapters surface decontamination will be treated, as the described mechanisms will be focused on surface rather than aerial contamination.

Then, to understand the importance of the current investigation, it is also relevant to briefly discuss about the resistance of the main type of microorganisms. Favero and Bond (2001) described in a graphical way the resistance of the main type of microorganism (Figure 14). It is quite clear that the prions and bacterial spores are at the top of the resistance level, while viruses, such as the SARS-CoV-2 are more susceptible to harassing environments.

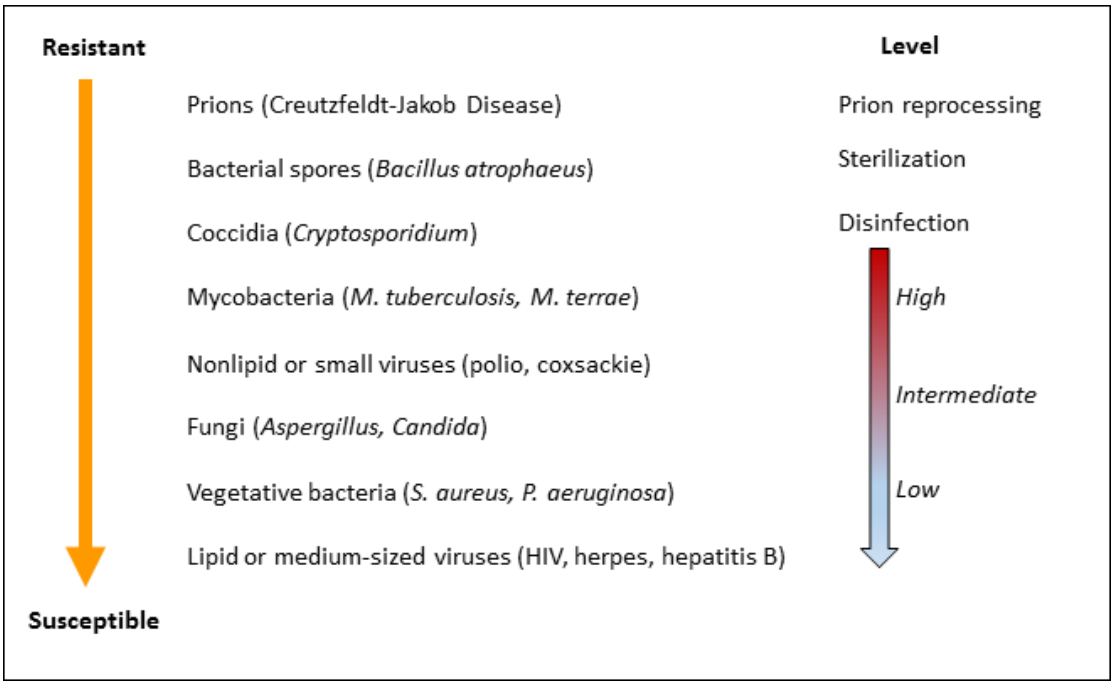

Figure 14 Level of decontamination versus Resistant microorganisms (Favero and Bond, 2001)

Therefore, considering that the hydrogen peroxide would easily decontaminate a surface with the subject microorganism, the next factor is ensuring that this agent is reaching all points and in a repetitive manner.

As shown in Figure 15, traditional surface disinfection methods have some advantages and disadvantages concerning the efficacy of this process.

Figure 15 Traditional surface disinfection methods (El Azab, 2019).

Then, automation and characterization of such systems appear to cover most of the uncertainties that were previously described. In next chapters further discussion about automated systems and SARS-CoV-2 will be done. Tests with similar technologies have already proved a repetitive deactivation even in hidden places and materials that apparently would be difficult to be treated in a such a manner.

3.3.5.2 HYDROGEN PEROXIDE TECHNOLOGY DURING COVID-19

For assessing the viability of this technology in the pandemic crisis, preliminary testing was planned. Even with not enough scientific rigour, this description aims to give a broader understanding of the importance of surface disinfection with automated cold decontamination methods in the current worldwide situation.

Two different events led the activities in this matter.

First of all, in May 2020, in the very beginning of the worldwide pandemic, the FDA released a press release where the hydrogen peroxide disinfection technology was mentioned (FDA, 2020b). The lack of Personal Protective Equipment (PPE), especially, facial masks, made healthcare professionals all over the world, to start reusing single-use PPE. This practice became even normal, exposing the first line professionals to risks not just of breakage of the PPE, but also, contamination due to the loss of efficacy. It is at this moment, when the FDA recalled a study done during 2016.

In this study, published by Battelle Memorial Institute (Columbia, Ohio) and sponsored by the FDA, hydrogen peroxide decontamination of face masks was proved to be efficient with the HPV technology (Bioquell's wet technology) (Richter, 2016). In this study, a testing bench was designed to ensure the reliability of the system, considering not only bioburden deactivation, but also penetration and mechanical resistance after certain number of cycles of decontamination.

The study resulted in a positive outcome reaching a complete decontamination of resistant spores, and in 2020, it is when, the FDA proposed to healthcare professionals the technology and the reuse of masks up to 20 cycles with the use of this technology. Battelle developed a system-container based where thousands of masks were treated simultaneously (Figure 16).

Figure 16 Battelle's decontamination system fully loaded (Richter, 2016)

On the other hand, during the whole pandemic, when the virus spread is in the latter phase, the surface decontamination in every local, public place or even open spaces are part of our day-to-day lives. This surface decontamination is in most cases done with systems that are somehow generating a mist as the technology here proposed.

These procedures do not consider the environmental conditions, no control system is behind, no standard operating procedure is in place, or no stable exposition time is ensured. The practice is delivering somehow extra certainty to the people. Still, it is an approach that should be somehow improved, overall, when discussing a technology to be applied in a health matter.

As soon as the FDA release was identified, together with the customer service department from Telstar as well as the microbiology team from Jose Collado S.A., a prototype was designed. The main purpose of the system was to decontaminate as much masks as possible in a short cycle time.

To do so, as described in Figure 17, a laminar flow cabin was used and special support, to ensure a minimum distance in between items, was designed.

Figure 17 Prototype for SARS-CoV-2 Decontamination

As the ionHP+ technology requires from a Programmable Logic Controller (PLC), a straighter forward nebulization system was integrated into the cabin. The nebulization was still controlled, but not recipe management was included.

In parallel, Jose Collado S.A. (Jose Collado, Barcelona, Spain), after discussing the FDA release, started an investigation together with the Quiron Hospital (Quiron Salud, Torrevieja, Spain). The study revealed that contaminated PPE could be disinfected with an automated method, in shorter cycle times than other procedures such as heat disinfection. In Figure 18, a set-up made by the Hospital is shown.

Figure 18 Automated disinfection method decontaminating different PPE in a Spanish Hospital.

3.3.5.3 CONCLUSIONS

All preliminary results in the previous activities delivered a positive result and, by that time, a promising countermeasure against the lack of PPE equipment in the healthcare environments was engineered.

The positive results were achieved even in the most hidden places of the PPE or masks within a controlled environment. Only, when the surfaces were showing a high dirtiness level, complete inactivation could not be achieved.

Therefore, in 2020, and in this hospital, an automated injection system as well as a dedicated area were installed to recycle the masks and disinfect the PPE equipment that was used during the treatment of positive COVID 19 patients.

4 HYDROGEN PEROXIDE TECHNOLOGY

To understand and characterize such a technology, engineering, physical-chemical and microbiological concepts should be first addressed. The aim of chapter 4 is not just to have an overview of each of the disciplines but also already introduce the Telstar's developed technology from all perspectives. Furthermore, validation, even if it is not a technological discipline, it is important enough to be considered throughout the development of the system.

4.1 PHYSIC-CHEMICAL PROPERTIES

No matter the type of technology applied, the hydrogen peroxide chemical is still "suffering" the same effects from the physic-chemical perspective. What matters to the physic-chemical behaviour is the formulation of the hydrogen peroxide solution (Scatchard et al., 1952). Thus, this chapter will discuss the main formulations present in the market, how do they impact the decontamination process and how would they behave in a specific environment. Physical-chemical parameters, such as vapour pressure and saturation, condensation, evaporation-diffusion, hydrogen peroxide decomposition and absorption-adsorption-desorption processes, will be described.

4.1.1 HYDROGEN PEROXIDE FORMULATION

As discussed in the previous chapter, the hydrogen peroxide molecule, with a molecular weight of 34.02 g/mol, is a chemical that in the present application, is always found as a solution in water. In this solution, the main chemical interactions are hydrogen bonds between molecules of water and hydrogen peroxide, which lead to the creation of polymers between the molecules. This close relationship should be considered when modelling a system with hydrogen peroxide as a sterilant. It does impact not just in the calculation of basic parameters, but also in measuring the presence of the molecule in the volume to be decontaminated (Watling et al., 2002). All properties to be discussed during the following paragraphs have in different ways, impact on the process. This impact, as well as the dependency on the water content, will be described:

- Density and viscosity: it is particularly important when discussing the particle size control and the volumetric control of the system. The density of the solution at 25 ºC is dependent on the % (w/w) of hydrogen peroxide, varying from 1 g/cm^3 to up to 1.44 g/cm^3 in pure solutions. Its viscosity, however, at 20 ºC ranges from 1.005 cP to 1.249 cP, again from low content hydrogen peroxide to higher content (Edwards, 1967).
- Surface tension: the surface tension plays a role in the particle generation and how the atomization nozzle would behave. The surface tension varies from 72.75 dynes/cm up to 80.4 dynes/cm in high content hydrogen peroxide. Its dependency on temperature is very low, being less than 0.1% variation from 0 ºC to 20 ºC (Edwards, 1967).
- Diffusion coefficient: the diffusion coefficient is important when discussing the distribution and reach of the deactivation principle to the microorganism to be eliminated. The diffusion coefficient of hydrogen peroxide vapour into the air was measured by McMurtrie and Keyes (1948) delivering values of 0.188 cm^2/sec at 60 ºC and 1 bar environmental pressure.

- Liquid-vapour phase equilibrium: Raoult's law considers the total pressure as the sum of the partial pressure of the individual components. It can be applied when no interaction in between molecules is taking place. The solution of water-hydrogen peroxide counts with a considerable difference between molecules when talking about volatility and the interaction between both is high. Therefore, Raoult's law cannot directly be applied. The equilibrium will be further discussed when reviewing vapour pressure and condensation (Watling et al., 2002).
- Boiling point: the boiling points in between both molecules are different, being the hydrogen peroxide one, larger than the water. While a 0.1 M of hydrogen (17.34 % (w/w)) has a boiling point of 103 ºC, a system with 0.9 M the boiling point is 145.1 ºC (Edwards, 1967).

Even though more properties could be considered (mainly thermodynamic properties), previous information is already enough to understand the impact of the water content in the hydrogen peroxide formulations.

The water content in hydrogen peroxide solutions is very variable, depending on the type of application. For instance, it might be used in values of 70-90 % (w/w) as a propellant or 1-2 % (w/w) in hair bleaching (Edwards, 1967).

In Cold decontamination methods, the concentration varies from 3-35 % (w/w), also depending on the grade of decontamination. If sporicidal activity is required, values above 7 % (w/w) are usually used (Monger, 1966).

The formulation, in addition to the water content, can be summarized by considering two components into the formula: stabilizers, that reduce the decomposition rate of the active compound, and enhancers of the deactivation capability. The type of formulation will give, in the end also the grade of the hydrogen peroxide: food, technical and semi-conductor grades (Toledo et al., 1973).

The stabilization is required because of the interaction of the hydrogen peroxide with other materials such as containers, piping or contaminats of the solution. The hydrogen peroxide itself is sensitive but stable. These stabilizers can be of organic nature for short term storage, or inorganic when longer periods are required. Both types have advantages and disadvantages, and for instance, the organic stabilizers are oxidized after a certain period and their effect is minimized. On the other hand, the inorganic stabilizers lead to residues after the hydrogen peroxide decomposition (Edwards, 1967). Examples of these types of stabilizers are sodium stannate, sodium malonate, hydroxyquinoline in the presence of phosphates/pyrophosphates, or chelating agents such ethylenediaminetetraacetic acid that act as sinks of metal ions (by forming intermediate compounds that reduce the contact of the hydrogen peroxide with them). Even if it is not a stabilizer in itself, the type of container to be used is very critical. It should be as inert as possible in contact with the active compound being the polymeric material the best in this sense (Monger, 1966).

The enhancers or substances promoting the deactivation are very wide, and recently, many formulators are even adding metals to the solution (Boyce, 2016). The most common compounds adding "value" to the deactivation are:

- Isopropyl alcohol, which in addition to have bactericidal properties, also aids in the wetting of the bacteria cells' walls.

- Enzymes that speed up the redox reaction.
- Fatty acids, that also have bactericidal properties.
- Acids, such as citric acid, lactic acid, or oxalic acid, speed the redox process, maintaining the required pH levels.
- Metals such as silver or copper would in themselves already enhance the bactericidal properties by toxic effects to the microorganisms.

The secondary effect of the additives is particularly important. Any additive, even in the ppm level, should be monitored in terms of residues. The field of application, mainly in Isolator technologies or pass-through boxes, implies a proper characterization of the long-term implications of using certain substances. Usually, the more stable or promoted activity, the more residues will leave at the end of the process, so a balance should be done when choosing the best chemical.

Figure 19 shows the importance in the shelf-life that a specific hydrogen peroxide solution might have depending on the type of stabilizer. While with no stabilization ends up reducing a 75% of the hydrogen peroxide content in 10 h, if Phytate is incorporated in the solution, this reduction takes place at around 20 h.

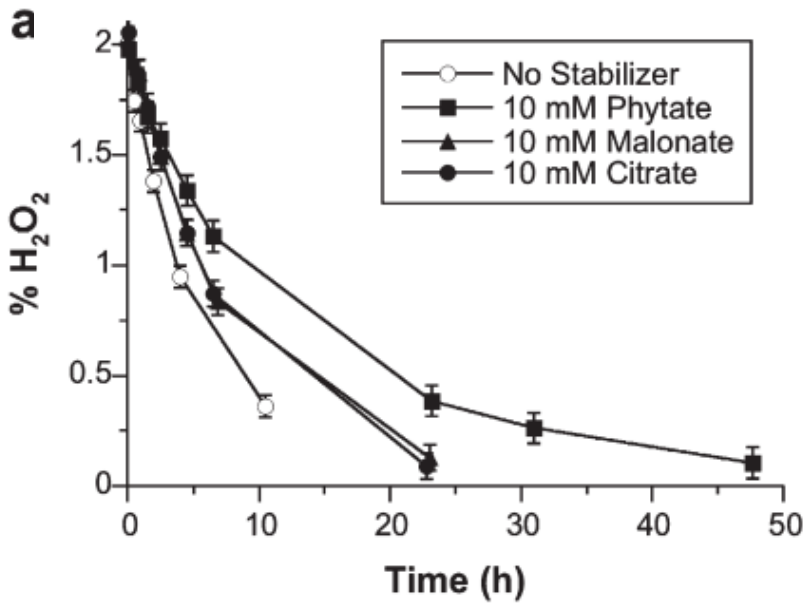

Figure 19 Decomposition of hydrogen peroxide without stabilization or with addition of phytate, malonate or citrate as stabilizers (Richard et al., 2007)

4.1.2 HYDROGEN PEROXIDE DECOMPOSITION KINETICS

One of the major advantages of using hydrogen peroxide as a biocide is, indeed, the way it is decomposed. There are, in theory, no residues at the decontaminated volume (only stabilizers or enhancers could leave so).

Hydrogen peroxide is a stable molecule at low, and medium pH and at moderate temperatures. The reaction, with up to 20 intermediate steps, is basically the one shown below. It is an exothermic reaction that can even be explosive with a high concentration of hydrogen peroxide and the suitable catalyst. The reaction is irreversible:

$$H_2O_2 \rightarrow H_2O + ½\ O_2 + 98.3\ kJ/mol$$

It is a first order reaction, function of the hydrogen peroxide concentration, that can be modelled in the following way:

$$\frac{-d[H_2O_2]}{dt} = k(T) \times [H_2O_2]$$

Equation 1 Decomposition hydrogen peroxide

Where $[H_2O_2]$ refers to the molar concentration of the solution in mol/L, and $k(T)$ to the reaction rate constant in s^{-1} which is function of temperature (T) in Kelvin.

The $k(T)$ can be experimentally calculated, analysing the hydrogen peroxide concentration over time. In this case, this value is modelled considering literature from various authors (Edwards, 1967; Khoumeri et al., 2000; Salem et al., 2000; Tachiev et al., 2000; Verce et al., 2008). The value is obtained minimizing the presence of a catalyst and its value over temperature is described in Figure 20.

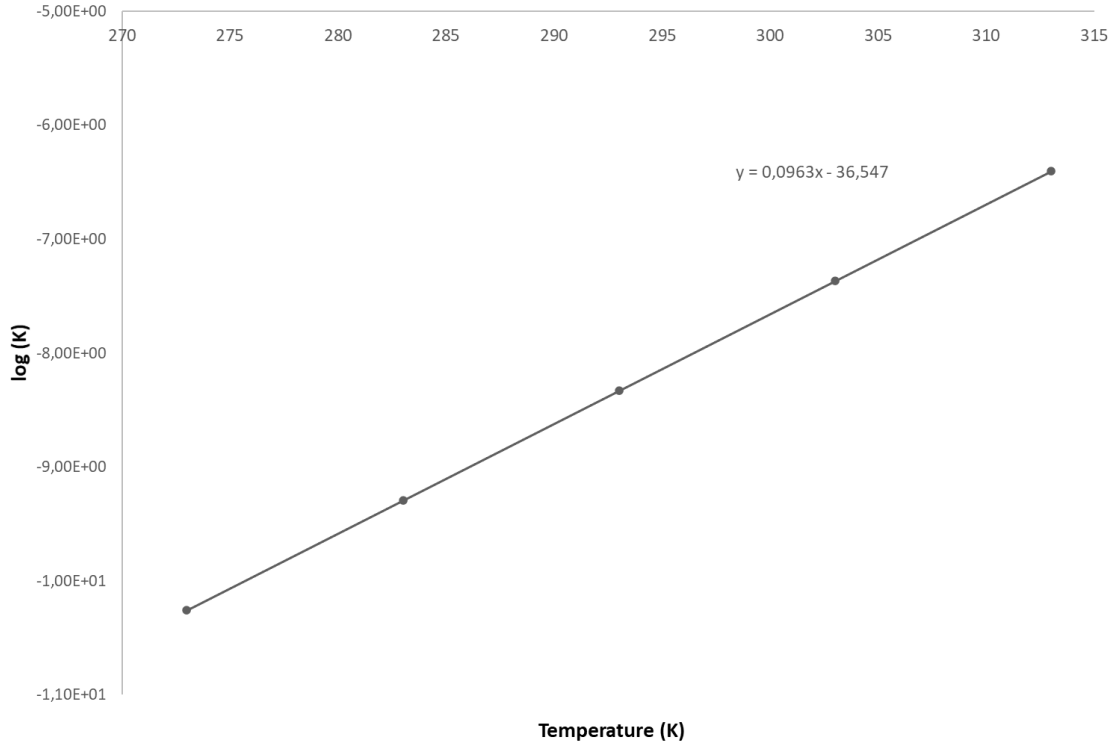

Figure 20 log k(T) vs Temperature

The exercise below (Figures 21 and 22) intends to show how the presence of a catalyst influences the kinetics of the decomposition.

Rearranging the equation 1, the final equation would be:

$$ln[H_2O_2]_t - ln[H_2O_2]_{t0} = -k(T) \times t$$

Equation 2 Hydrogen peroxide decomposition integrated in between t-t_0

Where $[H_2O_2]_t$ refers to molar concentration at a certain point in time, *t* (seconds), and $[H_2O_2]_{t0}$ the initial concentration. Again $k(T)$ is the reaction rate constant at a certain temperature (*T*) in Kelvin.

The Figure 21 shows how the hydrogen peroxide molar fraction (*Xi*) varies over time without a catalyst and at 293 K. While the Figure 22, shows the same exercise but considering a catalyst, active carbon, in between the solution.

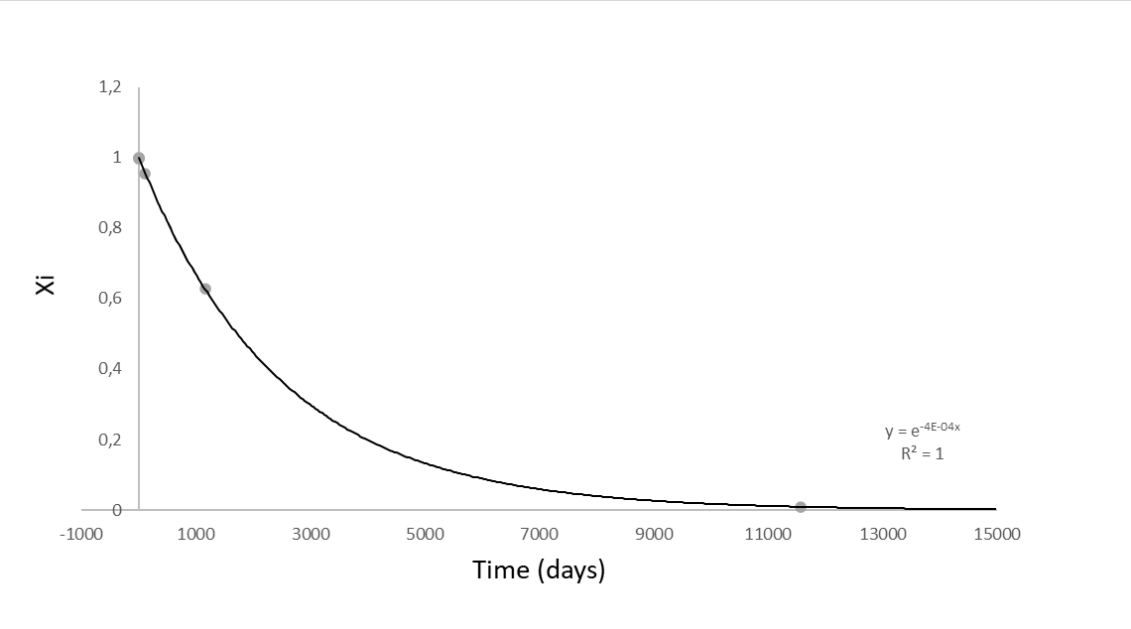

Figure 21 Hydrogen peroxide (Xi molar fraction) decomposition over time (no catalyst)

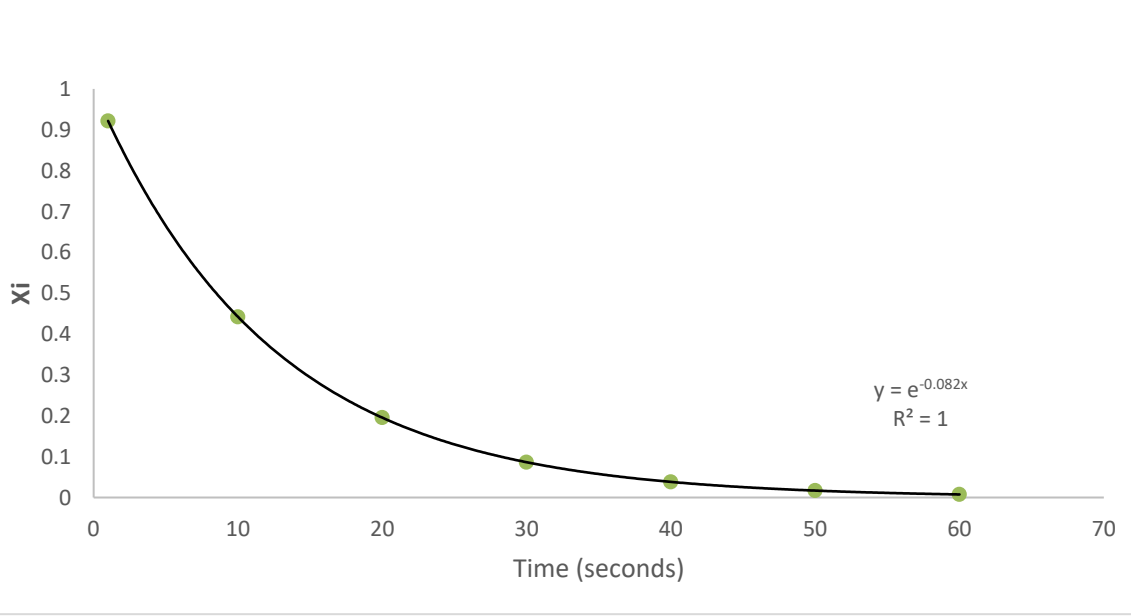

Figure 22 Hydrogen peroxide (Xi molar fraction) decomposition over time (with catalyst)

The exercise shows that at the same initial concentration and temperature, the total decomposition of the active compound can range from the order of seconds for a specific catalyst, to the order of even years without any catalyst. The first scenario where no catalyst is present is improbable. As discussed, the active compound is sensitive to the presence of metals and any other particle of certain elastomers, light, etc. Actually, as an example of the temperature impact over the decomposition reaction, at 343 K and

applying the same exercise, the decomposition takes place in the range of hours instead of years.

The decontamination process, as will be discussed in the next chapters, it is influenced by this kinetics modelling in two aspects:

1) Microbiological deactivation kinetics: Balance in between stability, activity, and residues. The more stable the solution is, the higher hydrogen peroxide concentration will remain in the solution to be injected (enhancing the repeatability). However, the activity would be minimized (less oxidation potential if too stable), and the residues to be left in the volumes to be decontaminated, would be larger.
2) Aeration: once the system has “finished” deactivating the microorganism (dwell time), the aeration phase starts. There is again a balance between stability and total aeration time. The lower the aeration time, the faster the process, and the higher production yield can be expected in a certain production facility.

4.1.3 THERMODYNAMICS GENERAL CONCEPTS

This point is significant in the understanding of every hydrogen peroxide technology, no matter which one. An initial description of basic concepts from the thermodynamic point of view will be done, focusing on hydrogen peroxide.

It might look too basic to start by the following: there are, basically, three states of matter, solid, liquid and gas (in extreme conditions, plasma can be generated). The changes in between them can be summarized in:

- Solid → Liquid: melting process; Liquid → Solid: freezing.
- Liquid → Gas: vaporization; Gas → Liquid: condensation.
- Gas → Solid: deposition; Solid → Gas: sublimation.

The atoms and molecules are bound together, and their kinetic energy increases as the states pass from solid to liquid and from liquid to gas phase (Pereira, 2019). In the present process, vaporization and condensation will be discussed.

Vaporization, as mentioned, is a process where, when applying energy to the liquid phase, the molecules increase their kinetic energy. The ones with higher energy than the attractive forces in between liquid molecules change their state, moving towards the gas phase. This gas phase creates a certain pressure over a system. If the surrounding pressure is lower than the pressure in equilibrium with the liquid phase at a certain temperature, the liquid would boil. However, if the surrounding pressure is still higher, the liquid would continue evaporating until an equilibrium is reached. The equilibrium is reached when the rate of condensation and the rate of evaporation are equal. It is then when the vapour pressure of a certain liquid is reached. This pressure is a function of the particular liquid as well as the temperature. The higher the temperature, the higher is the rate of evaporation, thus, the equilibrium is reached at a higher pressure.

The vapour pressure of every substance, as mentioned, is a core characteristic and can be empirically determined. Clausius-Clapeyron proposed the relationship in between temperature and vapour pressure (Rodgers and Hlll, 1978):

$$\log\left(\frac{P_2}{P_1}\right) = \frac{\Delta H}{4.57}\left(\frac{1}{t_2} - \frac{1}{t_1}\right)$$

Equation 3 Clausius-Clapeyron equation

Where P_1 refers to the vapour pressure at the Temperature 1 (t_1) and P_2 to the t_2. ΔH, refers to the latent heat of vaporization.

To characterize the first vapour pressure, P_i, at a defined temperature, Antoine equation, proposed that throughout experimental testing of the specific liquid, Antoine constants A, B, and C could be calculated and related in the following way (Rodgers and Hlll, 1978):

$$\log(P) = A - \frac{B}{t + C}$$

Equation 4 Antoine equation

This way, a pure liquid vapour pressure can be first determined and then characterized over a range of temperatures.

However, if, for instance, two substances are present in a certain solution, their vapour pressure is not just function of the temperature but also of the molar fraction of the substance in the liquid solution (*Xi*). This relationship was in 1880s stated throughout the following equation by the Raoult's law (Pereira, 2019).

$$Psolvent = Xsolvent \times P^0_{solvent}$$

Equation 5 Raoult's ideal law

where the $P^0_{solvent}$ is the pure vapor pressure of the solvent at a specific temperature and $Xsolvent$ is the molar fraction of this solvent in the solution. The Raoult's law assumes ideal behaviour of the molecules and that the interaction in between pure molecules are not affected by the other substance (Pereira, 2019).

In Figure 23, the molar fraction of one of the components is represented *versus* pressure. The larger the molar fraction of one component, the more weight would have in the total pressure of the system.

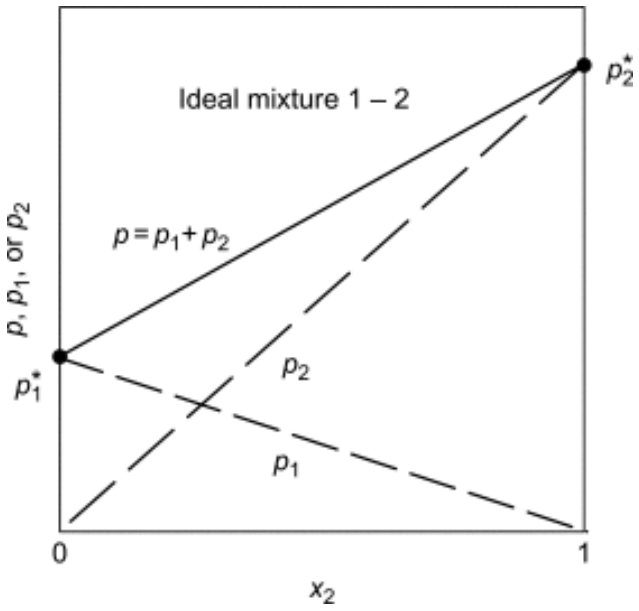

Figure 23 Vapour pressure of an ideal mixture in function of molar fraction (Soroush and Bahadori, 2017)

However, when interactions exist, it is then, when a correction should be addressed (Watling et al., 2002). This correction is done using activity coefficients that should be characterised for each solution. The Raoult's equation considering the activity coefficients is described in Equation 6:

$$P_{solvent} = \gamma_{solvent} \times X_{solvent} \times P^0_{solvent}$$

Equation 6 Raoult's law correction

Calculating the vapour pressure will be then "easy" to understand when a certain environment is saturated with a specific substance. When condensing occurs, the equilibrium is reached and saturation is achieved.

The hydrogen peroxide as a pure substance has a boiling point of 150 ºC and the water is barely 100 ºC. Also, the vapour pressures of both substances at a certain temperature are different, being the water one larger than the hydrogen peroxide one. For instance, at 25ºC, hydrogen peroxide has a vapor pressure of 300 Pa, while water has a vapour pressure of 317 Pa.

There are two important conclusions to be withdrawn from previous data:

1) The vapour composition will always be more concentrated in water than the liquid solution and the solution will remain with a higher hydrogen peroxide concentration.
2) The hydrogen peroxide will always start to condense (reach saturation) before the water does. Being therefore, the condensed phase, more concentrated than the solution.

An interesting description is given in patent US 4797255 (Hatanaka and Shibauchi, 1989) referring to the previous conclusions. Figure 24 describes two examples:

Example 1 (C-E and F-D):

- If a solution of 35 % (w/w) in hydrogen peroxide (C) is heated up to the boiling, 108 ºC, then the vapour in equilibrium would be 8 % (w/w) (E).
- Similarly, if a 71 % (w/w) (F) is heated up to 127ºC, then the vapour in equilibrium would be 35 % (w/w) (D) concentrated.

Therefore, it is always expected to have a significant decrease of concentration in the gas phase, when reaching the boiling point.

Example 2 (D-F):

Now, the solution is gasified. That means, that the whole solution is, throughout a flash distillation, moved to the gas phase. Then:

- Starting from a 35 % (w/w) solution, the gas phase remains with the same concentration (D).
- But, when the gas steam reaches a different temperature (lower), the liquid in equilibrium becomes more concentrated (as the first to condense will always be the hydrogen peroxide), 71 % (w/w) (F).

These two examples are of particular importance when discussing the hydrogen peroxide technology. The flash distillation is one of the most used processes to get a highly concentrated gas stream into the volume to be decontaminated.

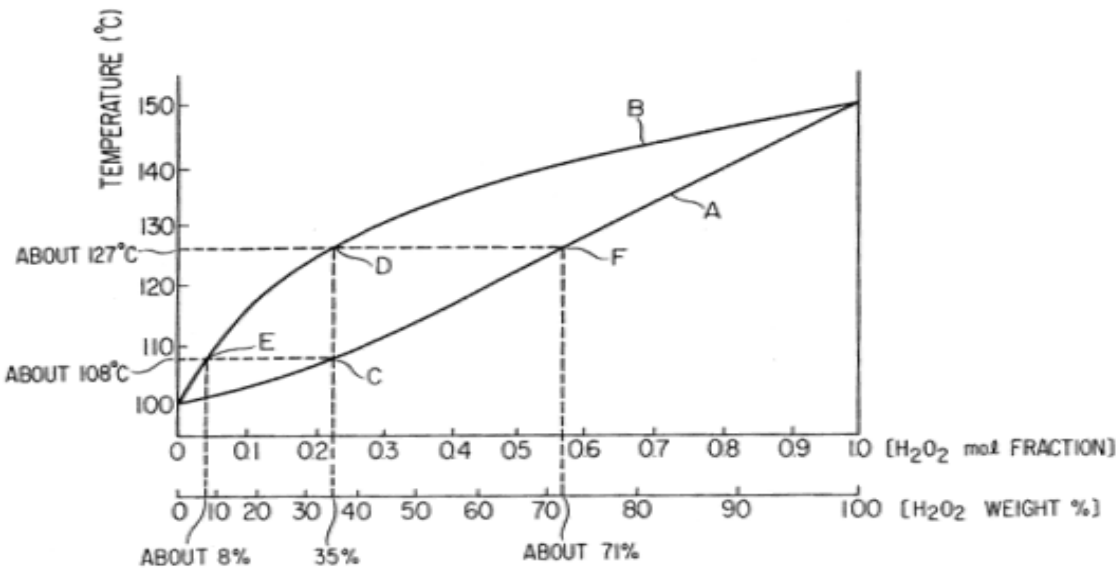

Figure 24 Boiling point of different Hydrogen Peroxide solutions. Line A refers to the boiling point of the mixture hydrogen peroxide and water. Line B refers to the gas composition at the boiling point (Hatanaka and Shibauchi, 1989).

In order to carry on with the thermodynamics understanding, and once understood the differences between hydrogen peroxide and water from the boiling and vapor pressure perspective, a specific solution will be characterized. The exercise intends to calculate the vapour pressure of a solution at different temperatures. To do so, the very first point is to calculate the vapor pressure of the pure components, using data already published by Keyes et al., (1947) and Scatchard et al., (1952) for water and hydrogen peroxide respectively:

$$log_{P_w}(T) = G + \frac{A}{T} + B \times log(T) + C \times T + D \times T^2 + E \times T^3 + F \times T^4$$

Equation 7 Water vapor pressure in function of temperature

$$log_{P_H}(T) = D + \frac{A}{T} + B \times log(T) + C \times T$$

Equation 8 Hydrogen peroxide vapor pressure in function of temperature

Where $P_{w,}$ *and* P_H refer to the vapour pressures of water and hydrogen peroxide respectively. The *T* (K) and A, B, C, D, E and F as Antoine constants are empirically defined.

Considering equation 6, the activity coefficient is still required to calculate the vapour pressure of each component of the mixture. The activity coefficients are also characterized empirically and were reported by Schumb et al., (1955) and represented by Equations 9 and 10.

$$\gamma_w = exp\left\{\frac{(1 - x_w)^2}{R \times T} \times [B_0 + B_1 \times (1 - 4 \times X_w) + B_2 \times (1 - 2 \times X_w)x(1 - 6 \times X_w)]\right\}$$

Equation 9 Activity coefficient of water

$$\gamma_h = exp\left\{\frac{{x_w}^2}{R \times T} \times [B_0 + B_1 \times (3 - 4 \times X_w) + B_2 \times (1 - 2 \times X_w) \times (5 - 6 \times X_w)]\right\}$$

Equation 10 Activity coefficient of hydrogen peroxide

Where γ_w and γ_h are the activity coefficients for water and hydrogen peroxide respectively, *T,* temperature in Kelvin, *R* the ideal gases constant, x_w and x_h the molar fractions of water and hydrogen peroxide and B_0, B_1 and B_2 empirical constants gathered by Schumb et al. (1955).

With both coefficients and the corrected Raoult's law equation the vapour pressure in equilibrium for a closed system can be calculated. As the calculations are tedious due to the number of variables, and the objective is to characterize the vapour pressure over different temperatures and molar fraction of the hydrogen peroxide, a programming software to develop algorithms and creation of models was used, MATLAB R2019a (MathWorks, Natick, MA, USA). With the definition of up to 6 functions, the following graph (Figure 25) was obtained. The same exercise could be done for water.

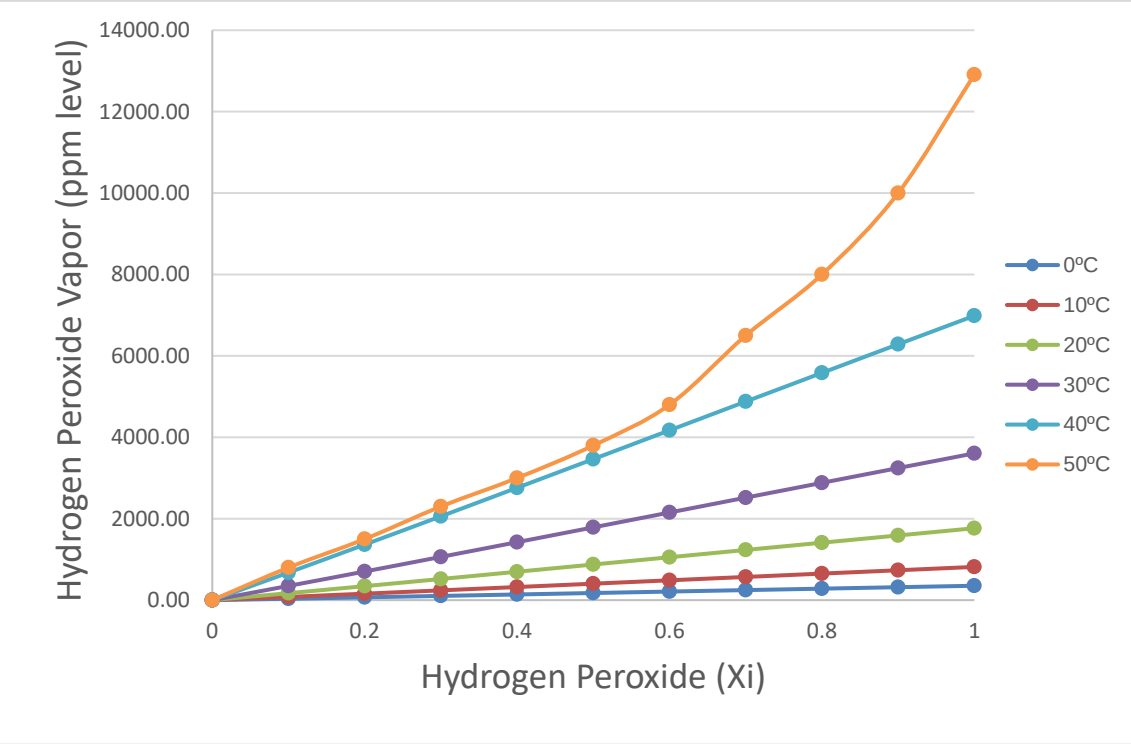

Figure 25 Hydrogen peroxide saturated vapor pressure in function of Temperature and Molar fraction of Hydrogen Peroxide

It is important to highlight the following:

- If the system is in equilibrium, this value is the maximum ppm level that can be reached. No matter the amount of hydrogen peroxide solution is injected (assuming there is enough to get the ppm level at the specified temperature), condensation will occur after that value is reached.
- To reach the equilibrium, there is a time of evaporation of the injected hydrogen peroxide (if injected in the liquid phase).
- The water content, both in the liquid phase and the Relative Humidity (RH) influence the total ppm level of the system.
- To get higher ppm levels, a dynamic system should be created. No equilibrium can be reached. An overheating (usually throughout flash distillation) has to be performed, and the system has to be maintained in dynamic conditions (for instance with recirculation).

Finally, to understand how the partial pressure, total pressure and vapor pressure are related, the Dalton equation should be addressed (Pereira, 2019).

$$P_{total} = \sum_{i=1}^{n} P_i$$

$$P_i = y_i \times Ptotal$$

Equation 11 Dalton's equation

Where y_i is the vapour composition of the substance "i", and P_i is the partial pressure for the same substance. The partial pressure would be calculated from Equation 11, so y_i

can also be gathered. Figure 26 shows how the vapor composition of hydrogen peroxide changes in function of the liquid molar fraction at 20 ºC.

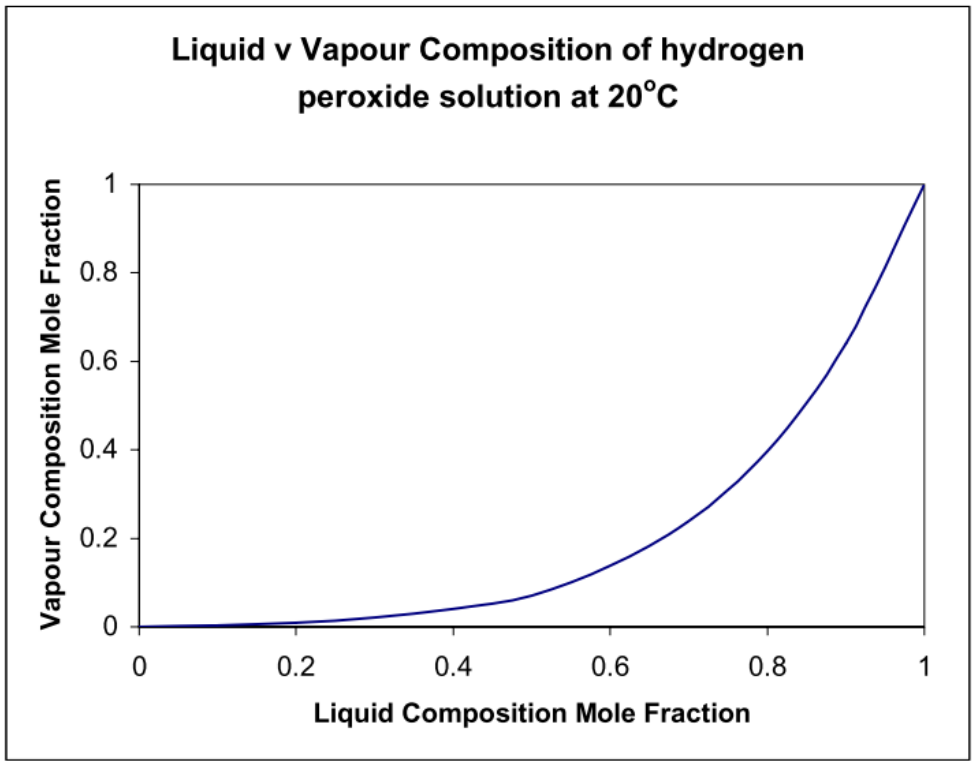

Figure 26 Hydrogen peroxide vapour composition in function of liquid molar fraction (Watling et al., 2002)

4.1.4 EVAPORATION, ABSORPTION, ADSORPTION AND DIFFUSION

These processes play an important role over the decontamination system. In this chapter, a basic understanding of the main factors to be considered will be done, but no modelling, nor deep analysis will be done.

4.1.4.1 EVAPORATION

The evaporation rate is, among other processes, defining when the equilibrium would be reached. The gas phase, mainly in processes where a mist is generated, is created by the evaporation of the particle. To understand how the evaporation is affected, it is interesting to describe the relationship that Seinfeld and Pandis (2016) published:

$$\frac{dmp}{dt} = -\frac{c}{4} \times \alpha \times \pi \times d_p^2 \times (Csat - Cg)$$

Equation 12 Loss of mass of particle in function of time (Seinfeld and Pandis, 2016)

Where mp refers to the mass of the particle, c is the mean molecular velocity (dependent on temperature and molecular mass of the substance), α the accommodation coefficient, d_p^2 the particle diameter and $Csat$ and Cg are the concentration of the substance till saturation and the actual one (Saleh et al., 2017).

The following should be highlighted when discussing about an atomization technology:

- The particle diameter affects the time to reach equilibrium.

- At the beginning of the process, the saturation $Csat$ *versus* actual concentration Cg will be high but then, the evaporation process will be slowed down, due to the reach of the equilibrium.
- The temperature will impact directly not just in c, but also in the $Csat$, being larger if the temperature is larger.

4.1.4.2 ABSORPTION, ADSORPTION AND DIFFUSSION

Absorption as a mass transfer process is also essential to understand the potential impact over decontamination. The absorption of hydrogen peroxide in different materials does not just have an effect over the material itself, but also on the decontamination efficiency. The Biot number describes the ratio of the inner mass transport resistance to the outer mass transport resistance (Yang and Mao, 2014). The Equation 13 describes this relationship:

$$B_i = \frac{\beta \times l}{K_i \times D_i}$$

Equation 13 Biot number Equation (Yang and Mao, 2014)

The factors β, l and K_i are mass transfer coefficients of the surrounding gas phase and that are mainly affected by the speed/flow scenario. The factor D_i is the diffusion coefficient of the species i in a certain material.

For instance, large Biot numbers show that no resistance is appearing in the outer surface (gas-solid), and the solid mass transfer would be limiting the absorption speed. This means as well during desorption, the concentration of the hydrogen peroxide on the surface is close to zero.

The speed of the hydrogen peroxide moving towards the inner layers of the system to be decontaminated would be the main mechanism to understand how absorptive a material is. That is given by the diffusion coefficient but also, using the Fick's second law of diffusion, the change in concentration could be characterized (Yang and Mao, 2014).

$$\frac{dC_{H_2O_2}}{\partial t} = D_{H_2O_2} \frac{d^2C_{H_2O_2}}{\partial x^2}$$

Equation 14 Diffusion Fick's Law

Where $C_{H_2O_2}$ is the hydrogen peroxide concentration, $D_{H_2O_2}$ the activity coefficient of the hydrogen peroxide in a specific material and *x* the transport's direction.

The greater the difference in concentration in between points, and the greater the temperature is, the faster the diffusion will be inside a certain substance. The saturation concentration of each material is different, as well as the diffusion coefficient. Figure 27 intends to show diffusion (bottom) and saturation concentration (top) of typical materials found in a clean room (Radl et al., 2011).

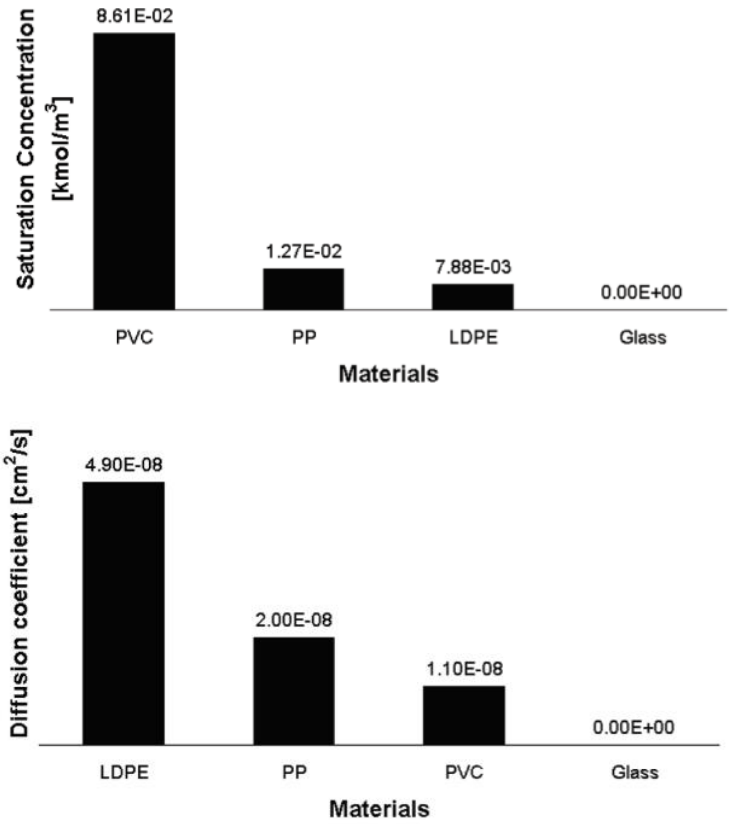

Figure 27 Saturation concentration and Diffusion coefficient - Materials in Cleanrooms (Radl et al., 2011)

As main highlights of this section, and relating them to the decontamination process, the following should be considered:

- The type of material to be decontaminated will impact in the actual hydrogen peroxide to reach the surface. This means that materials with high diffusion and saturation concentration would likely require higher volumes of sterilant to ensure decontamination in the material and leave enough quantity for the rest of surrounding surfaces.
- The hydrogen peroxide within the material, even if outer conditions are modified, will not be easily passed to the gas phase. The inner diffusion marks the desorption towards the gas phase. The only parameter to be modified with a certain impact would be the temperature.
- Aeration process, and therefore total cycle time, could become longer than expected due to the desorption process.
- Following use of the decontaminated material should consider that hydrogen peroxide might be released during a longer period than the aeration process considered. The safety level of 1 ppm could be reached while the materials are still releasing hydrogen peroxide.

4.2 MICROBIOLOGY

4.2.1 ACTION MECHANISMS OF HYDROGEN PEROXIDE

Hydrogen peroxide is a potent oxidizer. Even though it does have a low molecular weight compared to the main microorganisms' structures, its ability to penetrate cell wall/membranes can lead to a reaction with internal cellular components leading to apoptotic and necrotic cell death (Denyer and Stewart, 1998).

Its main mechanism of deactivation is based on the generation of Reactive Oxygen Species (ROS) in such a quantity that the defences against those are not enough. The reduction of the exposure to these ROS is a function of systems such as alkyl hydroperoxide reductase (Ahp) and catalases (KatG and KatE) among others (Seaver and Imlay, 2001). If not enough defence is present, then via Fenton's reaction, hydrogen peroxide will generate hydroxyl ions, against which there is no mechanism to reduce the damage.

Uhl et al., (2015) described two killing mechanisms: one is based on DNA damage due to Fenton's reaction and hydroxyl generation, and the other occurs when there is a higher concentration, and injury occurs in other macromolecules level (proteins and lipids). Unlike DNA damage, where the hydrogen peroxide is unreactive if no radicals are generated, the other macromolecules would be oxidised even in the absence of metals when the compound is close to proteins or cell membranes. Figure 28 represents both modes of action.

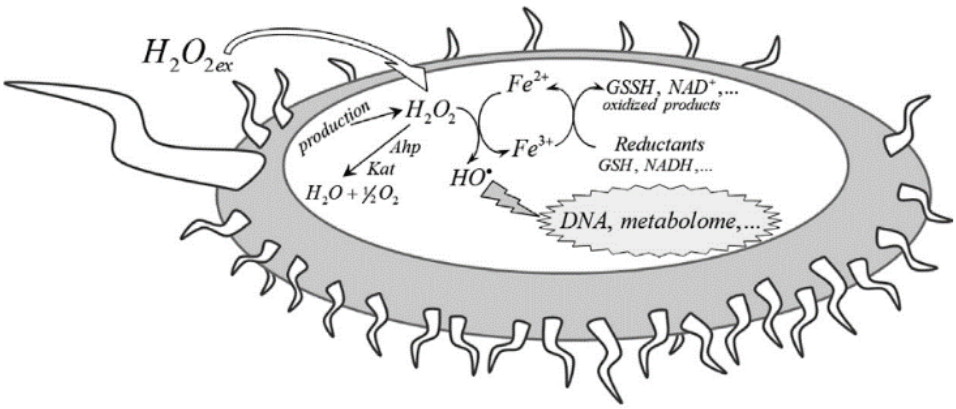

Figure 28 Hydrogen peroxide two mode of action representation. External hydrogen peroxide entering into the cell and via Fenton reaction (with Fe^{2+} as a catalyzer) producing hydroxyl radicals (Uhl et al., 2015)

In addition, a review performed by Linley et al. (2012) also discussed about the two modes of action that appear in *Escherichia coli* K12, when exposed to various concentrations of hydrogen peroxide (Figure 29). It was observed that cells were more susceptible to low concentrations (< 3 mM) than to intermediate concentrations (5-20 mM). With values above 20 mM, the number of surviving microorganisms was inversely proportional to the concentration of the disinfectant. This slight increase in surviving microorganisms with higher hydrogen peroxide concentration was related to the first mechanism of lethal action, where low levels of the oxidizer have greater impact in the DNA repair grown strains.

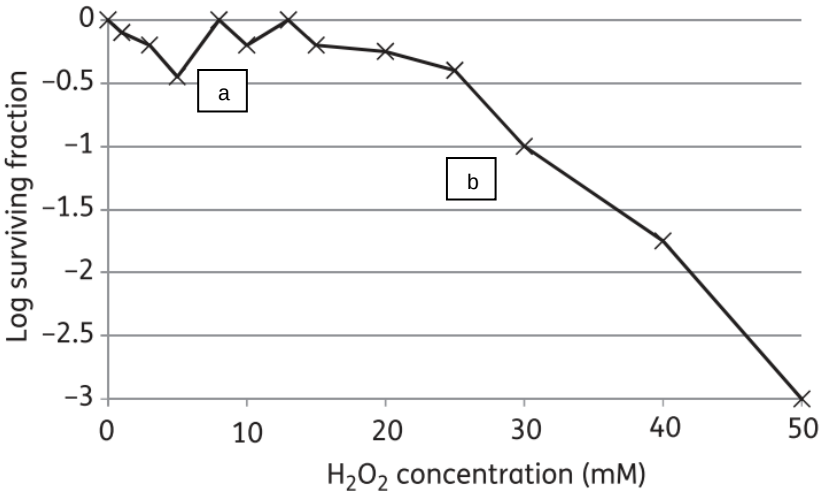

Figure 29 Surviving microorganisms in function of hydrogen peroxide concentration shows two modes of actions. a) where even with higher concentration the surviving fraction is higher and b) that after a certain concentration, the surviving fractions decreases with it (Linley et al., 2012)

However, not only the hydrogen peroxide concentration plays a role in the mode of action, but also the available free iron and the cell density can impact the inactivation kinetics. Regarding to cell density, further studies, such as the one carried out by Drinkwater et al. (2009), discussed about the effect of clumping. This effect is one of the reasons for higher D-values when the population grows from 10^4 or 10^5 to up to 10^6. The clustering effect appears when artificially manufacturing of commercial indicators is done, where a high concentration of microorganism is inoculated on a small surface. It is then, when the resistance of standalone microorganisms is not anymore valid, the D-Value might be longer than expected.

4.2.2 TYPE OF MICROORGANISMS AND FORMS

This chapter is not to discuss about all microorganisms present in the environment, but to discuss the most common biological systems that can pose an issue to the Pharmaceutical and Food industry.

Starting from the basics, microorganisms in both industries can be divided into two major groups, prokaryotic bacteria (their genetic material is not housed in a true nucleus) and viruses where there is not even a composition of cells. The viruses are mainly proteins and genetic material, either DNA or RNA (not both), that are inert outside of a host. Eukaryotic microorganisms, although might be relevant in specific cases of these industries, will not be considered in this section.

Bacteria can be classified according to their reaction to Gram staining. The Gram-positive bacteria have a thicker layer of peptidoglycan protecting the nucleus and the Gram-negative with only a thinner layer (Figure 30).

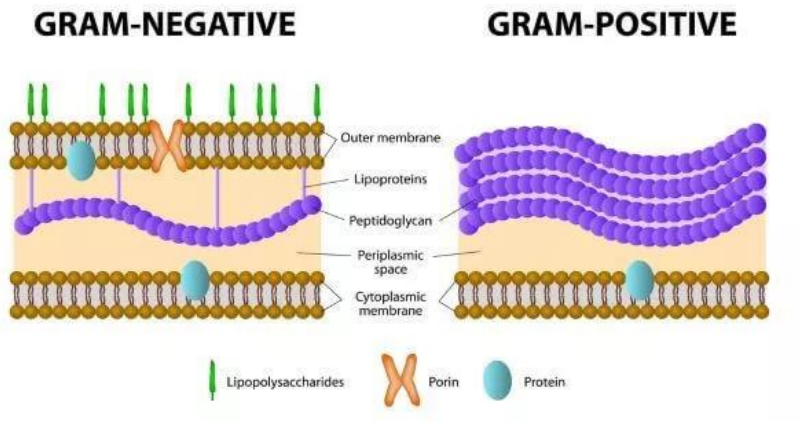

Figure 30 Gram positive versus Gram negative bacteria (Biology dictionary, 2021)

This classification has a certain significance, as their resistance to the disinfection differs depending on outer membrane type. Some investigations have proposed that Gram-negative bacteria persist longer than Gram-positive bacteria and, although it has been suggested that the type of surface does not influence the period of persistence, it has also been shown that longer persistence may occur on plastic or even on steel (Abreu et al., 2013). Even though there are other ways of classifying microorganisms (shape, nutrition, etc.), it is not part of the investigation to go in detail in this sense.

However, two factors differ some microorganisms from the other, and play an important role in this investigation: 1) their ability to adapt and survive to harsh environments, especially the sporulation capability, and 2) their ability to form multicellular communities to survive, i.e., their ability to form biofilms.

4.2.2.1 SPORES

The sporulation process is characteristic of more than 200 bacterial species. Most of those species are grouped in two genera of Gram-positive bacteria, the aerobic Bacilli and the anaerobic *Clostridia*. The process of sporulation (Figure 31) has a key step when asymmetric cell division occurs. The spore formation is assisted by the mother cell to undergo an autolysis process and finally release the final spore. Once the spore is generated, its structure confers the new entity a great resistance against adverse environments. It is created multilayer protection surrounding the cytoplasm that allows the spore to survive almost indefinitely, even in the absence of water and nutrients. The cortex, surrounding the core, has the objective of maintaining the dormancy status (Figure 32). The non-pathogenic spores are robust, making them useful not just as a validation tool but also as carriers/vehicles for vaccine inoculation. Nevertheless, the spores can also germinate again: if the environment becomes favourable, and enough water and nutrients are present, the spore would leave the dormant status and return to the vegetative form (Cutting et al., 2009).

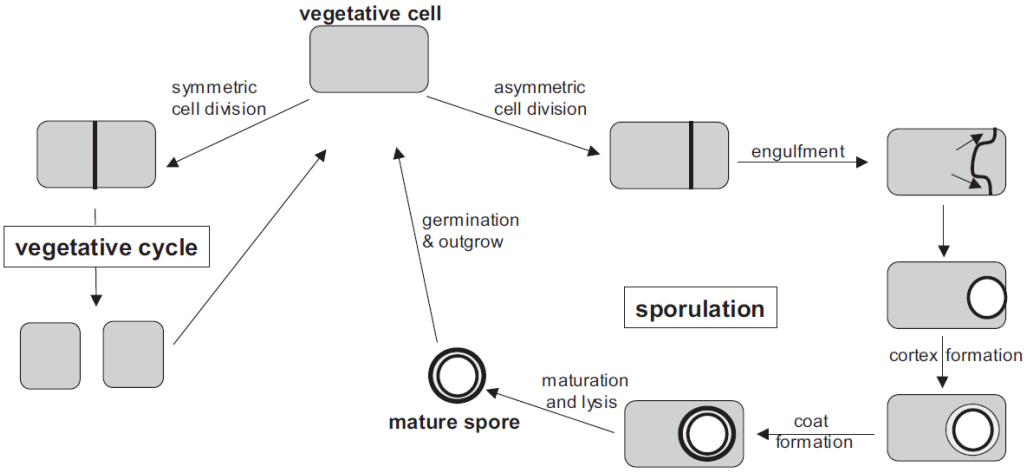

Figure 31 Sporulation process flow diagram (Cutting et al., 2009)

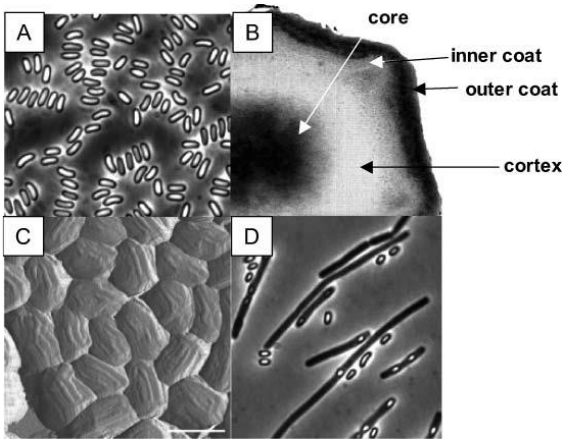

Figure 32 Microscopic analysis of bacterial spores. a) Using phase-contrast microscopy. b) Transmission electron microscopy. c) Atomic force microscopy. d) Phase-contrast microscopy of rod-shaped cells (Cutting et al., 2009).

4.2.2.2 BIOFILMS

The biofilms, in contrast, are a different way of responding to an attack or environmental difficulty. The bacteria generally exist as two types of population: planktonic cells, i.e., freely living in the environment, or sessile, i.e., as a unit attached to a surface or within the confines of a biofilm. The definition of a biofilm would be a conjunction of immobilized cells at a substratum and frequently embedded in an organic polymeric matrix of microbial origin (Garrett et al., 2008). To form the biofilm structure, adhesion to a substratum and coaggregation (including identification) processes occur. This biofilm can eventually grow because of the signalling process that appears in between cell-to-cell in microbial communities. The signalling process is called Quorum sensing, and it is in many cases modelled for the different types of bacteria (Figure 33) (Mattila, 2002).

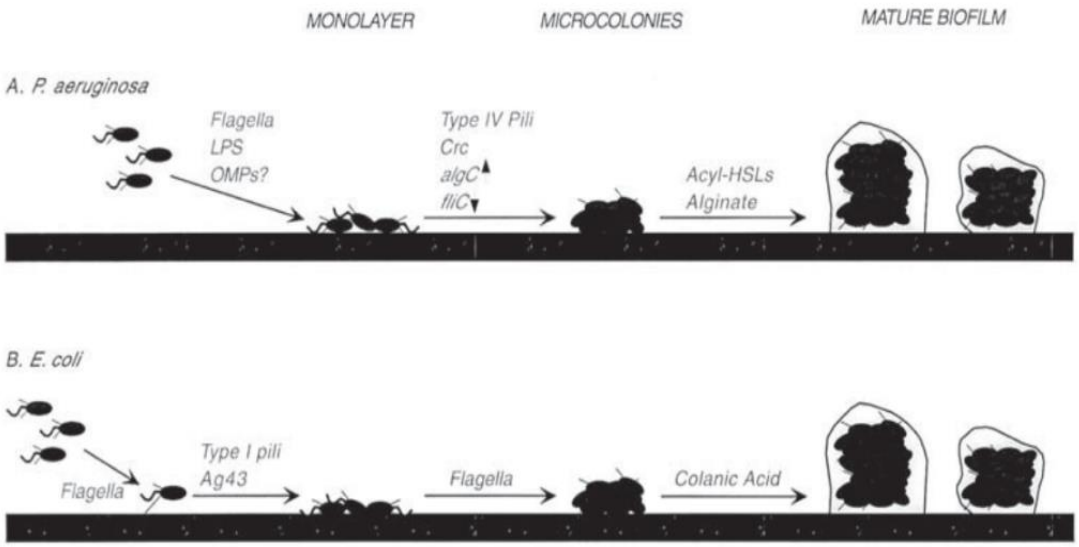

Figure 33 Biofilm generation process (Mattila, 2002)

This ability of the biofilm to create protective layers above the cells' community makes, in the case of certain sterilization technologies, even more difficult the penetration until the nucleus of the microorganism. These layers could be up to 75-90% of the total composition of cells and extracellular material. Therefore, the impact over the decontamination might be huge. The main factors influencing the creation of such a community is again the lack of nutrients, water or the exposition to harsh environmental conditions. Stress situations are the promotors of these kind of communities. It is particularly important that if the biocide is injected in an environment in a sublethal concentration, this slight harsh effect, can lead to the formation of a biofilm that was not present before (Mattila, 2002).

4.2.3 MICROBIOLOGICAL VALIDATION

The modelling of a decontamination process to ensure repeatability and robustness would require that the most significant answers from the system are used.

Without entering into the Pharmaceutical or Food industry yet, any process to be modelled should have input variables and a single or various answers from the system to be monitored. This answer, in the present investigation, is a microbiological response. Microbiology variability is bast, and therefore, it is mandatory for modelling, to consider certain assumptions to gain representatives of the whole microbial community. In addition, considering that for the pharmaceutical industry, part of this research, requires manufacturing in aseptic conditions, a well-documented and designed validation process should contemplate the mentioned variability and a good choice of the microorganism reference.

Thus, the current chapter intends to discuss further the validation process, and the uncertainties can pose to the modelling and validating system.

4.2.3.1 SELECTION OF MICROBIAL REFERENCES

Two aspects to be considered in the selection process are: a) the microbial bioburden representativeness, type, and concentration, and b) the microbial resistance to the selected decontamination process.

The bioburden is the characteristic microbial contamination in a certain enclosure, surface or system. Therefore, it is important to consider the most characteristic microorganisms present in the industry to receive the correct answer from the system to be modelled.

The pharmaceutical industry, in both the FDA and EMA guidelines, mention some examples of the main reference microorganisms to be tested (EMA, 2017; FDA, 2016):

- *Pseudomonas aeruginosa* (ATCC 9027)
- *Staphylococcus aureus* (ATCC 6538)
- *Escherichia coli* (ATCC 8739)
- *Salmonella enterica* (ATCC 14028)
- *Candida albicans* (ATCC 10231)
- *Clostridium sporogenes* (ATCC 11437)

Assays are performed with these microorganisms in vegetative form. The industry usually chooses not just to validate but also to monitor the decontamination process, analysing sporulated microorganisms (if there is) to detect the most resistant bacterial forms.

It is this fact that many times leads to an over-specified decontamination process. The process poses a challenge to achieve the microbial inactivation desired and a risk to the equipment, reducing the production yield and eventually posing a risk to the manufactured drug. In this sense, the cGMP advises monitoring the bioburden continuously and make a proper risk analysis of the specific manufacturing site (FDA, 2016). Then, a validation and monitoring should be done according to obtained results.

Discussing the microorganisms used as a reference for the food industry, the main concept is that the approach is different. While in the pharmaceutical industry the focus is on the environmental bioburden to ensure sterility of the final product, in the food industry, sterility itself is not required in most processes. It is accepted to have a certain microbial load and only specific microorganisms are monitored mainly in the final product.

An extract of the 2073/2005 Regulation (European Commission, 2005) would clearly show the mentioned approach of the food industry:

“Samples shall be taken from processing areas and equipment used in food production, when such sampling is necessary for ensuring that the criteria are met. In that sampling the ISO standard 18593 shall be used as a reference method.

Food business operators manufacturing ready-to-eat foods, which may pose a Listeria monocytogenes risk for public health, shall sample the processing areas and equipment for Listeria monocytogenes as part of their sampling scheme.

Food business operators manufacturing dried infant formulae or dried foods for special medical purposes intended for infants below six months which pose an Cronobacter sakazakii risk shall monitor the processing areas and equipment for Enterobacteriaceae as part of their sampling scheme.

Food business operators may use other sampling and testing procedures, if they can demonstrate to the satisfaction of the competent authority that these procedures provide at least equivalent guarantees. Those procedures may include use of alternative sampling sites and use of trend analyses.

Testing against alternative micro-organisms and related microbiological limits as well as testing of analytes other than microbiological ones shall be allowed only for process hygiene criteria.

The use of alternative analytical methods is acceptable when the methods are validated against the reference method in Annex I and if a proprietary method, certified by a third party in accordance with the protocol set out in EN/ISO standard 16140 or other internationally accepted similar protocols, is used.

If the food business operator wishes to use analytical methods other than those validated and certified as described in paragraph 3 the methods shall be validated according to internationally accepted protocols and their use authorized by the competent authority".

Some of the microbial references are:

- *Salmonella* spp.
- *Escherichia coli*
- *Listeria monocytogenes*
- *Bacillus cereus*
- *Campylobacter* spp.

The food industry is very broad and depending on the type of final product, the level of contamination to be allowed would be different.

4.2.3.2 BIOINDICATORS

Even if other factors such as physical conditions or type of load are important in the validation, when discussing this process, it is unavoidable to talk about bioindicators. Both the European and the United States Pharmacopeia (Council of Europe, 2021; FDA, 2016) require the use of biological indicators to validate any sterilization process.

Sterilization, as discussed in previous chapters, is mainly a probability of an absence of microorganisms, and therefore, using statistical methods when bioindicators are applied is unavoidable. Therefore, this chapter will discuss both items, the bioindicator itself and how data obtained from this analysis should be used.

Bioindicators are, in essence, standardized preparations of a specific microorganism with high resistance towards a specific sterilization technology (Sandle, 2016). The bioindicators are much more resistant than the typical bioburden, not just because of the type of microorganism, but also because of the load that is used for validation. The typical microorganism used for this purpose is basically spore forming bacteria that is prepared under certain conditions, regulated by the ISO 11138 or USP 55 (ISO, 2017; USP, 2020).

The type of bacteria to be used is very dependent on the type of technology used during the sterilization process. This dependency relies mainly on the mentioned resistance. For instance, for radiation technology, the European Pharmacopeia recommends the *Bacillus pumilus* or, for Dry Heat Sterilization, the *Bacillus atropheaus* is recommended. In the case of hydrogen peroxide, the Steam Sterilization reference is used, the *Geobacillus stearothermophilus,* which is the microorganism with the longest D-value on exposure to hydrogen peroxide according to published literature (Sandle, 2013).

The second important characteristic of the bioindicator is the number of microorganisms inoculated on a certain surface. The typical value for this population is $>10^6$, but other amounts can be used depending again on the technology and type of application. This artificial inoculation of such amount of population could eventually create the effect of clustering/clumping.

Finally, the type of carrier is also part of the characterization of the bioindicator. Mainly four formats are available commercially: strips, discs (Figure 34), suspensions (to be inoculated on any surface) and test tubes. The material of use is usually stainless steel, representing the most common component in both industries, pharmaceutical and food.

Figure 34 Bioindicator disc format

The statistical treatment of the bioindicators should be also discussed. The absolute sterility cannot be measured, and therefore, usually the already mentioned Sterility Assurance Level (SAL) is used. Reminding that term, basically to ensure sterility, 1 out of a million items could remain unsterile or even one in one million spores would remain in a specific surface. Then, this term, associated with the bioindicator itself, is part of the validation process. The bioindicator has a population of $>10^6$ (in most cases), to ensure that a certain logarithmic reduction is achieved. The fact of achieving 6 logarithmic reductions does not directly mean that sterilization is achieved in the system subject to the process. Both are different terms. Actually, to reach a SAL of 10^{-6}, already considered sterilization, the logarithmic reduction has to be equal to or more than 12 logs, starting from 10^6 (Table 6).

Table 6 Spore log reduction versus Log of microbial population for Sterility Assurance Level

Number of microorganisms	Log of microbial population	Spore log reduction (from original)
1.000.000	6	0
100.000	5	1
10.000	4	2
1.000	3	3
100	2	4
10	1	5
1	0	6
0.1	-1	7
0.01	-2	8
0.001	-3	9
0.0001	-4	10
0.00001	-5	11
0.000001	-6	12

So, the question would be how to measure 0.000001 microbial population. There are different methods to validate sterility (achieving 12-log reduction) using bioindicators. In this case, the overkill method will be discussed. The overkill method relies on the linearity of the deactivation model (considering the D-value), doubling the time or gas concentration exposure required to inactivate the microbial population in 6-log.

Then sterility process could be validated by this method. However, the issue would be how to count this logarithmic reduction using a “digital” answer. The way the bioindicators are evaluated, does not allow to do the counting. Basically, the BI is placed after sterilization in a culture medium and is incubated to an optimal time and temperature to recover the surviving spores. Therefore, no matter the surviving spores, if there is a remaining load capable of procreating, then a positive will be faced.

For instance, to evaluate the sterility after disinfection a statistic method has to be applied. A well-known method in microbiology is the Most Probable Number (MPN), which uses a series of dilutions to the extent that only a small proportion of the samples has a positive growth. The statistical basics of the MPN are founded in the appliance of a Poisson distribution of the samples.

The Poisson distribution is often used to model rare events. In the present case, the number of tubes showing growth in a diluted solution (otherwise, the number would be too high to fit the distribution proposed). Equation 15 shows the main components of the distribution.

$$p(x,\lambda) = \frac{e^{-\lambda}\lambda^{x}}{x!}$$

Equation 15 Poisson distribution

Where λ is the shape parameter which indicates the average number of events in a given time interval, and the x is the probability of finding the rare event. If the mean is too high, > 20, then Normal distribution should be applied. However, if too small, a discrete

treatment would better fit in the model (Halvorson and Ziegler, 1933; Montgomery and Runge, 2015). Figure 35 shows how to count throughout the MPN, applying a discrete distribution to a continuous one.

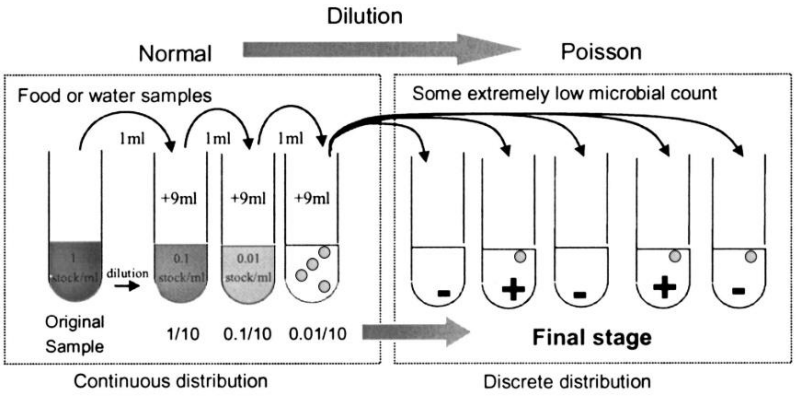

Figure 35 Classic procedure of MPN (Maiti and Bidinger, 1981)

Halvorson et al (1932) proposed Equation 16 to calculate the MPN, applying the Poisson distribution (Halvorson and Ziegler, 1933):

$$MPN = \ln \frac{n}{q}$$

Equation 16 Most probable number – Halvorson (Halvorson and Ziegler, 1933)

Where n is the number of replicates of a certain position and q is the number of positive growths.

With the MPN calculated, the exercise to get the Logarithmic Reduction (LR) of a particular process is dependent on the initial population. As an example, if a population of 1.6 x10^6, and three replicates are placed at position A, and only one out of the three replicates show growth, the LR would be still 6.597 applying this method.

It is clear then, that the validation process is not possible without an overall understanding of not just the physical-chemical process, but also consider the statistical approach of the microbiological answer.

4.3 ENGINEERING

As discussed previously, no matter the technology to be applied, the physical-chemical variables are part of the system and should be the basis of proper technology implementation. As commented in the introduction, the appliance methods are mainly three with many variations in between them. A summary of the different hydrogen peroxide technologies present in the market is shown in Table 7.

Considering previous concepts, it will now be easier to understand the principle of each of them. Every method will be reviewed considering the same previous theory:

Method 1: VHP (Vaporized Hydrogen Peroxide)

- Hydrogen Peroxide Formula: 30-35 % (w/w). Fewer stabilizers are added to ensure (food-semi-conductor hydrogen peroxide grade) reduction of residues in the system. It is common in vaporized systems, and no extra active ingredients are added.
- Thermodynamics: the system is not in equilibrium. It is overheated, and the solution is flash distilled to ensure all 35 % (w/w) vapour composition “goes” to the vapour phase.
- Evaporation process: Not limiting factor. There is no evaporation, unless in the distillation column.
- Absorption, desorption, diffusion: it is an important process. Once in contact with any material at a different temperature, the vapour phase would reach penetration and equilibrium. The penetration into the material would be higher.

To ensure the non-dynamic equilibrium, the system is continuously in motion. Recirculation or ejection are part of the process.

From the recipe perspective, the process should follow these steps:

1) Conditioning: The temperature and relative humidity (RH) of the volume to be decontaminated are in values of 30-35 ºC and 10-20 %RH.
2) Gassing: The concentration in gas phase of hydrogen peroxide is raised till the specified value. Usually, in the range of 800-1000 ppm.
3) Maintenance or dwell time: The concentration is maintained throughout injection to maintenance the specified level.
4) Aeration: The gas phase of hydrogen peroxide is reduced below 1 ppm.

With these steps, a dry system is claimed, where no condensation occurs, and only the gas phase of the chemical plays a role in the decontamination kinetics.

Method 2: HPV (Hydrogen Peroxide Vapor)

The principle of operation is the same than VHP, only that the following conditions are changed:

- Volume to be decontaminated is conditioned to higher %RH to promote a thin film of condensation in the surfaces to be decontaminated.
- For the same reason than previous statement, the volume to be decontaminated is conditioned to lower temperature.
- The gas phase concentration is not as high as previous system, as the dwell point is the main target. The concentration will be raised till saturation, and then wait for micro-condensation.

With this system a wet process is claimed, where condensation occurs, but in such a way that even if the deactivation is achieved, it is still gentle with the surrounding materials.

Method 3: Atomized Hydrogen Peroxide

- Hydrogen Peroxide Formula: 8-12 % (w/w). Stabilizers and other active ingredients are usually added to the formula to enhance the activity in deactivation.

- Thermodynamics: the system is in equilibrium. No extra heat or modification to the liquid phase is done. The vapour pressure limits the highest vapour composition that can be reached and is only function of the temperature.
- Evaporation process: it is a factor to be considered and might even be a limiting factor. Both the particle diameter and the temperature will be affecting when, the maximum vapour composition will be reached (particle diameter will not impact in the absolute value).
- Absorption, desorption, diffusion: none of these processes are as important as in other methods, but they still play a role. The absorption in the liquid phase is also possible. Although the penetration process is not as easy as with the vapour the absorption and desorption process should be considered.

There is a factor that was not discussed in previous methods, but that is a variable in the atomization process. It is the particle size and motion dynamics characterization within a certain system. The process intends to create particles that behave like the gas phase and that eventually reach every surface homogeneously.

From the recipe perspective, the process should follow these steps:

1) Injection: a validated volume of hydrogen peroxide is injected together with a stream of air. There is a gas phase that starts to raise and reaches, depending on the temperature, values in between 100 to 300 ppm.
2) Dwell time: no extra hydrogen peroxide is injected. It is only a time of exposure of the microorganism to the sterilant.
3) Aeration: the gas phase of hydrogen peroxide is reduced below 1 ppm.

Table 7 Main characteristics of the different hydrogen peroxide technologies present in the market.

	VHP (Vaporized Hydrogen Peroxide)	**HPV (Hydrogen Peroxide Vapour)**	**ionHP (Ionized hydrogen peroxide)**	**ionHP+ (Ionized Hydrogen Peroxide plus)**
Manufacturer	Steris Corp	Bioquell UK Ltd	Azbil Telstar SL (OEM SterCo)	Azbil Telstar SL (OEM J collado, S.A.)
Patent	EP 0486623	US 7025932	US 6969487	Not patented yet
Main physical-chemical description	This technology fully relies on **the gas phase of the hydrogen peroxide solution**. This phase is promoted from the environmental conditions point of view as well as the injection point. There is a flash distillation of the solution to ensure a safe and homogeneous injection. Then, the RH and Temp are maintained in a condition that avoids condensation all along the surfaces. In closed environments, a recirculation is performed.	In this case, even though the gas phase is initially promoted, the **deactivation relies in the microcondensation effect** that appears when the hydrogen peroxide "sees" a colder temperature than its vapour pressure equilibrium value. The conditions RH and Temp are also adapted to this effect and in both cases are different from other technologies.	The ionHP technology relies on the **liquid phase (stable phase at environmental conditions)** of the **hydrogen peroxide and instantaneous plasma effect of an arc of 17.000 volts**. The technology claims to generate extra radicals with a more powerful oxidation effect that ends up in the fact of using lower hydrogen peroxide concentrations as well as the "no need" of promoting gas phase. Therefore, no conditioning would be required.	The ionHP+ technology is an evolution of the former technology, ionHP, **also relying on the liquid phase (stable phase at environmental conditions)**. In this case, due to the type of sterilant as well as the different atomization system (smaller particles), the arc is not required to achieve even more effective results. There is no need for conditioning and the oxidizing power is enhanced **by the friction generated at the nozzle as well as the additional ingredients in the sterilant solution** (mainly isopropyl alcohol). The system, in addition, gains simplicity and, therefore, robustness. Finally, the PID controllers (for fluids injection) and RFID system ensures a reliable and safe decontamination system.
Type of sterilant	Hydrogen Peroxide 30-35% w/w	Hydrogen Peroxide 30-35% w/w	Hydrogen Peroxide 7.5% w/w	Hydrogen Peroxide 7.9% w/w
Cycle conditions	1) Conditioning phase: RH 10-20% + Temp 30-35ºC 2) Ramp gassing: 5-6 g/min 3) Decontamination: 3-4 g/min 4) Aeration: 2-5 h Total cycle time > 5h	1) Conditioning phase: RH 30-40% + Temp 30ºC 2) Ramp gassing: 1-2 g/min 3) Decontamination: 1 g/min 4) Aeration: 2-4 h Total cycle time > 5h	1) Conditioning phase: No need for conditioning 2) Injection: 15-20 mL/m^3 (10 g/min) 3) Dwell time: No extra injection 4) Aeration: 1-2 h Total cycle time > 1h	1) Conditioning phase: No need for conditioning 2) Injection: 20-30 ml/m3 (5 g/min) 3) Dwell time: No extra injection 4) Aeration: 1-2 h Total cycle time > 1h

	VHP (Vaporized Hydrogen Peroxide)	HPV (Hydrogen Peroxide Vapour)	ionHP (Ionized hydrogen peroxide)	ionHP+ (Ionized Hydrogen Peroxide plus)
Type of validation	10^6 *Geobacillus stearothemophilus** Unknown extra validations of the system (the Sterilant complies with appliable EN)	10^6 *Geobacillus stearothemophilus** Unknown extra validations of the system (the Sterilant complies with appliable EN)	10^6 *Geobacillus stearothemophilus** Unknown extra validations of the system (the Sterilant complies with appliable EN)	10^6 *Geobacillus stearothemophilus* 10^6 *Bacillus atropheaus* 10^6 *MRSA* 10^6 *ListeriaWith deactivation kinetics* of the dual system (Sterilant plus injection)
Deactivation kinetics	**Max of 1000 ppm** are reached and in contact with the microorganisms. The gas phase is in theory the only phase acting as a decontaminant and therefore it is expected longer exposure times. Exposure time for a 6 log reduction > 1h	**Max of 500-600 ppm** are reached and in contact with the microorganisms but then the liquid phase would condensate (considering equilibrium) at concentrations > 50% Exposure time for a 6 log reduction > 0.5 h (once system conditioned and injection is finished)	**Max of 150-300 ppm** during exposure are reached and in contact with the microorganisms but then main actor in deactivation is the liquid phase. Micro droplets are generated moving in the atmosphere as an air fluid. Exposure time for a 6 log reduction 30-40 min	**Max of 150-300 ppm**. Droplets are smaller, <5 microns and the particles completely follow the gas phase. Distributions is enhanced. 120.000-140.000 ppm reach the microorganisms and quicker deactivation is reached. Exposure time for a 6 log reduction 30-40 min considering worst conditions. Deactivation experiments show a nonlinear D-Value, reaching a full deactivation in 15 min in ideal conditions.
Advantages	1) Good distribution of the gas phase 2) If homogeneous temperature, no condensation - better materials compatibility	1) Good distribution of the gas phase 2) If homogeneous temperature, no condensation - better materials compatibility	1) Shorter turnaround cycles 2) No need for conditioning 3) Oxidizing power enhanced by the arc 4) Gentle with materials 5) Sterilant 7.5%	1) Shorter turnaround cycles 2) Simpler design, increased robustness 3) Oxidizing power enhanced by particle size and solution 4) Distribution enhanced by pulses and smaller particle size 5) Sterilant 7.9%+ 6) No need for pump calibration. PID control. 7) RFID for traceability (lot, expiration date)
Disadvantages	1) Dependant on the good distribution of temperatures. If not homogeneous, then different kinetics will be reached 2) Materials compatibility - High HP %w/w 3) High cost 4) Sterilant 30-35% HP - Corrosion and Logistics	1) Dependant on the good distribution of temperatures. If not homogeneous, then different microcondensation would take place 2) Materials compatibility - High HP %w/w 3) High cost 4) Sterilant 30-35% HP - Corrosion and Logistics	1) Distribution if not properly developed 2) Contained cost	1) Distribution if not properly developed

5 TELSTAR TECHNOLOGY DEVELOPMENT

5.1 FORMER TELSTAR TECHNOLOGY

Telstar used for several years an ionizing system that relied on an atomization nozzle and a voltage source to ensure decontamination. The approach is a modification of the atomization technology but with and extra ionizing system.

One of the main objectives of the thesis was to develop and characterize a decontamination system based on hydrogen peroxide for Azbil Telstar Technologies. When this investigation started, the system in use, was the SterCo's system (pseudonym of the licensing company due to confidentiality terms), which is a modification of method 3: Atomized Hydrogen Peroxide.

In the current section, an overview of the former system together with the first experiments will be done. It will allow a better understanding of the process and then being capable of evolving it. The former system is a patented technology, US7008592 (Sias et al. 2006).

The ionHP system was originally developed in 1999 by the Department of Defense of EEUU for biological warfare applications. The principle of operation is exactly the same as the Atomized Hydrogen Peroxide method, but, in this case, the liquid solution is forced to pass throughout a 17.000 V arc that theoretically enhances the system response. In the former system, in addition to liquid and air flow streams, a plasma arc supply was in place to ensure a proper ionization. The air and liquid flow streams were calibrated and expected to work repetitively after this process. No extra control over the injection pump was done. The pump was a dosing pump with a membrane system. The atomizing nozzle (Figure 36) provided by SterCo, did generate droplets in the 10-50 µm range, and the distribution was enhanced due to the ionizing effect. The nozzle position or the release valve was not considered in the design.

The hydrogen peroxide formulation counted with 7.5 % (w/w) hydrogen peroxide without specified extra active ingredients.

The system relied on the arc to ensure a proper distribution and inactivation process. The system was supposed to generate extra radicals that would remain active throughout the deactivation of the microorganism. These radicals would mainly come from the hydrogen peroxide solution and from the combination of it with air molecules, nitrogen and oxygen. The patent states that in addition to hydroxyl ions, others such as monoatomic oxygen (O^-) or nitrogen oxide ions would be generated and acting over the microorganism. The technology was used, as discussed initially, to combat biological warfare, and its appliance was designed to be a standalone system, not integrated into equipment of the pharmaceutical or food industries. The appliance was similar to the systems that are now applied against COVID-19 pandemic.

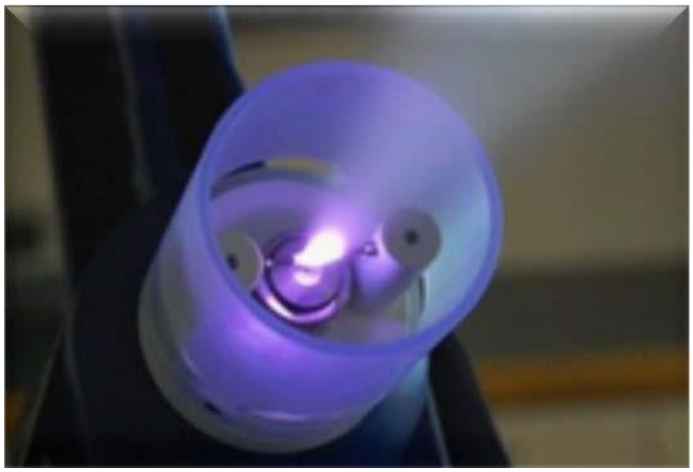

Figure 36 Ionisation nozzle acquired by Telstar

The main improvement areas of the system were related to the pharmaceutical requirements when applying a decontamination method. These requirements, already discussed during the Regulatory and Application chapters, can be summarized as follows:

- After a risk analysis, critical points are identified, and a known microorganism burden is applied. Then, the cycle development is done to achieve the target decontamination efficiency, usually a Sterility Assurance Level of 10^{-6} (probability of not more than one viable microorganism in an amount of one million).
- Parametric release after development and validation. The system has to ensure that the same circumstances are repeated each time the process is carried out. These circumstances are previously validated in the Process Qualification.
- The system has to be seen as a whole; this means that the design of the decontamination system has to consider the area where it will be applied.
- The solution has to be regulated and approved by the European Chemical Agency and registered as a Biocide according to the BPR.
- Any change in the design of any component has to be traced and documented according to the cGMP.

Considering these requirements, it will be easier to understand how events related to the robustness of the arc supply, non-controlled repetitiveness in the injection, or homogeneous supply of the sterilant, made Telstar be convinced of the need for a better assessment of the capability of the technology in use as well as integrate the knowledge of the process into the company.

The technology assessment was focused on analysing the most important variables affecting the process and evaluate the need for ionization.

5.2 STERCO's TECHNOLOGY EVALUATION

5.2.1 OBJECTIVE

This experiment aimed to evaluate the effect of different environmental and process variables over the ionized hydrogen peroxide technology treatments. The microbial lethality of *Geobacillus stearothermophilus* using commercial bioindicators was measured and correlated to the main identified variables.

5.2.2 MATERIAL AND METHODS

1) Main variables selection

The first selection of variables was done according to the previously discussed physic-chemical variables and the need to understand the impact of the ionisation process over microbial deactivation.

1) Dwell time (A): Time (minutes) of exposure of hydrogen peroxide over the microorganism. It is the time between the end of the injection of hydrogen peroxide into the system and the start of the aeration.
2) Ionisation (B): 17.000 V applied to the air and liquid stream. Its value is constant, and the expected effect was already discussed. Increased oxidizing effect throughout the generation of extra radicals.
3) Degree of nebulization (C): mL per minute of hydrogen peroxide solution divided by the air litres per minute injected in the same stream. The atomization nozzle creates different particle size of the hydrogen peroxide solution, depending on this ratio. The higher the ratio, the bigger the particle.
4) Total injected hydrogen peroxide (D): Volume (mL) of hydrogen peroxide solution into the total volume to be decontaminated. The larger the value, the more particles will be introduced into the system.
5) Environmental Temperature (E): Enclosure temperature (ºC). The vapour pressure of the hydrogen peroxide changes with the temperature. As discussed, the higher the temperature, the larger gas phase would be present.
6) Environmental Humidity (F): Enclosure water content (%RH). The dew point of the hydrogen peroxide solution will be dependent on temperature and the degree of air saturation.

2) Experiment layout and material

The equipment used for the injection followed the principle discussed in the STERCO's technology (shown in the right hand of the Figure 37). The system was integrated into a laminar flow cabin, model Bioptima (sponsored by Telstar, Terrassa, Spain) (1) and the injection nozzle (2) was placed in the front of the cabin panel. A hydrogen peroxide monitoring sensor (Drägër, Northumberland, United Kingdom) (3) was placed in the middle of the area, and a temperature and humidity sensor (Sensor Push, New York, US) (4) was also incorporated within the volume. In addition, to raise the temperature and environmental relative humidity, a heater and a water spray were used.

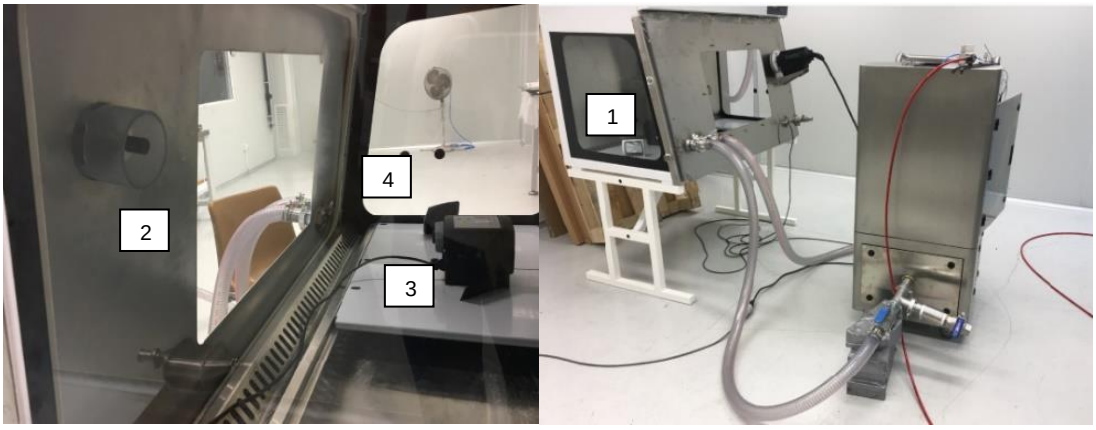

Figure 37 Equipment layout and injection system. 1) Laminar flow cabin, 2) injection nozzle, 3) Hydrogen peroxide monitoring sensor and 4) Temperature and humidity sensor.

3) Microbiological analyses

A series of bioindicators were placed into the system to understand the system's answer when varying the previous variables. A set of three bioindicators (BIs) with a bacteria population of 10^4, 10^5, and 10^6 spores/coupon were used in each position. The microorganism as spore form was the *Geobacillus stearothermophilus*. The BIs were purchased to Mesalab, Inc (Chassieu, France). These BIs were manufactured following the ISO 11138. After the decontamination process, the survival of the microorganism was evaluated putting the bioindicators into tubs with Releasat® Purple media (Mesalab, Chassieu, France), a specially formulated soybean casein digest culture medium containing the pH indicator Bromocresol Purple. Test results were obtained after incubation at 55 ºC for 24-48 h, and observing the medium colour change (from purple to or towards yellow and/or turbid) if any spores had survived the process.

The BIs were placed in different positions inside the cabin, as shown in Figure 38.

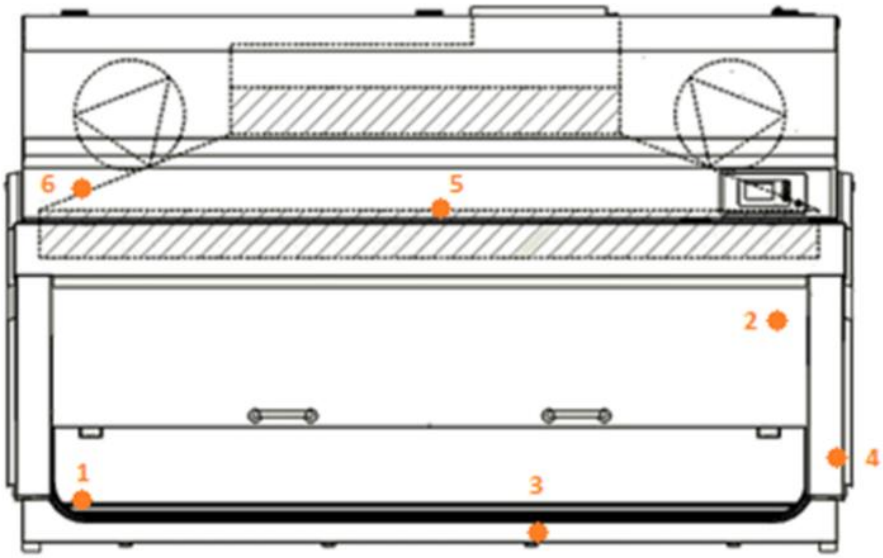

Figure 38 Bioindicators position layout into the cabin (Front image)

4) Statistical analysis

To better understand the impact of the input variables over the uncontrolled or answer of the system, an optimization method called Taguchi was used (Taguchi, 1993). The method was chosen due to the large number of variables identified and because the interaction between them appeared to be important (Table 8). The selected variables and levels were:

- Dwell time (A): 4 levels, ranging from 20 to 50 min. Previous experience showed that 30 min of dwell times already showed complete inactivation.
- Ionization (B): 2 levels, arc, and no arc (ionization).
- Degree of nebulization (C): 2 levels of nebulization ratio, smaller particles (1 mL/min of hydrogen peroxide solution and 9.5 L air/min) and larger particles (mL/min of hydrogen peroxide solution and 7.5 L air/min). The equipment in use only allowed to work in these ratios.
- Total injected hydrogen peroxide: 2 levels of injected hydrogen peroxide into the system (mL/m^3)
- Temperature (E): 2 levels of temperature (Ti), Max (> 50ºC) and room conditions (20-25ºC) Increasing or decreasing the gas phase in equilibrium.
- Relative humidity (F): 2 levels of relative humidity (RHi), Min < 30% and environmental conditions > 40%.

5.2.3 RESULTS

Regarding the physical-chemical aspects that took place during the treatments, it was observed that the fog generated at high temperatures was invisible. Once injected, the liquid drops were directly evaporated. In this case, the equilibrium was reached faster and favoured a higher hydrogen peroxide gas composition. Consequently, the maximum gas concentration measured in high temperatures overpassed the highest sensor limit, and therefore only 300 ppm were continuously measured.

Regarding microbiological lethality, the surviving fraction of *G. stearothemophilus* in the Bioindicators after treatment was lower, as expected, in the Bioindicators with a population of 10^4, 64 out 96 were inactivated, (66%), versus 59/96 in BIs with 10^5 (61.,4%) and only 46/96 in BIs with 10^6 (48%) (Table 8).

Table 8 Physicochemical variables of different assays and surviving of G. stearothemophilus (No growth/Positive growth in bioindicators) after treatment with hydrogen peroxide using STERCO's system

Assay	Physical-chemical variables						No growth*		
	Dwell Time (min)	**Ionisation**	**Ratio (liquid/air)**	**Concentration (mL/m^3)**	**Ti (°C)**	**RHi (%)**	**BI 10^4**	**BI 10^5**	**BI 10^6**
1	20	ARC	1/9.5	20	> 50	< 30	4/6	3/6	2/6
2	20	ARC	1/7	30	20-25	> 40	5/6	5/6	4/6
3	20	NO ARC	1/9.5	20	> 50	< 30	4/6	5/6	0/6
4	20	NO ARC	1/7	30	20-25	> 40	3/6	4/6	5/6
5	30	ARC	1/9.5	20	20-25	> 40	4/6	2/6	5/6
6	30	ARC	1/7	30	> 50	< 30	6/6	4/6	2/6
7	30	NO ARC	1/9.5	20	20-25	> 40	2/6	3/6	2/6
8	30	NO ARC	1/7	30	> 50	< 30	4/6	6/6	4/6
9	40	ARC	1/9.5	30	> 50	> 40	4/6	3/6	1/6
10	40	ARC	1/7	20	20-25	< 30	4/6	4/6	2/6
11	40	NO ARC	1/9.5	30	> 50	> 40	4/6	3/6	3/6
12	40	NO ARC	1/7	20	20-25	< 30	5/6	4/6	4/6
13	50	ARC	1/9.5	30	20-25	< 30	5/6	4/6	4/6
14	50	ARC	1/7	20	> 50	> 40	3/6	3/6	4/6
15	50	NO ARC	1/9.5	30	20-25	Min	3/6	3/6	2/6
16	50	NO ARC	1/7	20	> 50	> 40	4/6	3/6	2/6

* No growth (No growth BI/total BI) with a population of spores de *G. stearothermophilus* of 10^4, 10^5 and 10^6

Moreover, the worse locations in terms of inactivation of *G. stearothermophilus* were the positions 5 and 6 (data not shown), where the hydrogen peroxide in the liquid phase did not reach the positions in the same manner.

To understand the contribution of each factor, Taguchi's method (Taguchi, 1993) with 4 levels in factor Dwell time, and two levels in the rest of the factors were used. Also, the interaction between the factors Dwell time (A) and Ionization (B) was studied, and the Ionisation factor (B) with the rest of factors. The focus was placed on understanding the effect of ionisation and its interactions.

Therefore, 15 degrees of freedom were considered. In addition, to simplify the calculation and analyse the weight of the factors in the final answer of the system, only the results obtained with BIs with a population of 10^6 were considered.

The calculated contributions (%) in the lethality of *G. stearothermophilus* for each of the variables and interactions are summarized in Table 9. As can be seen, the temperature was the most relevant factor (23%). However, the contribution of the arc to the inactivation process shows that, alone, it is insignificant compared to the other variables of the process. The total contribution of this factor (0.94%) to the system's response, already directs the next developments towards the research and better control of other variables. It is particularly interesting to see that the larger the total injected hydrogen peroxide, the better efficacy is obtained only when the arc is not activated. Though, when the arc was activated, lower levels of total injected hydrogen peroxide were preferred. In addition, the ratio of liquid/air, and therefore the particle size, did not play an important role when the arc is activated. However, if the arc was deactivated, the ratio clearly affected the lethality of *G. stearothermophilus*. In this case, the system response improves when the particle size becomes larger.

Table 9 Factor contribution (%) to the system's response to obtain a lethality of 10^6 (6 logs) *according to Taguchi's method.*

FACTOR/S	CONTRIBUTION (%)
Temperature (E)	23.44
Ionization-Concentration (BD)	15.00
Degree of nebulization (C)	15.00
Ionization- Degree of nebulization (BC)	15.00
Dwell time-Ionization (AB)	10.31
Relative humidity (RHi) (F)	8.44
Dwell time (A)	6.25
Concentration (D)	3.75
Arc/No arc (B)	0.94
Ionization-Temperature (BE)	0.94
Ionization/Relative humidity (BF)	0.94

5.2.4 DISCUSSION AND CONCLUSIONS

Unger-Bimczok et al. (2008) suggested that the temperature and relative humidity play a key role in the lethality process caused by hydrogen peroxide. They demonstrated that the higher the micro-condensation (larger humidity and lower temperatures), the D-value would be smaller. In these experiments, it has been confirmed the high impact of the temperature over the lethality of the process, and how high values of this factor could reduce the microbial efficacy, by decreasing the micro-condensation rate, and reducing the total particle volume (Table 8). In this sense, it is important to consider that in the maximum level of temperature (> 50 ºC), having the gas phase promoted, and the reached ppm level being high (> 300 ppm), it was not enough to inactivate the high populated bioindicators.

However, and still at high temperature levels, complete inactivation was obtained in low populated bioindicators (10^4), and hidden positions such as the position 5 (above the filter), showed the best results at this condition (75% of inactivation in BI 10^5) (data not

shown). This fact confirms that the application of hydrogen peroxide promoting the gas phase, would be a good option when hidden areas should be reached and a more homogeneous distribution of the biocide is required (Chen and Chen, 2010; Davies et al., 2011; Linley et al., 2012).

Another important conclusion is related to the effect of ionization. The most significant result was related to this variable's low contribution (or relevance) in the microbial lethality (Table 9). The low effect of the ionization process can be related to the ions' lifetime when no continuous plasma is promoted. The ions would have a lifetime of milliseconds (or even microseconds) if no continuous energy is maintained (Attri et al., 2015). In contrast, the lethality process is in the range of minutes.

When analysing the relationship between other factors and ionisation, particle size showed one of the most important contributions in microbial lethality (Table 9). When the arc is not activated, the particle size variable (ratio liquid/gas) became important (Table 8). The assumption made at this point, is that while the ionization plays a role in the distribution, the degree of nebulization (particle size) becomes the main factor controlling the distribution and the interaction of the active compound to the spore when the arc was deactivated. Also, in accordance with Sandle (2013), it was observed that the variables, dwell time or concentration did not show a high effect in the lethality process unless analyzed together with other variables.

In conclusion, the parameter ionization (arc) could be discarded from the recipe, being more relevant to focus on other parameters as temperature, particle distribution and hydrogen peroxide concentration when developing the new technology.

5.3 ENGINEERING TELSTAR's TECHNOLOGY – ionHP+

Once the ionization of the previous system was discarded due to the results of the previous experiment, the development of the new system was mainly focused on three aspects: (1) automation and integration over a higher-level system, (2) particle generation and distribution (atomization), and (3) thermodynamics and formula understanding over the system's mass balance and microorganism inactivation.

Telstar's system, ionHP+ (name given during the development of the thesis), developed together with José Collado, S.A. (José Collado, Barcelona, Spain) during this investigation, is an atomization hydrogen peroxide technology that relies on the capability of particle distribution to ensure the decontamination. Also, there is a gas phase that achieves its maximum when the equilibrium is reached.

The development and characterization of the process allowed selecting not just components, but also to develop a way to create recipes to ensure the decontamination repetitively.

5.3.1 AUTOMATION AND INTEGRATION

The system is usually integrated into higher-level equipment (as discussed, Isolator technology or Passthrough box) that controls the decontamination system. Two Programmable Logic Controller (PLC) work together to ensure that the process follows the specified steps (Figure 39).

Both systems are usually the "container" to be decontaminated (a passthrough box, an STI or even a clean room), together with the decontamination system itself. Both systems should be characterized and coordinated to a ensure proper decontamination.

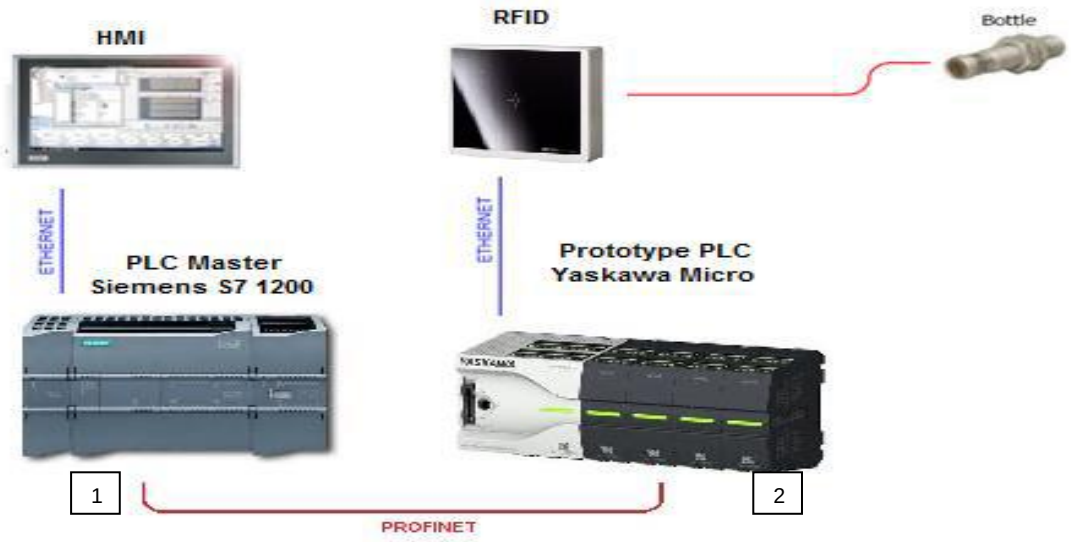

Figure 39 Telstar control system architecture. (1) PLC from the higher-level equipment and (2) PLC from the cold decontamination equipment

In Figure 40, both systems are graphically shown. The right side of Figure 40 describes the decontamination system, with each of the components (they will not be disclosed due to confidentiality terms) that would be integrated into the higher level equipment (left side). This equipment, with a volume that can vary between 0.5 m^3 and up to 20 m^3,

integrates the decontamination system and the relieving and filtering components (blue circles).

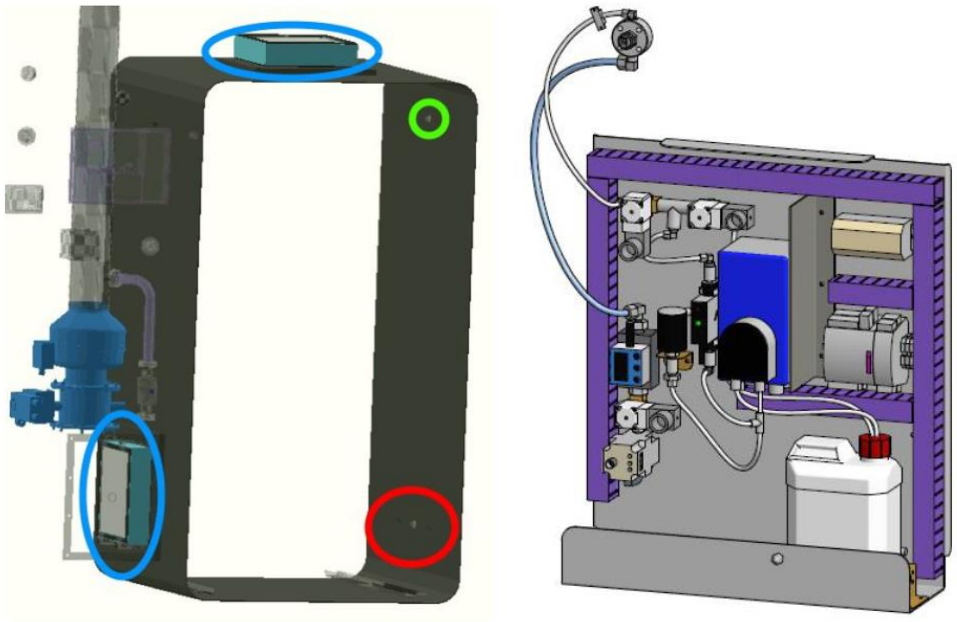

Figure 40 Passthrough box and Decontamination system ionHP+. Left-hand side a BioSAS with an exhaust and inlet filters (blue circles), one hydrogen peroxide nozzle (green circle) and one air nozzle (red circle. Right-hand side an atomization system formed by the control, injection and liquid components needed for the hydrogen peroxide process.

5.3.2 ATOMIZATION PROCESS

The atomization process intends, throughout a disturbance, to create droplets in the micro or even nanoscale from a liquid jet. The disturbances might be of a very different nature, and they can come from pressure or speed fluctuations, surface displacement or even temperature differences (Ashgriz, 2011). Figure 41 shows two types of disturbances by pressure difference. While the upper side of the image shows a non-uniform disturbance, the bottom side shows a homogeneous one.

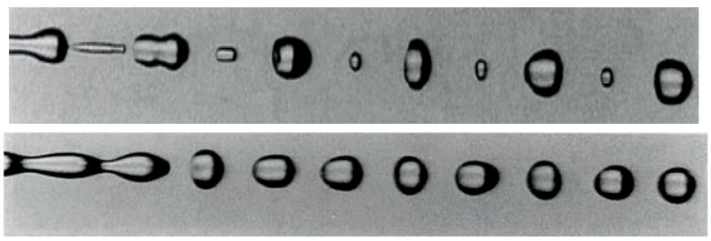

Figure 41 Two type of disturbances into the same liquid jet showing uniform and non-uniform generation (Ashgriz, 2011).

In the present investigation, the disturbance is done through a stream of air that directly interacts with a very high-speed liquid jet. This process is done in one of the most important components of the system, the nozzle. The nozzle (Figure 42), commercially available, can create a different disturbance depending on the incoming air and liquid flow that arrives to its entrance. This disturbance difference will impact not only in the particle size but also in the fog pattern that will be generated onwards. Figure 42, in

addition to represent the nozzle itself, also shows the main characteristics of the fog pattern. A and B represent the spray pattern's width at different distance from injection that can vary from 7.5 to 15.0 cm, and from 22.0 to 25.0 cm respectively. The total distance of spray projection (C) ranges from 1 to 3 m. These values are dependent on the ratio of liquid to air specified in the injection program.

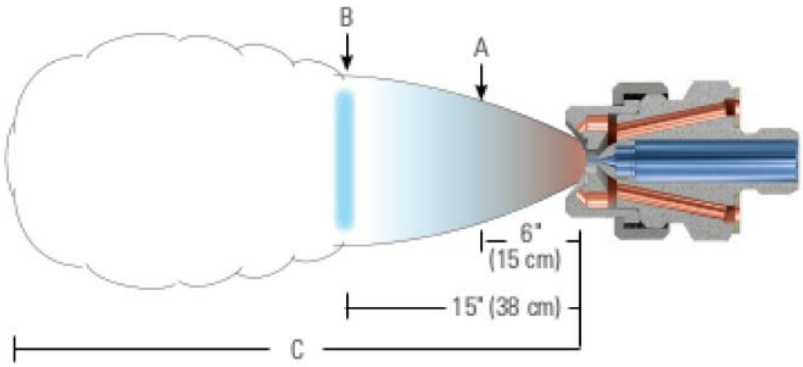

Figure 42 Nozzle graphical representation (A and B are spray pattern width and C is the total length)

The particle size can go from < 1 µm to up 10 µm and the jet size might vary from values of 50-100 mm in the largest side of the created ellipse and 10-50 mm in the smallest part. Figure 43 shows the created jet close to the nozzle position.

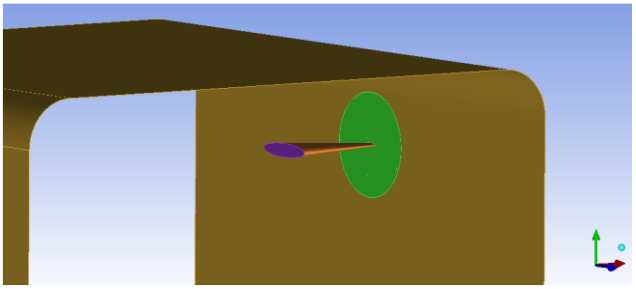

Figure 43 Created jet close to the nozzle position

Therefore, it is clear that air and liquid flow control into the system plays an important role. In microflows, the control of these parameters is done using a control PID (Proportional Integral and Derivative) tool provided by the PLC and two air and liquid flow sensors. Those sensors are the input variable to the PLC, and depending on the read value, the controller will manage to send a signal to the injection pump as well as to the air pressure regulator (the sensors, injection pump or even PLC specification have been part of the development. However, they are not disclosed in the present document due to confidential terms).

Then, once the particles have been created and they start to enter into the volume, the dynamics of the particle should be understood.

Firstly, assuming a monodispersed distribution of particles (and without the use of fluid simulations), meaning the same size for every particle, the total amount of particles injected e.g., in 2 min at a specific flow of 5 mL/min would be described in Table 10:

Table 10 Number of generated particles of each diameter and per second (and 120 seconds) at a dosing flow of 5 mL/min of sterilant of Hydrogen Peroxide

Diam. [µm]	Diam. [m]	Vol. [m3]	Mass [kg]	Flow [mL/s]	Num. Drops 1 s	Num. Drops 120 s
0.1	1.00E-07	5.24E-22	5.31E-19	8.33E-08	1.59E+14	1.91E+16
0.5	5.00E-07	6.54E-20	6.64E-17	8.33E-09	1.27E+11	1.53E+13
1	1.00E-06	5.24E-19	5.31E-16	8.33E-09	1.59E+10	1.91E+12
2	2.00E-06	4.19E-18	4.25E-15	8.33E-09	1.99E+09	2.39E+11
6	6.00E-06	1.13E-16	1.15E-13	8.33E-09	7.37E+07	8.84E+09
10	1.00E-05	5.24E-16	5.31E-13	8.33E-09	1.59E+07	1.91E+09

These number of particles are injected into a large volume where they would be dispersed into a continuous phase. In the particle motion characterization, two effects should be considered: dynamic conditions where the particle is following the air streams at high speed, and then, once the injection is stopped, the drop movement is more affected by gravity and intermolecular forces (depending on size). The position and dimension of the relief valve to control the volume pressure is a component also to be considered in the system when characterizing the distribution.

5.3.3 HYDROGEN PEROXIDE FORMULA

The hydrogen peroxide formula that has been used during the development is a solution commercialized by José Collado S.A. The solution main components are: 8% (w/w) hydrogen peroxide and 9.99 % (w/w) isopropyl alcohol. Other ingredients are not specified in the present investigation due to confidentiality terms.

5.3.4 HYDROGEN PEROXIDE THERMODYNAMICS

Once particles are characterized, a mass balance was done to aid in the understanding of the whole process. The characterization of the amount of liquid and gas phase present in an atomized technology applied in a known volume is the main target of the mass balance. As a consequence, an understanding of the effect of the temperature over the process will be assessed and will serve as a tool for proper recipe development.

Figure 44 shows a schematic diagram of the mass balance of the process, where *HP* refers to hydrogen peroxide and *Liquid phase* to the hydrogen peroxide that is injected into the system. *Vapor phase* refers to the gas phase that is generated till saturation is reached. The *Decomposition reaction* refers to the injected hydrogen peroxide that suffers a process of decomposition over time and the *Existing water* to the water in the form of environmental Relative Humidity (RH). This water can be present either in vapour or condensed phase. Finally *Vapour phase and Condensed water* refers to the Extra water that is added to the system via injection.

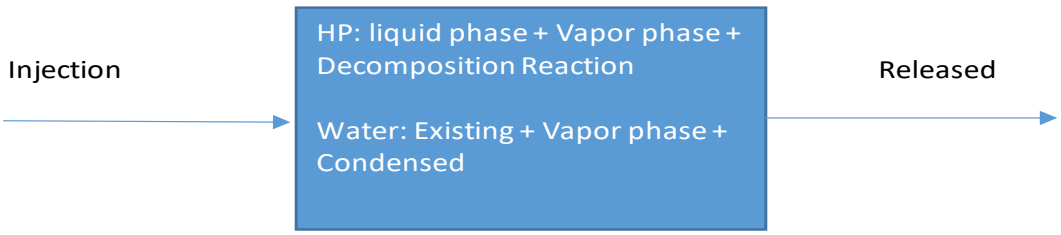

Figure 44 Mass balance hydrogen peroxide. Injection and released main streams into the system.

Therefore, a mass balance for each component of the system could be done. Below, the balance is already rearranged to understand what would remain for the decontamination:

Balance for water

$$nr(w)+ni(w)+ne(w)=no(w)+nc(w)+ng(w)$$

What remains?

$$nc(w)+ng(w)=nr(w)+ni(w)+ne(w)-no(w)$$

Balance for HP

$$ni(hp)=nr(hp)+nc(hp)+ng(hp)+no(hp)$$

What remains?

$$nc(hp)+ng(hp)=ni(hp)-nr(hp)-no(hp)$$

Equation 17 Mass balance water and hydrogen peroxide

Where each of the elements of the mass balance are:

- *nr (hp):* decomposed hydrogen peroxide.
- *nr (w):* water formed after hydrogen peroxide decomposition.
- *ni (hp):* injected hydrogen peroxide into the system.
- *ni (w):* injected water into the system.
- *nc (hp):* condensed hydrogen peroxide in the system.
- *nc (w):* condensed water in the system.
- *ng (hp):* gas phase of hydrogen peroxide in the system.
- *ng (w):* gas phase of water in the system.
- *ne (w):* existing water in the system.
- *no (w):* released water out of the system.
- *no (hp):* released hydrogen peroxide out of the system.

The objective is to get the quantity of gas phase and liquid phase remaining for the hydrogen peroxide at a specific temperature, *nc (hp)* and *ng (hp).*

With a system with the following characteristics:

- Volume to be decontaminated = 600 L

- Pressure = 101325 Pa
- Temperature = 293 K
- Releasing pressure = 400 Pa
- Injected hydrogen peroxide concentration = 20 mL/m^3

The following can be calculated:

1) Injection (*ni (hp)*): 0.028 mol (Table 11).

Table 11 Calculation of injected hydrogen peroxide in mols.

Parameter	Values
Solution HP[HP]	8 %
Density solution	1-014 g/mL
M(hp)	34 g/mol
M(w)	18 g/mol
Injection V	12 mL
Injection m	12.16 g
Injected HP	8 g
ni (hp)	0.028 mol

2) Decomposition of hydrogen peroxide (*nr (hp)):* 0 mol. It is assumed that no catalyser is present, and that the formula has enough stabilizers to ensure a constant biocidal activity.
3) Released hydrogen peroxide (*no (hp)):* 0.00069 mol. Assuming that all injected hydrogen peroxide remains in the gas phase till condensation occurs (saturation is considered the dew point). After 9 seconds of injection, all hydrogen peroxide will remain in the liquid phase. As per Figure 45, 2.4% of the hydrogen peroxide injected will be exhausted throughout the system. The vapour composition in function of time has to be calculated to estimate the total hydrogen peroxide lost throughout the relieving valve (Figure 45). It is not the same the potential loss at the beginning of the injection than at the end. With the use of the ideal gases law as well as the Boyle Mariotte law, and the technical specification of the relieving valve, the calculation can be performed.

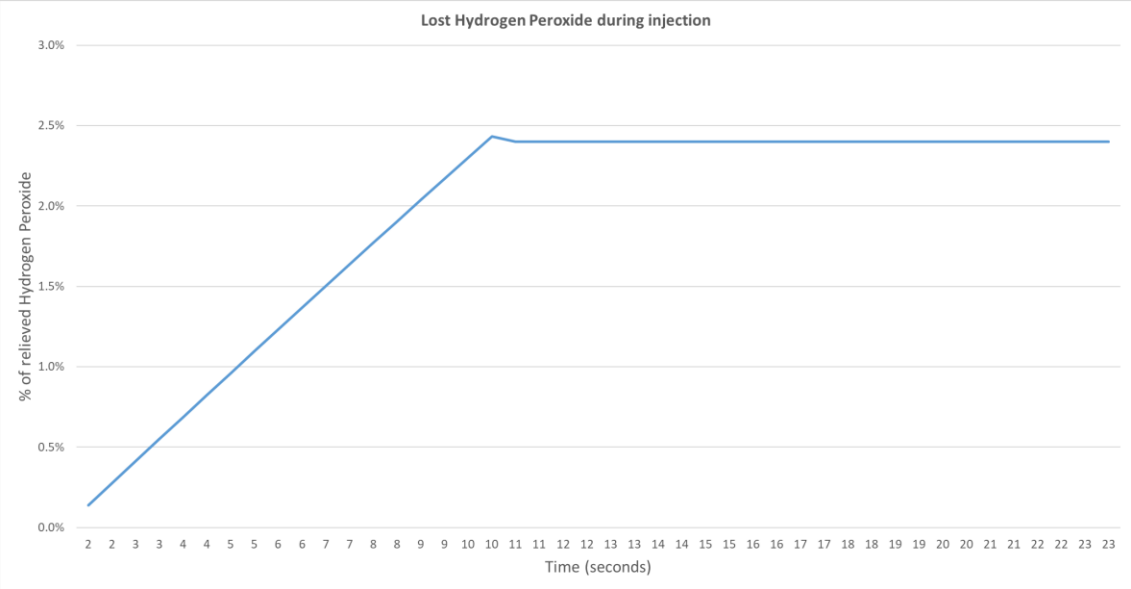

Figure 45 Hydrogen peroxide relieved throughout the pressure control system (after 9 seconds equilibrium is reached and no more hydrogen peroxide into the gas phase and therefore the vapor composition remains constant).

$$P \times V = n \times R \times T$$

$$P_1 \times V_1 = P_2 \times V_2$$

Equation 18 Ideal gases and Boyle Mariotte law

Where P refers to Pressure, V to volume, n to the number of mols, R ideal gases constant and T to Temperature.

Once the *no (hp)* and the *ni (hp)* are calculated (and assuming that no decomposition takes place), the last exercise would be to assess the proportion between the condensed and gas phase. Both values can be calculated considering that the equilibrium is reached. This means that hydrogen peroxide injected beyond the vapour pressure at the specified temperature will condense. The vapour composition will be given by the existing water content and the evaporated hydrogen peroxide. In this sense, the particular values for this exercise are:

4) Gas phase (*ng (hp)):* 0.00309 mol.
5) Condensed phase (*nc (hp)):* 0.02485 mol.

The system should reach 134 ppm in equilibrium at 293 K. This gas phase will be evenly distributed and fulfil the whole volume.

On the other hand, the rest of the hydrogen peroxide, in the form of particles, will remain in the liquid phase, first in motion due to the air stream and then in slow motion due to convection, diffusion and gravity forces.

Instead, if the temperature is raised, for instance, up to 10ºC, reaching 303 K, the maximum ppm level to be reached should be close to 280 ppm. If the temperature falls to up to 283 K, then the ppm level and therefore the gas available for deactivation will be in the range of 60 ppm.

It is important to understand this balance, as the remaining liquid phase is the one that will be distributed in the form of particles.

5.3.5 CONCLUSIONS AND NEXT STEPS

A prototype can be built considering the previous technical specifications.

The accurate control of air and liquid flows, the characterization and prediction of the available gas phase in each temperature, together with a proper understanding of the fluid and particle dynamics, can lead to a first prototype design. The integrated design should consider not only the hydrogen peroxide decontamination technology itself but also the volume or equipment where the system will be placed.

An analysis of all experiments related to the validation of the prototype will be done. Afterwards, a computational fluid dynamics (CFD) simulation will be performed to better predict the particle distribution, and then, this prototype will be tested from the microbiological perspective.

The microbiological analysis will have three main parts: one related to the variability of the microorganisms itself, a second, related to the impact of the particle reach and temperature over the previously identified inactivation models and a third one focused on the impact of the type of bioindicator in use when assessing the decontamination process kinetics.

6 TECHNOLOGY MODELLING - ionHP+

6.1 PROTOTYPE PERFORMANCE ANALYSIS

The development of the ionHP+, a technology that does not rely on the arc, was done in collaboration with Jose Collado S.A. The development process itself generated an important set of data in real conditions. In this case, there is no specific experimental design. The analysis was done by clustering and classifying data, with the main objective of gaining insights about the developed technology.

6.1.1 OBJECTIVE

This assessment aims to evaluate the impact of the different ionHP+ process variables over the generation of available gas phase of hydrogen peroxide and the microbiocidal activity. The ultimate objective is not just to understand the impact but also predict the behaviour of both variables by the analysis of the generated data.

6.1.2 MATERIAL AND METHODS

1) Process variables and microbiological analyses

More than 100 assays were performed for this study, of which up to 64 were selected to evaluate what variables and conditions were the most relevant. These assays were performed in three types of volumes of cabin (Figure 46).

Figure 46 Three volumes or benches used. Left hand: first prototype; Center: final prototype; Right hand: proof of concept of the new technology.

Again, the variables to be monitored and with expected impact over the process are the Degree of nebulization (Nr, air (L/min)/ hydrogen peroxide (mL/min)), the total injected hydrogen peroxide (mL/L of volume to de decontaminated), the environmental temperature (Ti, enclosure initial temperature in ºC) and the environmental humidity (RHi, Enclosure initial water content expressed as %RH).

On the other hand, the variables to be measured as an outcome of the process are the hydrogen peroxide gas phase and the microbiological efficacy. The hydrogen peroxide gas phase concentration (in ppm of hydrogen peroxide corresponding to 1.39 mg/m^3 (based on 34 g/mol and 25 ºC, 1 atm)) will be measured by the sensor Polytron 7000 (Dräger).

The Efficacy will be calculated as described in Equation 19:

$$Efficacy = \frac{BId}{BIt} \times 100$$

Equation 19 Efficacy of the hydrogen peroxide system

Where *BId* refers to the number of bioindicators with total lethality and *BIt* to the total number of bioindicators in the assay. The spore of use was a commercial BI of *Geobacillus stearothermophilus* acquired from Mesalab. The population of the bioindicators was in any case > 10^6 per coupon. The position of the BIs was always in the "open" area of the volume (not above the filter or similar hidden areas), and a maximum of 6 BIs per test were used. Microbiological analyses were performed as described in the previous chapter.

2) Statistical Analyses

The statistical analysis was done using the Minitab 18 (Minitab Inc. State College, Pennsylvania, US). One-factorial analysis of variance (ANOVA) was used to compare the lethality obtained after applying different treatments. The Tukey test was used to obtain paired comparisons among sample means. Also, frequency histograms were used to obtain the frequency distribution of microbial inactivation and hydrogen peroxide gas phase concentration after applying ionHP+ treatments. Finally, Regression analysis were used to model the hydrogen peroxide gas phase concentration in function of the different process variables (so-called "inputs"). Moreover, contour and surface plots were used for representing the processes with higher efficacy or gas phase concentration. In all analyses, *p* values < 0.05 were considered to be significant.

6.1.3 RESULTS

To discard the impact of having different test benches, a Tukey's range test was applied with 95% confidence individual intervals to ensure that all data was comparable. Results are shown in Figure 47, and as can be seen, no statistical differences were observed in the efficacy of tests applied on the lethality of the *G. stearothermophilus*. All of them showed high variability over the efficacy variable (output), but all of them crossed as well the zero, which is a signal, in the used statistical method, to discard significant variables in between the comparison.

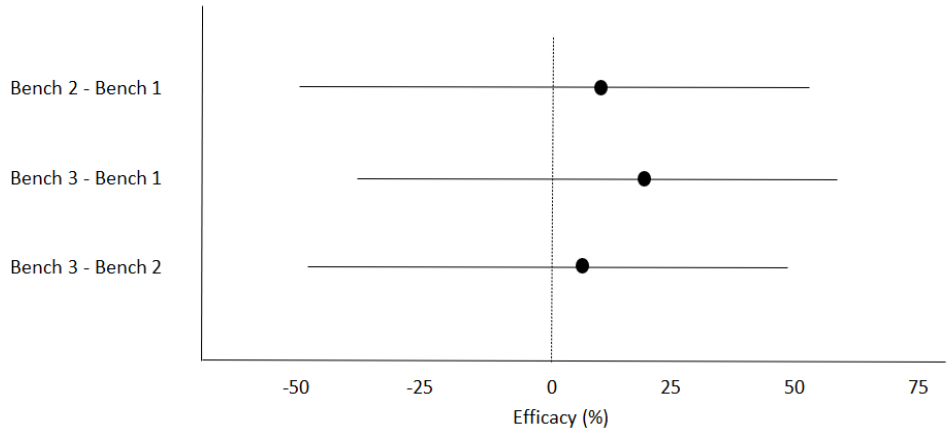

Figure 47 Tukey's range test for bench comparison on the lethality of G. stearothermophilus

Since no statistical differences were observed in between the test benches, a statistical analysis was carried out considering all available data. The histogram of both systems

responses (microbial efficacy and hydrogen peroxide gas phase concentration) showed that the efficacy value with higher frequency is clearly between 85-100% of inactivation (Figure 48a), and the ppm level registered with the highest frequency was between 91.75 and 161 ppm (Figure 48b). The average for both answers, microbiocidal efficacy and ppm level, was 83% and 140 ppm, respectively. In very few tests, and when the temperature was higher, the gas phase was >300 ppm.

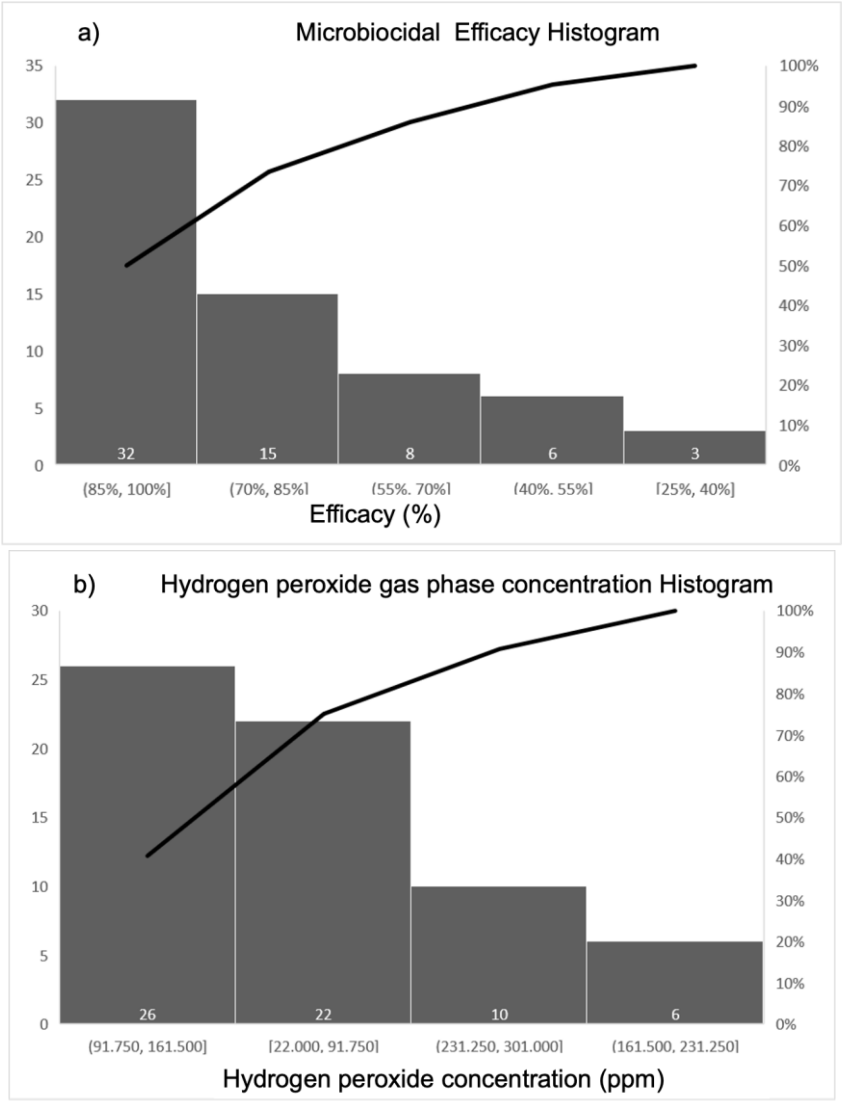

Figure 48 Histogram of both system answers: a) Efficacy (number of deactivated bioindicators/total of bioindicators, and b) hydrogen peroxide gas phase concentration (ppm).

Based on previous experience gathered with the decontamination system, two levels were defined for each input variable (temperature, relative humidity, Degree of nebulization and total of H_2O_2 injected). Considering these levels in the input variable, the answer on the efficacy is shown in Table 12.

Table 12 Mean ± standard deviation of different input levels on the microbiocidal efficacy (%).

Level definition of the input variables	**Input variables (Mean ± SD)**	**% Efficacy (Mean ± SD)**	**F value**	**p value**
High Temperature (≥ 25 ºC)	32.2 ± 9.9	77 ± 21	2.48	0.120
Low Temperature (< 25 ºC)	17.3 ± 3.4	88 ± 18		
High Relative Humidity (≥ 60%)	68.9 ± 7.4	81 ± 20		
Low Relative Humidity (> 60%)	44.1 ± 10.4	85 ± 22	0.05	0.832
High Degree of nebulization (≥ 10 l of air/mL H_2O_2/min)	17.7 ± 2.9	82 ± 22	0.06	0.804
Low Degree of nebulization (< 10 L of air/mL H_2O_2/min)	4.4 ± 4.6	84 ± 19		
High total injected H_2O_2 (≥ 0.02 mL H_2O_2/l volume)	0.024 ± 0.005	76 ± 26	3.26	0.076
Low total injected H_2O_2 (< 0.02 mL H_2O_2/l volume)	0.015 ± 0.00	86 ± 18		

The efficacy was higher than the mean, in values of low temperature, low concentration of H_2O_2, low nebulization ratio and low relative initial humidity. Besides, one-way ANOVA was applied for each independent variable and considering the discussed levels (Table 12), it was observed that even if none of the variables show a *p*-value below 0.05, there were clear differences between temperature and concentration, and the other two variables. Also, the F-value showed a higher value for these two variables, meaning that, the between-group variance is larger than the within-group one.

For this reason, one more level was added to evaluate the effect of the temperature variable (> 30 ºC, 20-30 ºC and < 20 ºC). Figure 49 shows an ANOVA for three levels of temperature. Significant statistical differences appear in between the extreme values (> 30 ºC and < 20 ºC). When comparing values with the intermediate level (20-30 ºC), no statistically significant results were obtained. Apparently, in lower temperatures, the inactivation was enhanced.

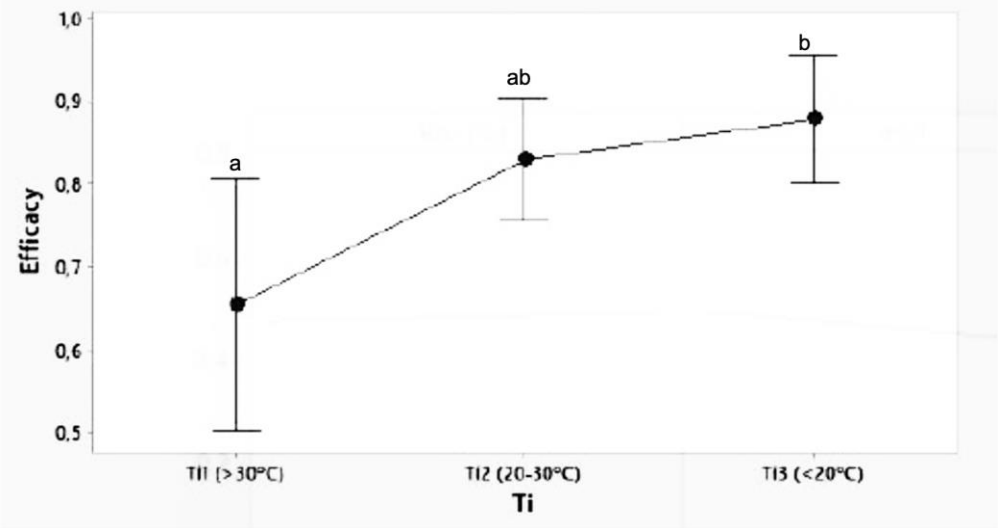

[a-c] Different letters indicate statistically significant differences (p < 0.05) between groups.

Figure 49 ANOVA for three levels of temperature

Even though, prediction models were applied for both answers, no significant results were obtained for the microbiological efficacy answer. Regarding the ppm of H_2O_2 level prediction, even if it could be theoretically calculated, the effect of the environment, absorption, diffusion etc., will impact the theoretical vapor pressure in equilibrium. However, a model presented in the Equation 20 was adjusted with a R^2 of 0.72 ($p < 0.05$). Figure 50 shows graphically the correlation between the predicted maximum gas phase and the real value.

$$ppm_{\max} = -25.6 - 1.091 x Rhi\ (\%) + 4203\ x\ \mathrm{mL}/l + 6.247\ x\ Ti\ (^{o}C) + 0.501\ x\ Nr$$

Equation 20 Max ppm level regression model

In the model, as Table 13 shows, the temperature and H_2O_2 concentration are the values with a lower *p*-value. In addition, their coefficients values and standard error show both their higher weight in the prediction model compared to the rest of the variables, and the higher precision in the estimation. The Variance Inflation Factor (VIF) value with a value higher than 5 would mean that the particular regression coefficient should be discarded. In this case, all of them are in between 1 and 5, showing a moderate correlation.

Table 13 Statistical coefficients of equation 19

Parameters	**Coefficient**	**Standard error**	**p-value**	**VIF***
Constant	-25.6	41.4	0.539	
RHi (%)	-1.091	0.474	0.025	1.24
Injection H_2O_2 (mL/l)	4203	1804	0.023	1.78
Temperature (º C)	6.247	0.848	0.000	1.78
Nebulization (Nr) (l air/ml of hydrogen peroxide)	0.501	0.971	0.608	1.17

*VIF: Variance Inflation Factor

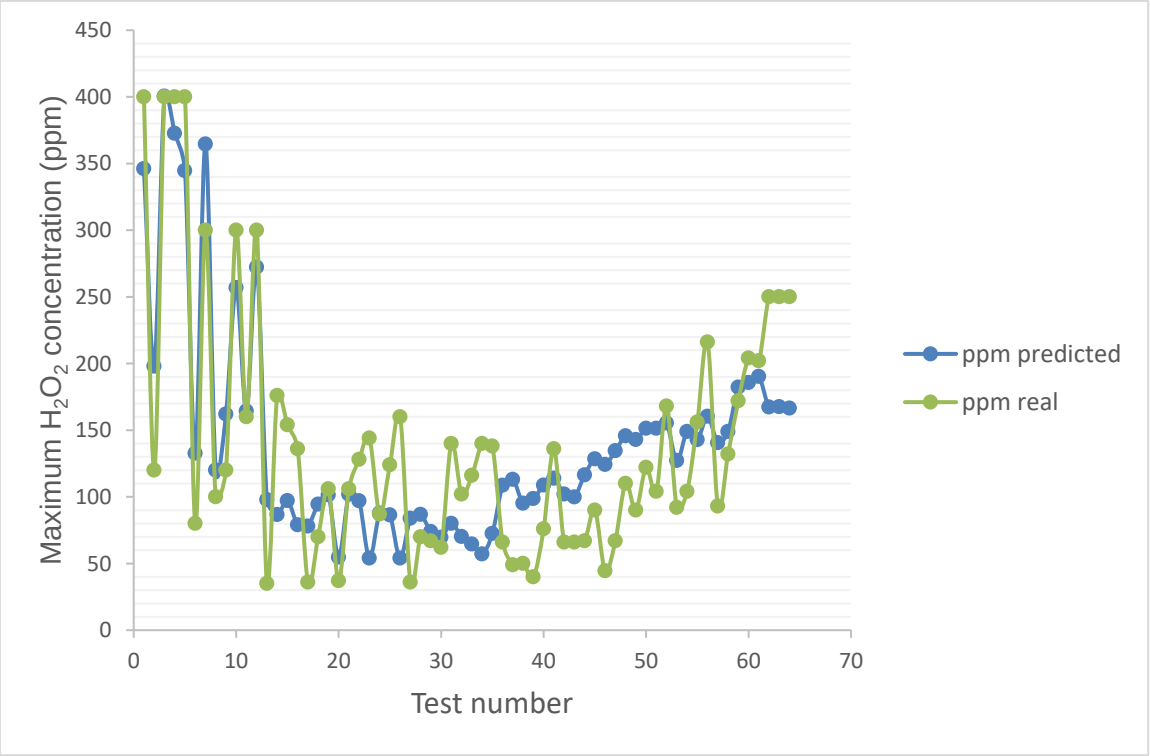

Figure 50 Predicted H_2O_2 concentration versus real ppm level

To correlate different operating variables, with the maximum hydrogen peroxide concentration and microbiocidal efficacy, Minitab visual analytical tools were used: contour and surface plotting. Results are shown in Figure 51, and it can be observed that the higher the temperature, the higher the ppm level of H_2O_2 reached in the system (Figure 51b). Also, it can be seen how the microbiocidal efficacy is again affected by temperature, especially at low temperatures (Figure 51c) and how the nebulization ratio did not show a significant effect on the microbiocidal efficacy (Figure 51d).

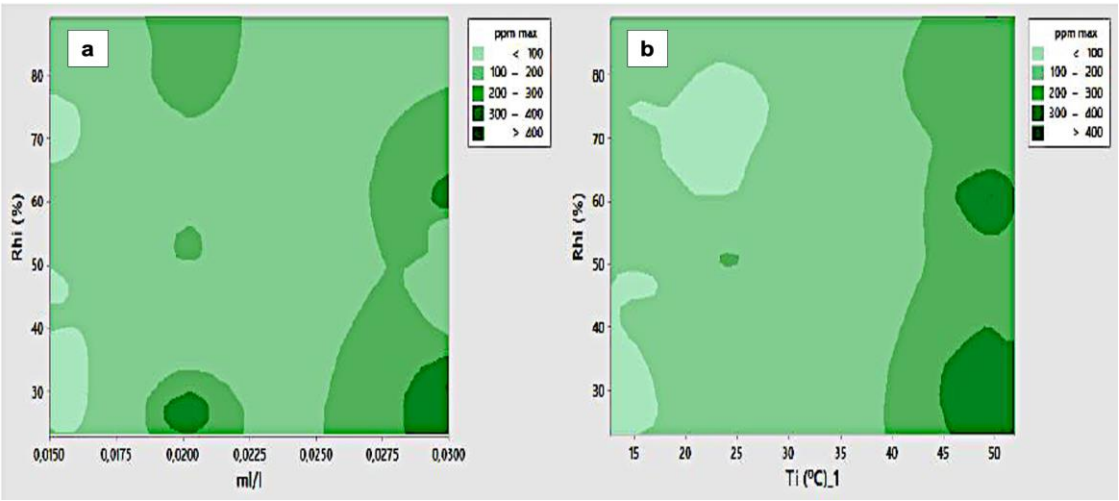

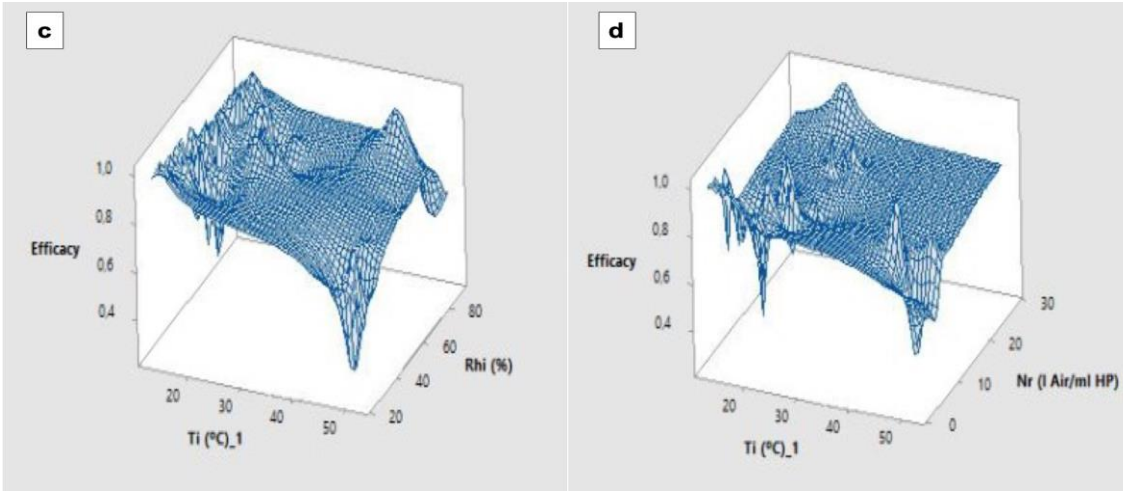

Figure 51. a) Contour plot of maximum concentration of H_2O_2 (ppm max) versus degree nebulization-Initial relative humidity and b) initial temperature-initial relative humidity; c) surface plot of microbial efficacy versus initial temperature-initial relative humidity or d) initial temperature-degree of nebulization.

6.1.4 DISCUSSION AND CONCLUSIONS

The evaluation of the relationship between the four variables of the system (degree of nebulization, initial temperature and relative humidity and hydrogen peroxide total injection) and how the system reacted measuring the two selected answers (gas phase of the hydrogen peroxide and the microbicidal efficacy) delivered valuable conclusions.

The temperature, directly related to the environmental saturation, showed a significant relationship with the available gas phase and the microbial efficacy. The larger the temperature, the higher the gas phase, reaching values over 300 ppm. The relationship was modelled for this particular environment, but it is important to consider that, as published by Ito et al., (2016) the material or the geometrical model of the volume will modify the available gas phase. On the other hand, it is important again to remark, that this higher gas phase concentration, was not related to a higher efficacy. In fact, this has been already reported by other author that concluded that while factors like hydrogen peroxide concentration had a high influence in the microbial inactivation effectiveness, the temperature (in high values) had a negligible impact (Kirchner et al., 2013). Lower temperature will clearly enhance the condensation, leading to a contact in between the microbial load and the hydrogen peroxide in a much more concentrated value. When the hydrogen peroxide solution (in the liquid phase) directly contacts a bioindicator, a 120,000-140,000-ppm concentration of hydrogen peroxide actuates over the microorganism. Consequently, the inactivation should be almost immediate. Whereas when the gas phase is involved, a maximum of 400-500 ppm can be achieved, so longer contact times would be required.

The initial relative humidity, also directly related to the environmental saturation, did not show an important influence. Initially, as proved by other publication, a higher initial relative humidity would have end in a higher condensation but less hydrogen peroxide availability in the gas phase and less microbial lethality (Møretrø et al., 2019). However, in this analysis, even if the gas phase was impacted in the same way than the previous study, the microbial efficacy did not show any influence. As there was not a controlling

system to adjust the relative humidity system during the process, the fact of starting at low or high Rh did not show a clear effect on the microbial efficacy response.

Finally, the nebulization ratio and the hydrogen peroxide injection variables showed no clear trend in the microbial effect. The gas phase was influenced by the injected hydrogen peroxide, but the microbial effect was not modified. How the particles are distributed, as well as how the amount of particle would impact the microbial result remain without a clear answer after this experiment. The hypothesis would be that the smaller particle size, the better homogeneity would be achieved. However, factors such as the geometrical volume, the release valve position, or the materials load, could lead to different results than expected.

6.2 PARTICLE GENERATION AND DISTRIBUTION

6.2.1 OBJECTIVE

During previous assessments it was clear that the particle generation process is key in the understanding of the technology.

Particle generation depends not just on the type of atomization nozzle but also on the air and liquid injection conditions. Furthermore, the way the nozzle is placed, as well as its relative position versus the air relief will considerably impact the main objective of the atomization technology: to reach a good distribution of the hydrogen peroxide in the liquid phase, similar to how it would be achieved in the gas phase.

The main objectives of this experiment were:

- Characterize the distribution of particles over different positions of the system to be decontaminated.
- Assess how the particle size impacts over its distribution in a specific volume.
- Assess the maximum distance between particles.

6.2.2 MATERIAL AND METHODS

A Computational Fluid Dynamics (CFD) software was used to predict how changes in certain parameters affect the behaviour of the fluids and the mechanical parts of equipment they interact with. Data analyses and further interpretation were performed together with Termo Fluids S.A., a spin-off of Universitat Politècnica de Catalunya (Terrassa, Spain). Up to 5.9 million volumes (mesh) were specified. Also, 256 Central Processing Units (CPU) and 5 days were needed for the simulation.

A single volume was studied, with a single position of the nozzle (model not disclosed) and a single position of the air relief. Figure 52 shows the passthrough box and position of the nozzle (blue circle) and relief valve (green circle).

Figure 52 Passthrough box for Computational Fluid Dynamics (CFD) simulation: Relief (green circle) and nozzle (green circle)

In addition, four stages were selected and studied. The stages were shorter in time than real conditions, but they were considered representative while computationally efficient:

- Injection phase: 2 minutes
- Exposition: 2 minutes
- Air pulse: 2 seconds
- Exposition: 2 minutes

Particle size was varied to understand the fluid phenomena under different sizes: 0.1, 0.5, 1, 2, 6 and 10 µm particle diameter. These sizes could be obtained by varying the air to liquid ratio. The ratio at this simulation was: 100 L/min of air and 5 mL/min of hydrogen peroxide solution. A dispersed multiphase flow was considered. A continuous phase (air) and a dispersed phase was formed by droplets of hydrogen peroxide. The carrier phase was specified incompressible, considering that the relief valve will always remain open.

The droplets were considered rigid spheres. About 150,000 droplets were injected for each particle diameter, so a total of 900,000 droplets were in the system. It is a very small fraction of the real conditions (0.0007% in 10 µm particle diameter). Still, according to the simulation, it was feasible and representative of the particle dynamics. No other processes such as evaporation, nucleation or heating were considered in the simulation. And every droplet that touched a surface was considered an adhered particle.

The working environmental conditions were:

- Pressure: 101,325 Pa
- Temperature: 298.15 K
- Air density: 1.184 kg/m^3
- Air dynamic viscosity: 1.84 x 10^{-5} Pa · s

The speed at the nozzle outlet was too high to be simulated (Figure 53), consequently, 15 cm from the nozzle was considered as the starting point of the simulation.

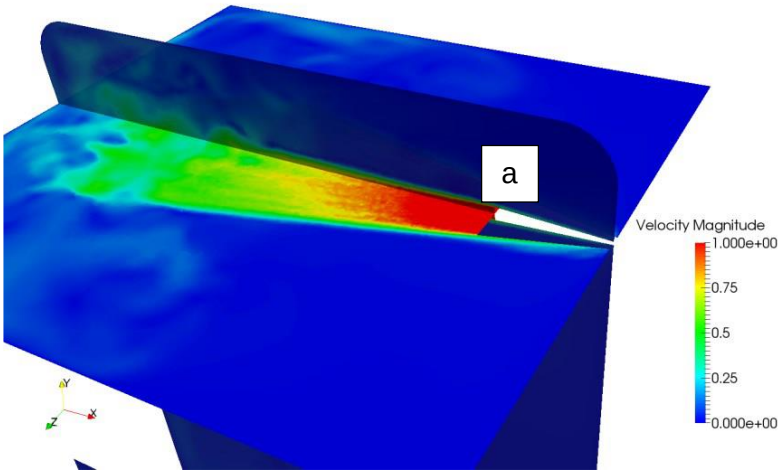

Figure 53 Speed characterization at the nozzle position in m/s. a) Starting position of the simulation

6.2.3 RESULTS

The instantaneous simulation results were stored every 0.25 seconds, aiming to study the dynamic evolution of the droplets within the pass-through box. The data saved for each time-step was related to the speed particle (m/s), and the position and the diameter was related to the colour (Figure 54). The simulation showed that the jet initially impacted against the opposite wall of the nozzle to later create a recirculation vortex in the injection plane that makes the flow, and the droplets, move backwards. The droplets also began to move downwards close to the front wall. Due to their inertia, some droplets got in contact with the wall and stuck to it (stuck particles are represented by red colour) (Figure 54).

Moreover, due to the change in direction that is taking place in the doors' corners and in the spray plane, it could be appreciated that some droplets got stuck to the lateral's walls. After approximately 25 seconds from the start of the injection, the first droplets arrived at the exhaust, where the air relief system was placed. Also, at this moment, some droplets started to come in to the nozzle region. While the injection was active, this flow pattern remained constant, increasing the droplet concentration throughout the cabin. The stuck particles were mainly in the areas in front of the nozzle, roof and lateral walls close to this point (Figure 54).

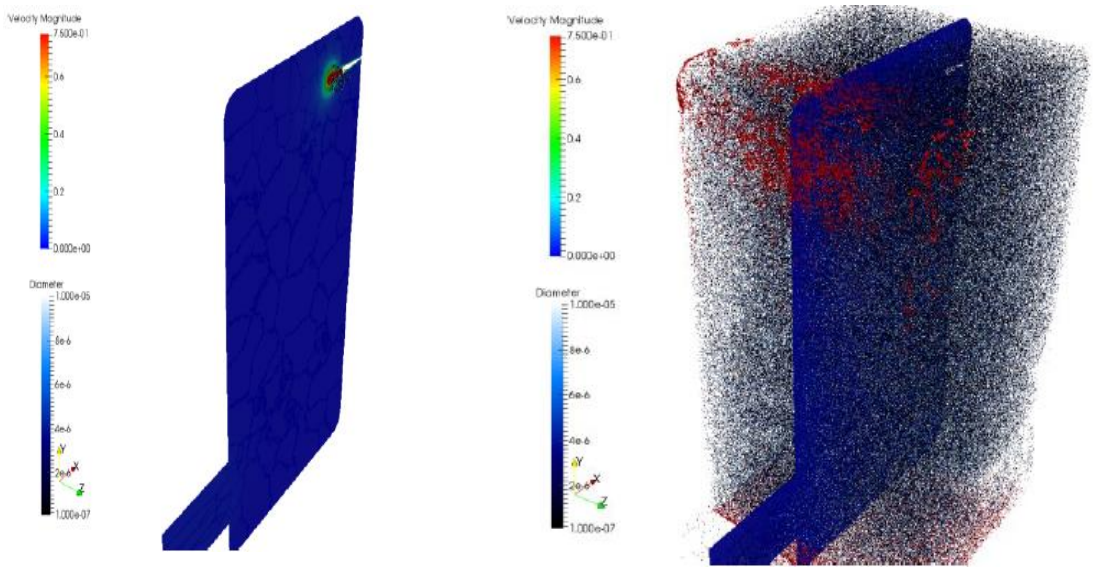

Figure 54 Computational Fluid Dynamics (CFD) simulation. Results after 0.25 sec (left) and after 125 sec (right).

To better assess the results, the cabin was divided into 80 quadrants (x, y, z). As shown in Figure 55, 4 levels on *x*-axis, 4 levels in *z*-axis and 5 levels in *y*-axis were done.

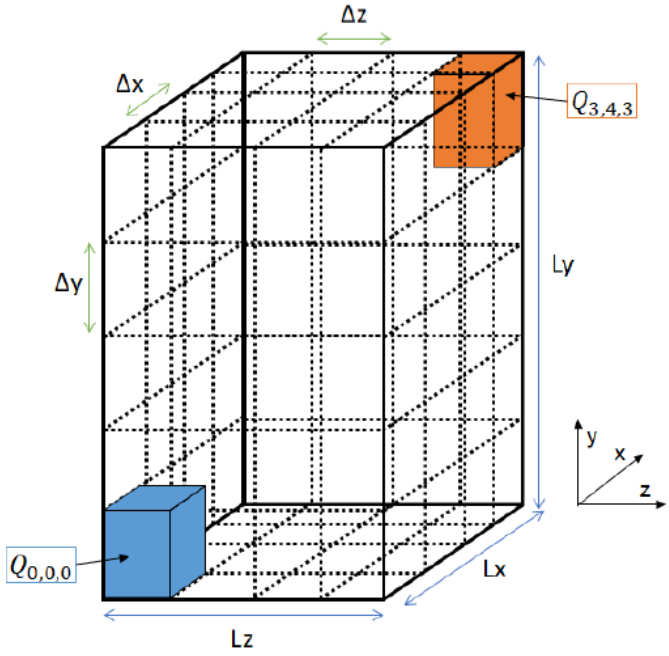

Figure 55 Quadrants division of the BioSAS. Two quadrants are specified $Q_{0,0,0}$ and $Q_{3,4,3}$

The cabin regions with a lower droplet concentration were the bottom corners of the wall, where the spray nozzle was installed. Between 0.6 and 0.5 % of the particles were in these quadrants just below the nozzle and close to the floor ($Q_{3,0,3}$). However, around 1% of particles would be present in quadrants where a more optimal distribution was obtained ($Q_{2,4,4}$) (Figure 56). Another observed effect (Figure 56) was the difference between particles equal to or above 6 µm and below this size. The particles below that size were not affected by gravity and could remain in suspension for a long time, likely, longer than the whole inactivation process.

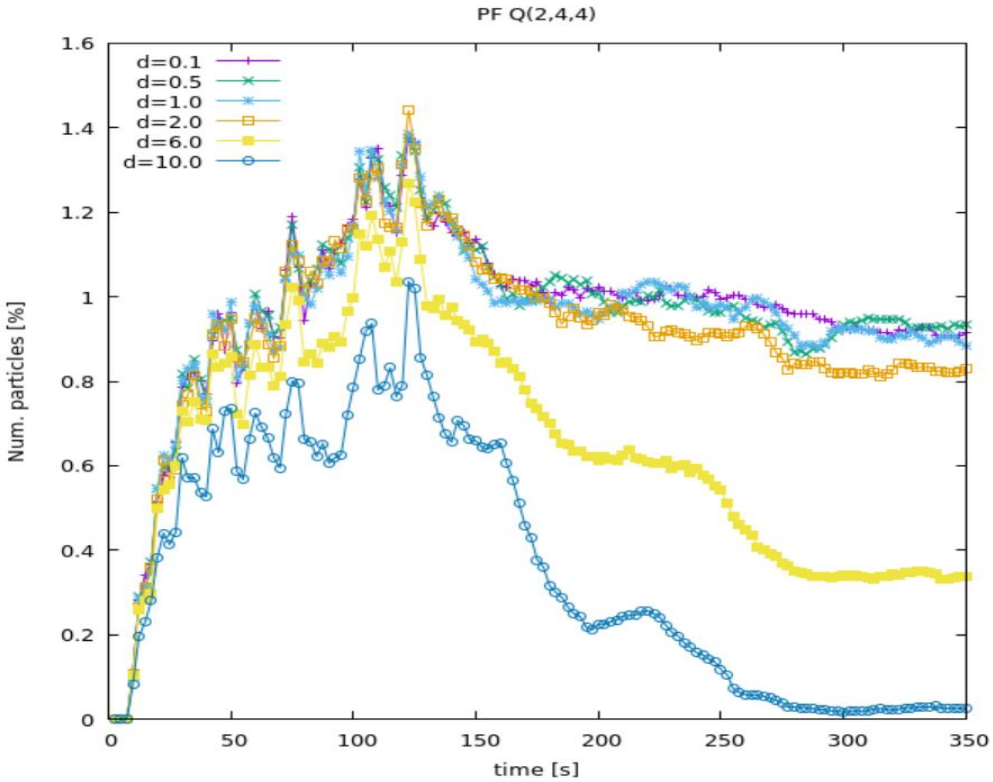

Figure 56 Number of particles (%) in function of particle size (d, μm) and time (s) in the quadrant $Q_{2,4,4}$ of cabin.

In terms of the adhered or stuck particles, approximately around 3% of all particles remained attached to the upper side of the walls (Figure 57a). In contrast, in the case of the bottom quadrants (Figure 57b), up to 25% of the particles of 10 µm diameter were deposited. If longer simulation time would be given, all particles in between 10 µm and 6 µm particles would probably contact the bottom quadrants.

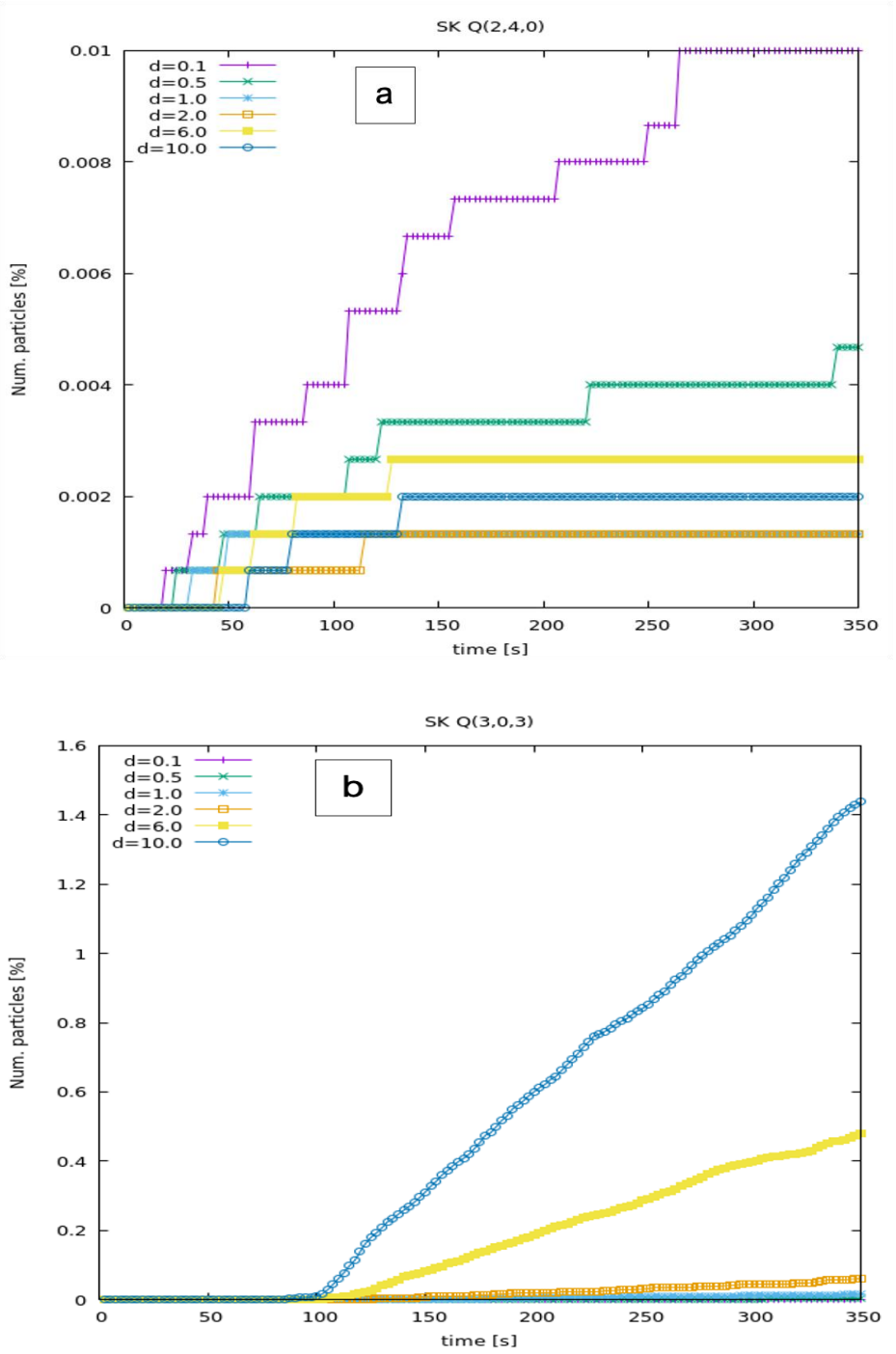

Figure 57 Stuck particles in function of particle size (d, μm) and time (s): a) upper side of the walls of the cabin ($Q_{2,4,0}$), b) bottom of the cabin ($Q_{3,0,3}$)

The particle size distribution differences are also visually explained in Figure 58. The initial distribution for all diameters was very similar, meaning that all of them tend to follow the flow streams (Figure 58a). However, particles of 10 μm, as was commented previously, were affected by gravity, while that effect was almost negligible in the lightest ones. Moreover, it can be seen how the droplets that followed the streamlines close to the cabin roof were the lightest ones. Only a few droplets tended to adhere to the roof of

the cabin, while no droplet of 10 µm was attached to the roof (Figure 58b). The air pulse effect was appreciable just in a very limited space of the decontaminated cabin.

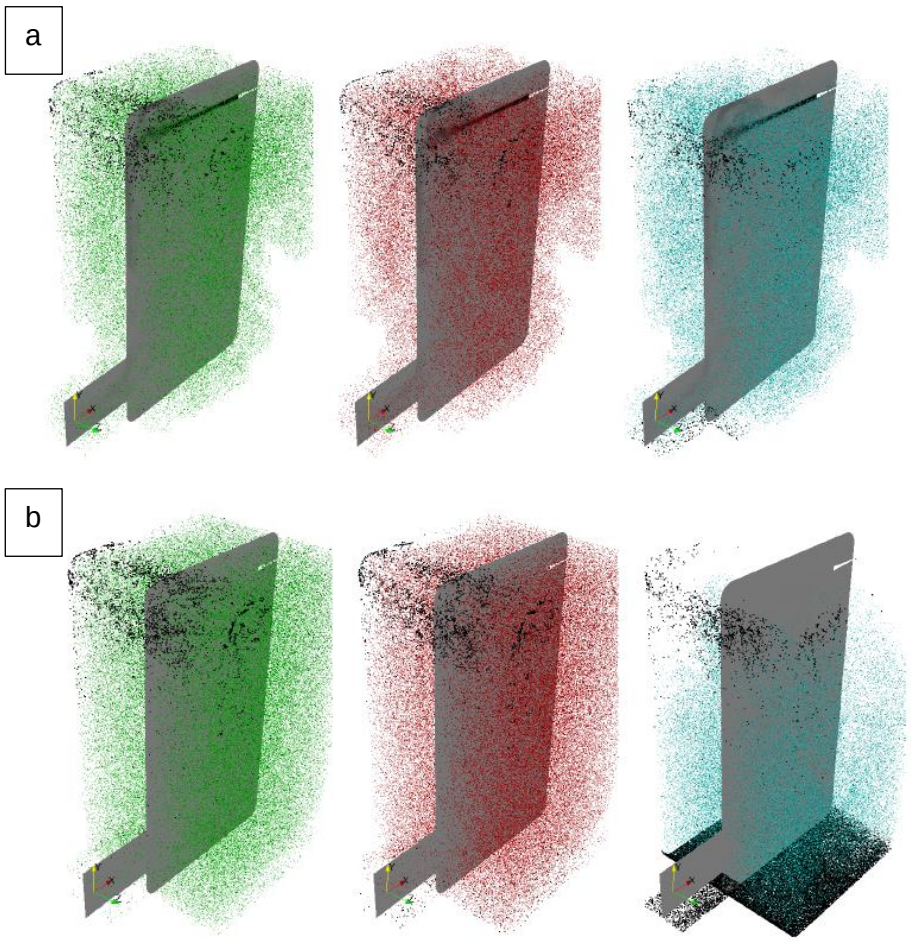

Figure 58 CFD simulation at different particle sizes (Green: 0.1 µm, Red: 1 µm, Blue: 10 µm) at different instants. a) Top image instant at time 25.5 s and b) bottom image at time 300.25 s.

The minimum average distance in between particles of the same size also delivered significant results. Since the distribution was similar for any particle size, the distance in between them was given by the quadrant division. To consider a more realistic scenario, an extrapolation considering all particles injected was done. The results are shown in Figure 59. Applying this correction factor, it can be clearly seen, how for the smallest droplets, the minimum average distance was reduced various orders of magnitude, reaching average values of 1 µm. This was the expected behaviour since a much higher number of droplets were injected.

However, for larger particles (10 µm) the average distance was in the range of 150 µm.

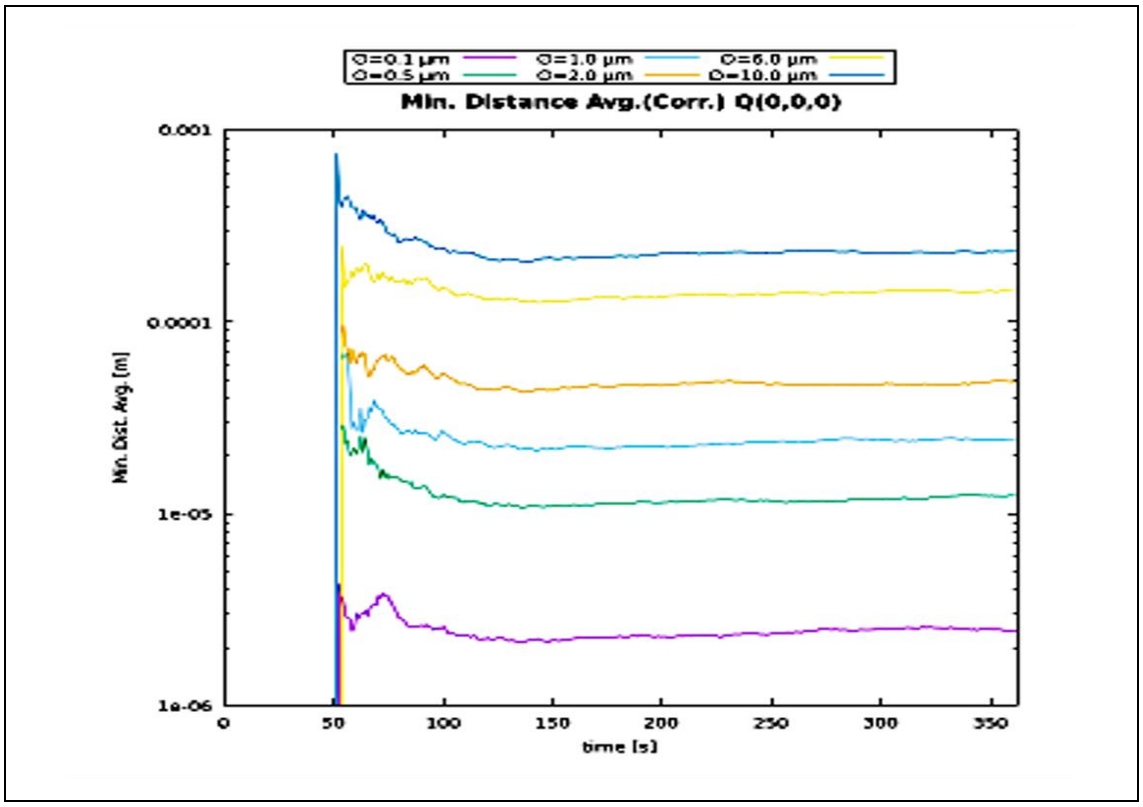

Figure 59 Minimum average distance in between particles (m) of different sizes in quadrant Q (0,0,0) of the cabin

6.2.4 DISCUSSION AND CONCLUSIONS

The atomization is a complex and challenging process to predict due to the high number of physical processes occurring in a very short lapse of time. Turbulences, convoluted interfaces, or coalescence are some of the interactions that occur and should be modelled to get a higher level of predictability (Ashgriz, 2011). In this case, the motion of the drops was simulated using Lagrangian-Eulerian models. The drops are simulated first in a turbulent scenario to then, during the exposition time, in a stationary state.

In the cabin, the turbulent phase is mainly driven by the output speed of the nozzle (air and liquid flow) and the relief and nozzle relative positions. Consequently, even though particles above 6 µm are also affected by gravity, the flow patterns created during the injection are the main promoters of the distribution. In principle, no matter their size, they would follow the air streamlines and cover all volume areas if the air pattern reached that position, no matter their size.

However, due to the mentioned relative position, there are quadrants where the particle density is lower. Therefore, is expected a lower probability of reaching full inactivation of the whole surface by the liquid phase. In the simulated case, these quadrants are just below the injection position, but they could change if the position of the relief valve would be the opposite, or the volume had material inside to be potentially decontaminated. Therefore, a study of the airflow characterization with different loads would improve the results of the decontamination cycle by ionHP+.

An important fact to be discussed is the number of adhered particles. The droplets tend to get stuck in regions of the domain with noticeable flow direction changes, which in this case, would be the upper part of the volume. Under these circumstances, certain droplets do not strictly follow the streamlines, but adhere to the walls when contacting them (the largest the particle, the larger the inertia and the easier it to come out of the air streamline). Therefore, any prominent disturbance due to material loading pattern, trays or the trolley design will also impact in the particle distribution. The lightest droplets can follow the streamlines closer to the cabin's roof and be transported towards the nozzle area.

In particles bigger than 6 μm, the gravity effect plays an important role during the exposition time. Meaning that, vertical surfaces have fewer chances being contacted with the hydrogen peroxide particle during the exposition. In addition, if shadows are created, or some items act as an “umbrella” for the spores, it decreases the probability of contacting with some of the hydrogen peroxide particles. Mei and Gong (2017), during a study focused on particle deposition in indoor air (with no such a high-speed incoming air injection) also proved that the impact of gravity over particles in the range of 10 μm significantly influenced the air stability.

Regarding the distance between particles of the same size, it is interesting to comment that the average distance can range between 1 to 200 μm, depending on the particle size. This fact is relevant because the spore average size can range from 0.5-1 μm (Yoshino et al., 2015). Moreover, in the case of bioindicators, the number of spores per cm^2 is in the range of 1.6×10^6. Then, if considering a 0.5 μm spore radius and assuming a homogeneous distribution of the spores, the average distance between the spores would be 4-5 μm. Therefore, only the particles in the lower range (smaller) would theoretically cover every spore. This is a significant assumption, as the spores are not always homogeneously distributed (Raguse et al., 2016), and overall, the particles are no rigid spheres (Figure 60), mainly when the droplet reaches a surface (Ashgriz, 2011).

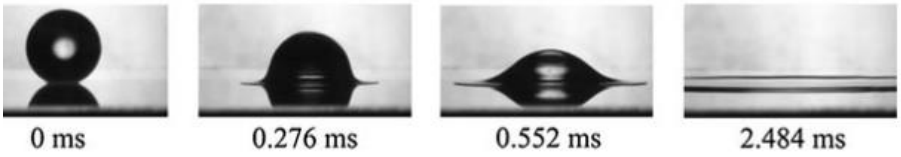

Figure 60 Droplet after surface contact (Ashgriz, 2011)

In conclusion, the Computation Fluid Dynamic (CFD) simulation enhanced the importance of three main factors in the design of an automated system to ensure homogeneous decontamination of a certain volume: 1) It is essential the characterization of the airflow pattern, especially considering the position of the nozzle and the relief valve and any other interaction with a solid interface that impact in the behavior of the air streamlines; 2) the particle size should be as small as possible to ensure a good distribution in points where the turbulences are higher. Only the lightest particles can reach positions of the roof and above the nozzle, and 3) the timing of the different stages is important. The injection phase should be long enough to ensure that the particles reach every point of the volume. The larger the specific surface to be covered, the longer the injection phase would be required.

It is important to recall that processes with potentially high impact on the decontamination system have not been considered in the simulation. Evaporation, condensation, coalescence, or nucleation are processes that if included in the exercise would clearly improve the predictablity of the particle status when reaching the microorganisms.

6.3 MICROBIAL LETHALITY ASSESSMENT

6.3.1 LETHALITY ASSESSMENT OF REPRESENTATIVE BIOBURDEN IN THE PHARMACEUTICAL, FOOD AND HEALTHCARE INDUSTRIES

6.3.1.1 INTRODUCTION AND OBJECTIVES

Without a thorough understanding of the microbial inactivation mechanisms occurred when hydrogen peroxide is applied, it would be impossible to predict the microbiocidal effectivity of the technology proposed in this dissertation. The perfect microbiocidal prediction model should ensure, with a probability of 1 in 1,000,000, that all potential biological contamination is inactivated (when sterility is the target, obviously). However, the biological and experimental variability makes it nearly impossible to get a coefficient of determination (R2) with this magnitude (0.999999) in a prediction model (Halvorson and Ziegler, 1933). The objective of the present modelling process is to reduce as much as possible the different uncertainties associated with the on going microbiological processes.

The first variable encountered when analysing the system from the microbiology perspective is the quantitative and qualitative variability of the microbial contamination on the surfaces and the environment. Also, the sensibility to the hydrogen peroxide might differ between microbial groups. As discussed in previous chapters, some microorganisms with high resistance to one biocide method could be easily decontaminated by other methods (Møretrø et al., 2019; Raguse et al., 2016; Sandle, 2013). Therefore, choosing the proper microorganism and clearly evaluating its inactivation kinetics is crucial for obtaining the best prediction model. There are published papers referring to the kinetic understanding, but mainly focused on HPV and VHP processes where the gas phase is the principal player in the inactivation process (Ali et al., 2016; Linley et al., 2012; Møretrø et al., 2019; Unger-Bimczok et al., 2008).

In the technology subject of study of this dissertation, the *Geobacillus stearothermophilus* is the reference (mentioned along the regulatory review). This reference will be compared, firstly, with the *Bacillus atrophaeus*, as there are inconclusive published experiments about its resistance versus the current reference. Pottage et al. (2012b) compared both spores observing how the first was more resistant than the second one. However, Pruß, K. et al. (2012), proved that the most resistant spore against this technology would be the second.

On the other hand, even if spore forms have been historically recognized as the most resistant biological form, other vegetative microorganisms are starting to increase their relevance showing high resistance against outside processes, being the genetic mutations one of the main reasons for that adaptation (Panchal et al., 2020). Therefore, and considering that the present atomization technology is starting to be, not just used in the pharmaceutical industry, but also in the Healthcare or Food industries, other microbial groups should be evaluated. Microorganisms such as methicillin-resistant *Staphylococcus aureus* (MRSA), or *Listeria monocytogenes* are selected as examples of significant microorganisms of such industries, being reported their high resistance against other decontamination methods (Choi et al., 2012; French et al., 2004).

In Hospital operating theatres, the MRSA is currently one of the most important microbiological risks. The traditional cleaning and disinfection methods are not capable

of removing it from the contaminated surface, and its spread across Europe's hospitals is becoming a real threat to the operating theatres (French et al., 2004). A study published by Voss et al (1994) was already pointing out its increase, proving that close to 13% of the *Staphylococcus aureus* screened strains (in a >7.000 strains test) were methicillin resistant. In addition, its occurrence varied from <1% in Scandinavian countries to >30% in southern Europe, Spain, or Italy, for instance (Voss et al., 1994). This evolution of the *Staphylococcus aureus* led this strain to be the reason for up to 20.000 deaths and 119.000 infections in the United States during 2017, as reported by the Center for Disease Control and Prevention (CDC) (CDC, 2019). Additionally, the EFSA has published an analysis remarking the importance of the subject microorganism due to the increased resistance and its association to infections in pigs, cattle, horses, poultry or even pets ("Analysis of the baseline survey on the prevalence of methicillin-resistant *Staphylococcus aureus* (MRSA) in holdings with breeding pigs, in the EU, 2008 - Part B: factors associated with MRSA contamination of holdings", 2010). Moreover, it is starting to be considered an occupational hazard for the food industry stakeholders and should be considered as a critical microorganism in the decontamination of surfaces.

Finally, and regarding *L. monocytogenes*, it is a well-known foodborne pathogenic microorganism that causes listeriosis, with one of the highest dead rates in foodborne infections (Huang, 2013). Its adhesion to equipment or cleanroom surfaces is a vector of contamination, and its removal, mainly from hidden spaces or edges, is not yet resolved (Back et al., 2014). In few studies, such as the one published by Choi et al. (2012), it has been demonstrated that the subject microorganism, if no sanitization method is applied, can survive up to 7 days from a starting concentration of 10^4-10^5 CFU/mL approximately. In the same study, hydrogen peroxide technology was used at 0.5 %(w/w), and the results showed a good deactivation reaching 4-log reductions in 10 minutes and below 1 $\log_{10}$(CFU/mL) in 60 minutes. The authors mentioned the importance of hydrogen peroxide concentration and the environmental conditions, but no further study was made.

Therefore, the importance of this investigation relies on the use of an atomized hydrogen peroxide technology (in particular the developed ionHP+) for surface decontamination against four critical microorganisms that are causing severe problems, not just in the industrial and life science areas but also in the day-to-day lives of the public across the world.

6.3.1.2 MATERIAL AND METHOD

1) Process engineering

A specific prototype was built. A simplified drawing of the Piping and Instrumentation diagram (P&Id) is shown in Figure 61. The nozzle position is well represented in Figure 61b, and the dimensions of the isolator are still the same than in previous experiments, 0.6 m^3:

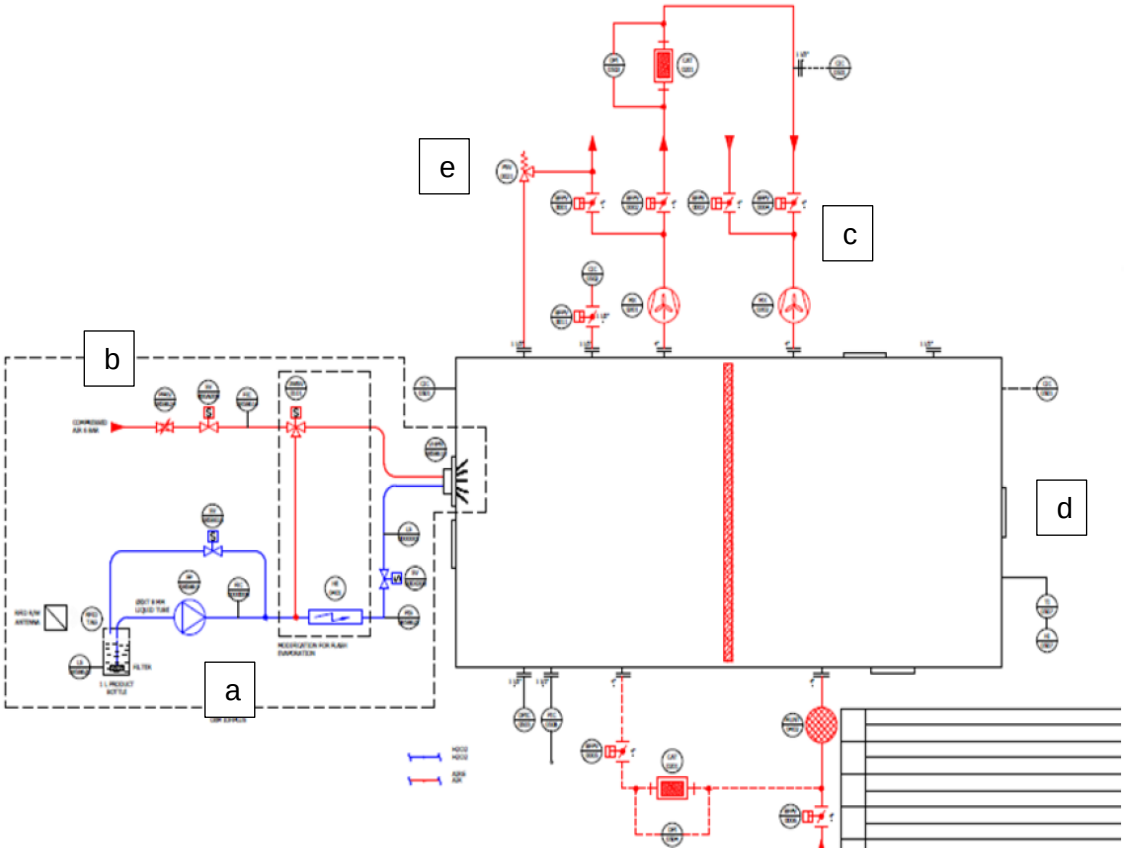

Figure 61 Piping and Instrumentation diagram Laboratory prototype. a) Liquid injection system with a dedicated flow, pressure and air detection sensor. b) Air injection system with pressure and flow sensors. c) Aeration system with two dedicated fans and filters. d) Hydrogen peroxide, micro-condensation and pressure sensors. e) Relief valve.

Circulating fans to ensure faster aeration after the exposition time were incorporated into the system. A pressure sensor to control the relieving pressure and a relief valve at the bottom of the volume was installed. This way a control of the airflow streamlines was achieved. A specifically designed port was manufactured to allow a safe extraction of the bioindicators while performing the decontamination cycle (Figure 62a). A temperature and RH monitoring sensor (Sensor Push, New York, USA) was included in the system (Figure 62c). A Recipe control throughout a Programmable Logic Controller (PLC) and Human Machine Interface (HMI) was installed (Figure 63a and 63b). To measure the hydrogen peroxide in the gas phase the same sensor Polytron 7000 (Dräger) was used. However, in this case, it was placed in the middle of the volume (Figure 62b). Models and brands of some pieces of equipment have not been disclosed due to confidential terms.

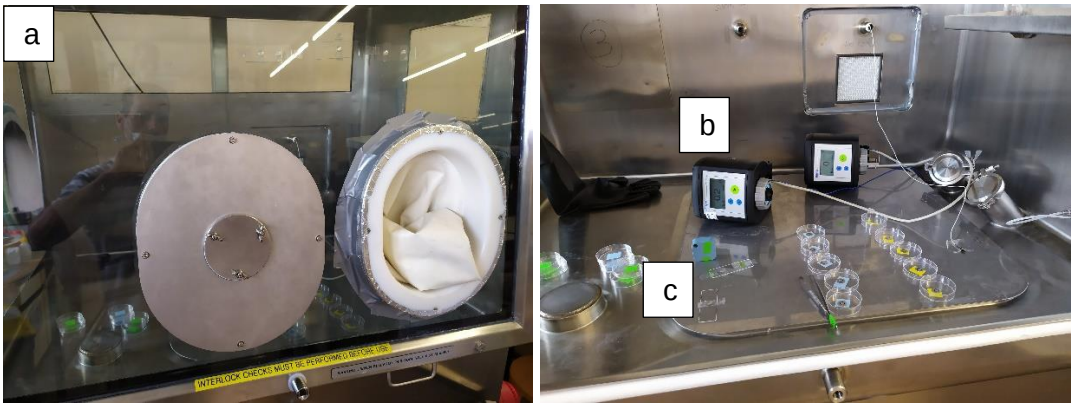

Figure 62 Extraction port a), Hydrogen Peroxide sensors b) and Temperature and Relative humidity sensor c)

The process recipe was constant with the following setpoints: airflow of 80 L/min, liquid flow of 5 mL/min, an exposition time of 40 min and a total injection of 12 mL of hydrogen peroxide. Thus, no particle variation nor distribution disposition was expected, leaving all the process parameters constant in all the microbiological tests.

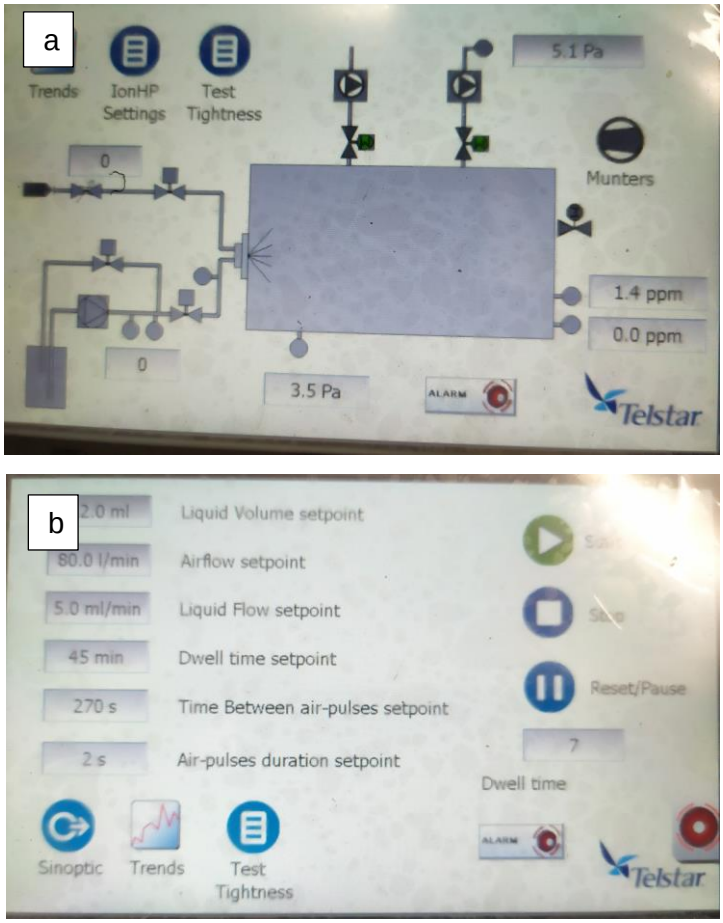

Figure 63 a) Synoptic of the HMI and b) Recipe setting screen

2) Inactivation Evaluation: Microbiological analyses

For this study, the position of the bioindicators was specially selected to ensure a total contact of the particles. According to the simulation study, the floor quadrants were the ones more likely to receive bigger particles. Even if the generated particles were below

6 μm, coalescence and nucleation processes (Spiegelman and Alvarez, 2015) would make the particles fall in the floor quadrant by the gravity effect, and contacting the bioindicators (Figure 64).

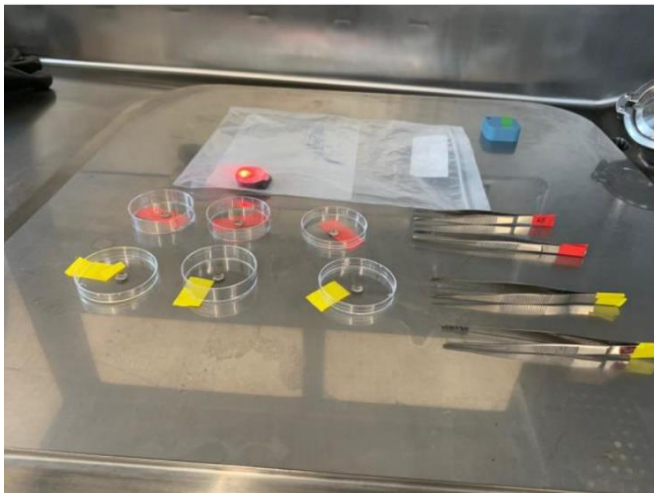

Figure 64 Bioindicators position in the isolator/cabin

The bioindicators were manufactured following the next steps both for the spore forming microorganisms and the vegetative forms:

Isolation, purification and spore-producing

Purification of microorganisms of commercial BIs was performed as follows. Coupons of *G. stearothermophilus and B. atrophaeus* were placed in tubes of Trypticase Soy Broth (TSB, Oxoid) for 24 h at 55 ºC and 30ºC, respectively. Afterwards, the strains were streaked in Petri plates of Trypticase Soy Agar (TSA, Oxoid, United Kingdom) and incubated in similar conditions. During incubation at their respective temperatures, the plates were placed inside a container with a flask with water, to minimize dehydration of the agar. Isolated and purified colonies were streaked in a TSA slant tube and then stored at 4ºC till the moment of use.

Then, the spores were produced following the method of Wells-Bennik et al. (2019) with some modifications. Strains were inoculated in 10 mL of Tryptone Yeast Broth (TYB) containing 10 g/L of tryptone (Oxoid), 5 g/L of yeast extract (Oxoid) BD), and 5 g/L NaCl (Panreac, Castellar del Vallés, Spain). The incubation was performed for 24 h at 55 °C or 30 ºC, depending on the strain. After that, 2 mL of this culture were added to various Roux culture bottles with TSA supplemented with 0.13 mM $MnSO_4$, 1 mM $MgSO_4$, 1 mM $CaCl_2$ and 13 mM KCl (Panreac), and the pH was adjusted to 7. Roux flasks were incubated at 55ºC and 30ºC for the corresponding microorganisms for 7 days. After 7 days of incubation, spores were harvested by adding approximately 10 mL of cold sterile water to the surface of each Roux flask. Spore suspensions of three Roux flasks were pooled and washed four times in cold sterile water by centrifugation at 7500 g for 10 min in an Eppendorf 5804R Centrifuge (Eppendorf, Hamburg, Germany). Sediment was resuspended with 15 mL of water. In order to eliminate the remaining vegetative forms, thermal treatment of 75 ºC for 30 min was applied. The spore's suspension was stored at 4ºC until use.

Bacterial strains preparation

Methicillin-resistant *Staphylococcus aureus* CECT 4438 (MRSA) strain was obtained from the Spanish Collection of Type Cultures (CECT) (University of Valencia, Valencia, Spain). The *L. monocytogenes* Scott A strain (serotype 4b) was obtained from the Department of Animal and Food Science in the Universitat Autonoma de Barcelona (Universitat Autonoma de Barcelona, Barcelona, Spain) and was selected for its high resistance to technological treatments. The *L. monocytogenes* RO15 strain was obtained from the Faculty of Food Science and Engineering of the Galati Dunarea University of Josy of Galati (Galati, Romania). It was isolated from surfaces of meat industries and was selected for its high resistance to disinfectants.

The strains, originally lyophilized, were recovered in TSB. After incubating for 24 h at 37°C, they were streaked on Petri dishes with TSA and incubated at 37°C for 24 h to verify the identity and purity of the culture. From this culture, isolated colonies were streaked in TSA slant tubes, incubated at 37°C for 24 h, and subsequently stored at 4°C (working cultures). These working cultures were maintained on TSA slants at 4 ºC for a maximum period of 9 weeks.

For this study, both strains were prepared according to the protocol described by Pottage et al. (2012b). Both *L. monocytogenes* and MRSA strains were incubated for 20 h at 37 °C in 10 mL of TSB and Brain Heart Infusion broth (BHI, Oxoid), respectively. Subsequently, they were centrifuged at 3000 x g for 10 min at 4 °C, repeating this process three more times with distilled water. Finally, a 1 mL dilution of the culture was made in 9 mL of sterile distilled water to reach a final concentration of 6 to 7 log CFU/mL.

Preparation of bioindicators

All tests executed with own-manufactured bioindicators used stainless steel AISI316 coupons, 2B grade, 1 cm diameter, and 1 mm thickness. Discs were prepared according to the protocol described by Chen et al. (2015) with minor modifications.

Before use, discs were washed by a 12 h immersion in 1000 mL of an aqueous 10% detergent concentrate solution (ADIS, Madrid, Spain) and rinsed three times by a 10 min immersion in 1000 mL of sterile distilled water at 21 °C. The washed stainless-steel coupons were dried at a temperature of 55-60 ºC, and an area of 0.6 cm in diameter was encircled by a permanent marker. Finally, all discs were sterilized in a vapor autoclave at 121ºC for 15 min.

An inoculum of 40 µL of spore suspension (6-7 log CFU/ml) of *G. stearothermophilus* or *B. atropheaus* was deposited within the marked area of the stainless-steel coupon and were dried for 1 h in a safety hood (Telstar, Terrassa, Spain), until they were visibly dry. Discs were stored at 4ºC until use.

For vegetative strains, an inoculum of 40 µL of the bacterial suspension, were deposited within the marked area of the stainless-steel coupon and were dried for 1-2 h in a safety hood (Telstar) until they were visibly dry. For the experiments, these bioindicators were used immediately.

Treatments and determination of the achieved inactivation

Bioindicators were removed from the isolator and placed in a 5 mL solution of Dey-Engley neutralizing broth (DENB, Sigma-Aldrich. St Louis, USA) in a 50 mL tube with 3

g of sterile glass beads of 2 mm diameter (Vidra Foc, Barcelona, Spain). Then, to promote the recovery of spores adhered to the surface, the tubes were placed in a Branson 2510 ultrasonic bath (Danbury, USA) with a frequency of 40 kHz for 5 min. Subsequently, they were vortexed for 2 minutes. A series of decimal dilutions were done in Phosphate Buffered Saline (PBS) solution (Lonza Accugene, Rockland ME, USA) and were plated in TSA using an Eddy jet spiral plater (IUL Instruments, Barcelona, Spain). Low microbial counts were enumerated by the pour plate method in 1mL of sample or bioindicator. Incubation was done at 55 ºC and 30 ºC for the *Geobacillus stearothermophilus* and *Bacillus atropheaus*, respectively. The bacterial strains, *Listeria monocytogenes* and MRSA were incubated at 37ºC. Finally, plates were counted manually or in an automated IUL Flash and Go colony counter (IUL micro, Barcelona, Spain).

Chen et al. (2015) suggested that this method for recovering the microorganisms from the bioindicators in these surfaces became a key step towards a good characterization of the inactivation study. For this reason, an assay of repeatability was performed previously on the recovery, considering the initial concentration of spores stated in the commercial biological indicator's datasheet as a control. The average recovery was 94.1%, with an acceptable standard deviation (2%) (data not shown).

The method used to calculate the inactivation kinetics of the ionHP+ technology was based on the survivor curve method. The calculation considered the difference between the logarithm of the initial count (without treatment) and the final count (after treatment), using the Equation 21:

$$Lethality\ \left(Log\frac{CFU}{g}\right) = Log\ (\frac{N_0}{N_r})$$

Equation 21 Lethality calculation

Where N_0 is the Initial count expressed as spores or CFU/bioindicator and N_f the count obtained after the application of the atomized hydrogen peroxide treatments.

Data analysis and modelling

Seven experiments for *Geobacillus stearothermophilus* and *Bacillus atrophaeus* were performed. A set of 12 points in time was planned, between 0 a 45 min.

In addition, three experiments for MRSA and *L. monocytogenes* strains were performed. A set between 7 and 10 points in time was planned between 0 a 25 min.

The 4D value, representing the time to achieve a 4-log reduction, was used as the main parameter to assess the resistance of each microorganism. The 4D value is appliable both to logarithmic-linear and non-log-linear inactivation models (Buchanan et al., 1993).

The GInaFIT computer tool (Geeraerd et al., 2005) was used to determine the bacterial inactivation curve and 4D value. In relation to the goodness-of-fit value of the models used, an often-used criterion for judging whether or not a model fits well, is the coefficient of determination (R^2), which is the ratio of the sum of squares due to regression to that of the total sum of squares of the response variable around its mean. Similarly, another goodness-of-fit value, is the adjusted R^2 (R^2_{adj}), which is based upon de variances (i.e., the mean squares) rather than upon the sum of squares. The R^2_{adj} attempts to penalize

the inclusion of redundant parameters. However, the use of either of these values, alone, for non-linear regression is sometimes inappropriate, usually leading to a rather overoptimistic view of the success of the modelling process (Ratkowsky, 2004; Geeraerd et al., 2005). Therefore, more suitable goodness-of-fit measures of non-linear models have been used, concretely the Root Mean Squared Error (RMSE) that is defined as a measure of the discrepancy between observed and predicted values. A low RMSE value means better adequacy of the model to describe data (Pérez-Rodríguez and Valero, 2013; Ross, 1996).

The prediction bands of the graphs, the standard error (SE), and the confidence intervals (CI) of the different parameters and statistical measures were obtained using the GraphPad Prism computer tool (GraphPad Software Inc., San Diego, CA, USA).

6.3.1.3 RESULTS

Physic-Chemical parameters

During all treatments, similar trends were observed in the physical-chemical parameters. Figure 65 represents the model of the most common values of each critical physical-chemical variable during all the process steps: (a) injection, (b) dwell time and (c) aeration.

The temperature did not vary much during the cycle itself and not even in between cycles. In this case (Figure 65), the temperature was 21.18 ± 0.13 ºC, and the variation between cycles was ± 2.44 ºC. The slight decrease observed in temperature at the beginning of the cycle, just after injection, was related to the initial evaporation, which is an endothermic process and tends to decrease the environmental temperature. Then, when saturation was reached, and condensation started, the temperature slightly rose again.

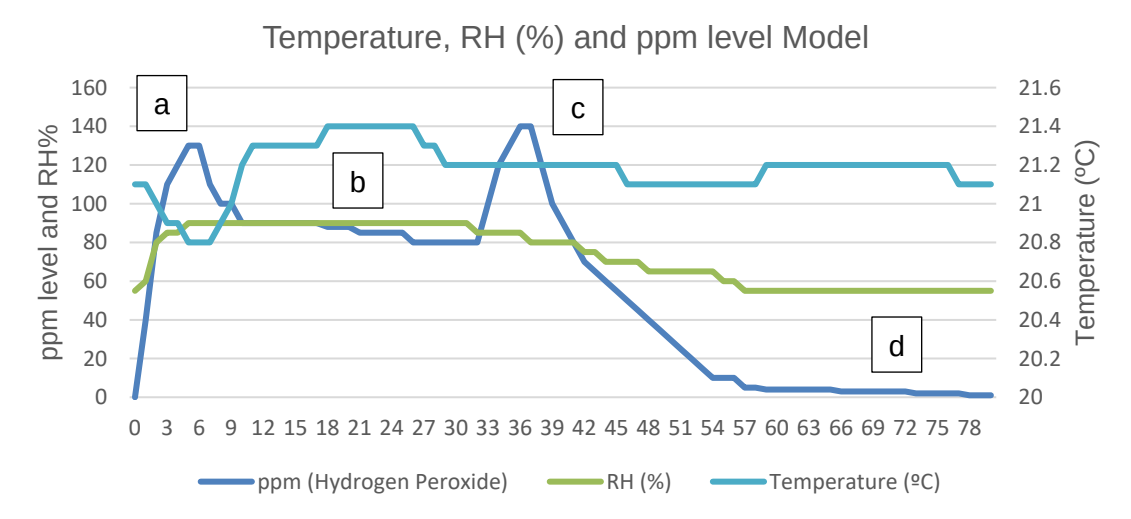

Figure 65 ppm level, RH (%) and Temperature model representation. a) Injection phase, b) Dwell time, c) Start of aeration, d) End of aeration

The differences in concentration of hydrogen peroxide gas (ppm level) were evident between the different phases of the cycle. At the beginning of the injection and till equilibrium is reached, the ppm level got values of 120-130 ppm. Later during the dwell phase, the concentration decreased as the hydrogen peroxide started decomposing in contact with metals (Salem et al., 2000). The mean value during dwell time was 92.5 ±

13.94 ppm. An interesting effect appeared when the aeration started. The atmosphere was renewed with fresh air, and the equilibrium was broken. Part of the condensed hydrogen peroxide evaporated, and the gas phase of hydrogen peroxide, even if no more injection was done, reached similar levels than during injection (Figure 65c). The aeration was a long process, with more than a 30 min cycle to reach a value below 1 ppm (safe hydrogen peroxide gas level). The absorption of the hydrogen peroxide into the materials within the isolator, and the evaporation, made that once all hydrogen peroxide in the gas phase was removed, the limiting step was not related to the exhaust or renewal of air, but with the internal diffusion of hydrogen peroxide within the different materials (Radl et al., 2011).

The relative humidity increases with the injection of the hydrogen peroxide solution. The F66-SR (Jose Collado S.A.) is a water-based solution, with more than 80% of water content, so water is nebulized into the system. Evaporation takes place, and as the relative humidity is not controlled during the exposition time, the air is saturated with both molecules, water, and hydrogen peroxide. The RH reaches 89.4% ± 2.27 during exposition.

Microbial inactivation

The injection step, even if not specifically designed for microbial inactivation, already showed an effect in the lethality process. As an example, in the case of the experiment performed with *L. monocytogenes* Scott A at least 1-log reduction was obtained (Figure 66), in the first two minutes, while the injection was still taking place. Therefore, for modelling the microbicidal effect of hydrogen peroxide, time 0 min was considered as the beginning of the injection (not the beginning of the exposure time or as previously named, dwell time).

Lethality and inactivation modelling of spore formers bacteria

The inactivation models with a better fit for both spore formers were adjusted to a Weibull and a Log-linear models, proposed by Marfart et al. (2002) and Bigelow and Esty (1920), respectively (Figure 66 and Table 14). A description of the mentioned models is shown in Equations 22 and 23.

$$Log\ (N) = Log\ (N_0) - \frac{Kmax \times t}{ln10}$$

Equation 22 Log-linear or Bigelow Model (Bigelow and Etsy, 1920)

$$Log\ (N) = Log\ (N_0) - \left(\frac{t}{\delta}\right)^p$$

Equation 23 Weibull or Marfart Model (Mafart et al., 2002)

Where N_0 refers to the initial population, the $Kmax$ parameter refers to the inactivation constant of the linear model, δ refer to the time to achieve the first log-reduction, p to the shape of the inactivation curve and t the time of treatment.

Bacillus atrophaeus showed significantly higher resistance against atomized hydrogen peroxide than the other tested microorganisms. Figure 66 represents both spore formers

inactivation curves with the best fit statistical parameters for *B. atropheaus* (log-linear) and *G. stearothermophilus* (Weibull).

While for the complete inactivation of the *G. stearothermophilus* no more than 30 min were necessary, the *B. atrophaeus* spore required more than 40 min of exposure. Consequently, the estimated 4D value of *B. atropheaus* was 24.75 min and the one for *G. stearothermophilus* was 21.60 min. Both models showed a clear dependence on the exposure time, with a steeper reduction (higher $Kmax$ in the Log-linear model (Table 14)) in the pharmaceutical reference (*G. stearothermophilus*) than in *B. atropheaus*.

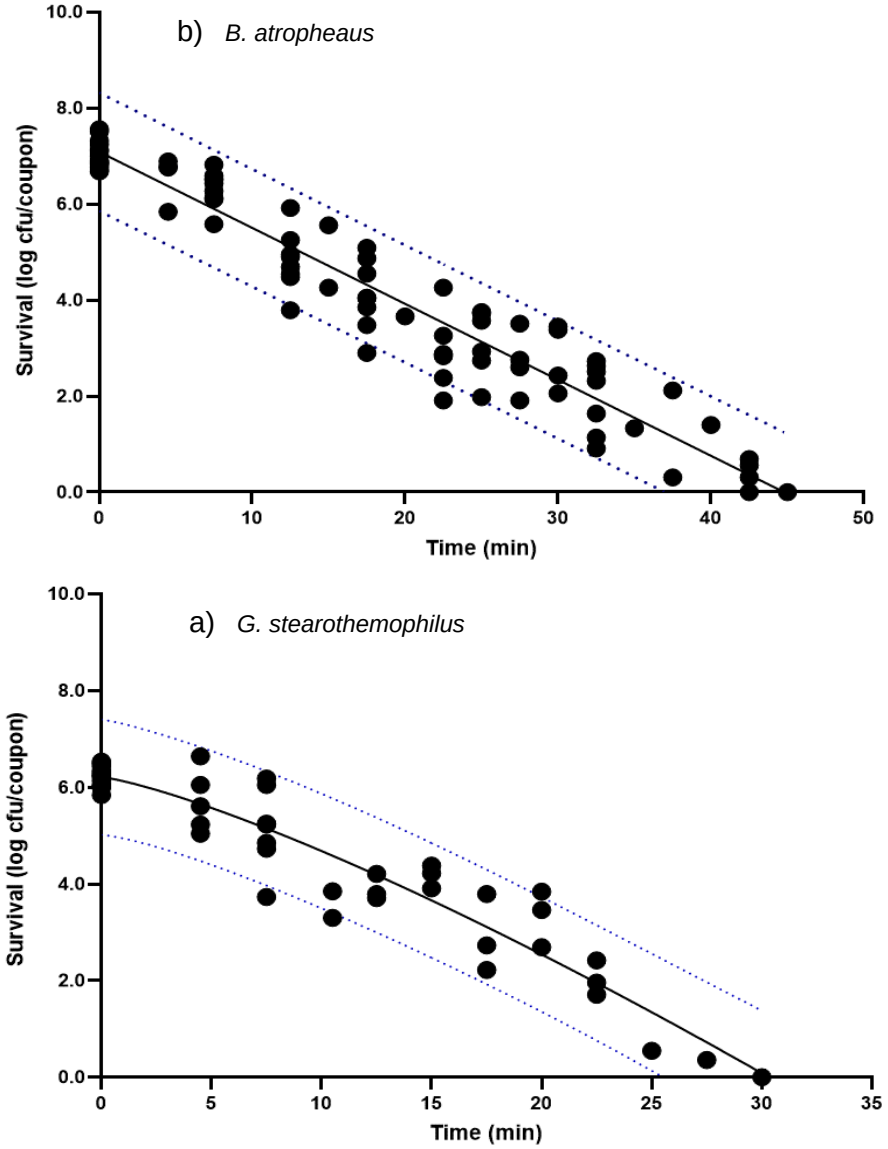

Figure 66 a) Inactivation model of B. atropheaus (Log-Linear) and b) G. Stearothermophilus (Weibull) during a hydrogen peroxide atomization process. The dotted lines show the prediction intervals.

A statistical summary of the model fitting is shown in Table 14, including the 4D estimated value, standard deviation and 95 % confidence intervals (CI) of four model parameters fit. The δ and p values in the Marfart model could be interpreted as the time required for the first log-reduction by the action of the atomized hydrogen peroxide, and the shape factor of the Weibull distribution, respectively. These parameters delivered results worth to be highlighted. As Cerf (1977) mentions, the bacterial resistance cannot only be observed from the linearity perspective but also considering concave or convex forms that enhance the fitness of the model towards reality. As reflected in Table 14, the δ value is higher in *G. stearothermophilus* than the *B. atropheaus* due to the greater resistance shown in the first minutes of the exposition. In addition, as can be observed, the p value showed certain convexity (p>1) in the *G. stearothemophilus* spore; however, after that, the remaining cells are more affected (Martinus and Van Boekel, 2002) by the action of the atomized hydrogen peroxide, showing a higher inactivation constant ($Kmax$) than the *B. atropheaus*. In addition, both the confident intervals (CI) and the adjusted coefficient of determination ($R^2_{adjusted}$) showed that the *G. stearothemophilus* spore results were more unpredictable than the ones from the *B. atropheaus*. The higher CI and lower $R^2_{adjusted}$ with a smaller analyzed data population showed that *G. stearothemophilus* behaved differently against the atomized hydrogen peroxide technology. Other factors not considered in this investigation might affect the prediction model.

Table 14 Statistical indexes and parameter estimation (mean, standard deviations and 95% confidence intervals) of the inactivation model used for B. atropheaus and G. stearothermophilus during the atomization technology ionHP+

		B. atropheaus		***G. stearothemophilus***	
Parameter	**Unit**	**Log-linear**	**Weibull**	**Log-linear**	**Weibull**
Log (N_0) ± SE	log CFU/coupon	7.09 ± 0.11	7.16 ± 0.15	6.40 ± 0.13	6.21 ± 0.14
Log (N_0) (95 % CI)	log CFU/ coupon	6.87-7.30	6.87-7.45	6.14-6.65	5.92-6.50
K_{max} ± SE	log CFU/min	0.36 ± 0.01		0.45 ± 0.02	
K_{max} (95% CI)	log CFU/min	0.34-0.39		0.40-0.49	
δ ± SE	min		5.74 ± 0.80		7.15 ± 0.93
δ (95% CI)	min		4.35-7.36		5.32-9.19
p ± SE	-		0.95±0.06		1.26±0.12
p (95% CI)	-		0.84-1.08		1.03-1.55
4D	min	25.65	24.75	20.70	21.60
R^2 (adjusted)	-	0.924	0.924	0.900	0.909
RMSE	-	0.610	0.612	0.602	0.575

N_0: the initial population, K_{max}: inactivation constant of the linear model, δ: time to achieve the first Log-reduction, p: the shape of the inactivation curve, 4D: time to achieve a 4-log reduction, RMSE: Root Mean Squared Error.SE: standard error; 95 % CI: 95% confidence interval

Lethality and inactivation modelling of vegetative bacteria

The inactivation models with better fit were adjusted to a Weibull and a Log-linear models for both *L. monocytogenes* strains and Weibull and log-linear model with shoulder (Geeraerd et al. 2000) for MRSA (Figure 67 and 68 and Table 15).

A description of the log-linear with shoulder is shown in Equation 24.

$$Log\ (N) = Log\ (N_0) - \frac{Kmax\ \times t}{ln10} + \frac{\log_{10}(e^{Kmax \times SI})}{(1 + e^{Kmax \times SI} - 1) \times e^{Kmax \times t}}$$

Equation 24 Log-lineal model with shoulder or Geeraerd (Geeraerd et al. 2000)

Where N_0 refers to the initial population, the $Kmax$ parameter refers to the inactivation constant of the lineal section, the SI to the duration of the shoulder effect and t the time of treatment.

Both strains of *L. monocytogenes*, Scott A and RO15, showed a much lower resistance than the previous spore formers and the MRSA strain. In both cases, the total reduction was achieved in the first 10 minutes of exposition (Figure 67).

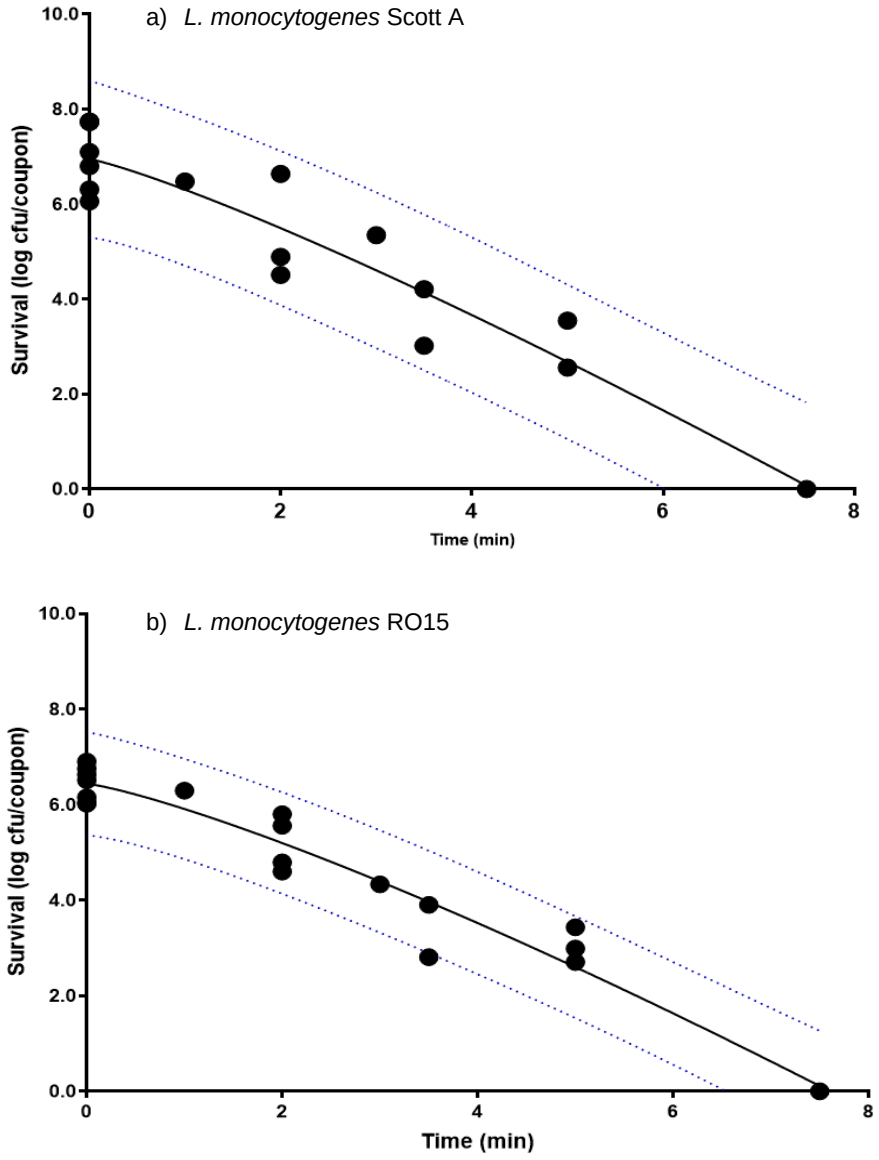

Figure 67 Inactivation models of a) L. monocytogenes Scott A *and b) L. monocytogenes RO15 during a hydrogen peroxide atomization process. The dotted lines show the prediction intervals*

A statistical summary of the models fitting of both *L. monocytogenes* strains and MRSA is shown in Table 15, including the estimated value, standard deviation and 95 % confidence intervals (CI) of six model parameters fitting.

Figure 67 and 68 represents both *L. monocytogenes* and MRSA inactivation curves, with the most significant statistical model. Both strains of *L. monocytogenes* are showing a very similar 4D value, with a slightly higher resistance in the strain RO15, 5.04 min versus 4.80 minutes. In this case, the RO15 had a higher p value, therefore, showed a light higher resistance at the beginning of the exposure.

Regarding the MRSA strain, as can be seen in Figure 68 and Table 15, the inactivation curve shows a convex shape (p>1) or a shoulder time of 5.3 min, which is related to higher resistance of bacterial population at the beginning of the atomized hydrogen peroxide treatment. The δ value was even higher than the *G. stearothermophilus* which, between the spore former bacteria, showed the greatest resistance in the first fold reduction. However, after this first phase, the inactivation kinetic constant ($Kmax$) of the MRSA was significatively higher (0.71 log cfu/min), and the 4D value obtained was lower (18.97 min) than the spore former. To achieve a complete lethality, more than 20 min of exposure were required.

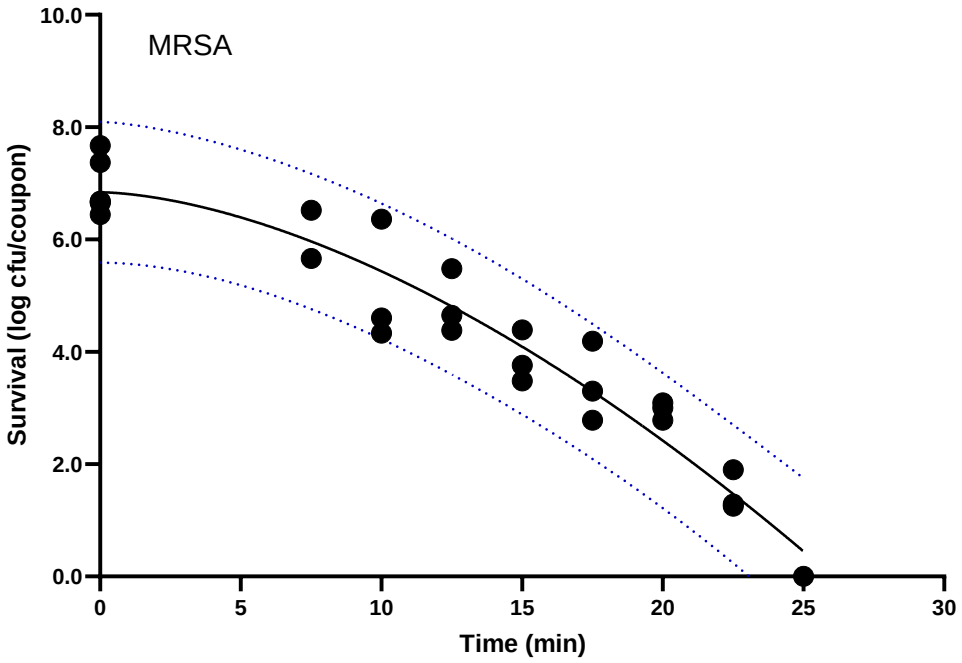

Figure 68 Inactivation model of Methicillin-Resistant S. aureus (MRSA) during a hydrogen peroxide atomization process. The dotted lines show the prediction intervals.

Table 15 Statistical indexes and parameter estimation (mean, standard deviations and 95% confidence intervals) of the inactivation model used for L. monocytogenes Scott A, L. monocytogenes RO15 and Methicillin-Resistant S. aureus (MRSA) during the atomization technology ionHP+.

		***L. monocytogenes* Scott A**		***L. monocytogenes* RO15**		**MRSA**	
Parameter	**Unit**	**Log-linear**	**Weibull**	**Log-linear**	**Weibull**	**Log-linear shoulder**	**Weibull**
Log (N_0) ± SE	log cfu/disc	7.11 ± 0.24	6.95 ± 0.28	6.67 ± 0.18	6.42 ± 0.19	6.89 ± 0.24	6.89 ± 0.22
Log (N_0) (95% CI)	log cfu/disc	6.60-7.63	6.35-7.56	6.23-6.97	6.07-6.81	6.40-7.38	6.46-7.34
K_{max} ± SE	log cfu/min	2.10 ± 0.15		2.00 ± 0.12		0.71 ± 0.04	
K_{max} (95% CI)	log cfu/min	1.79-2.41		1.70-2.12		0.63-0.81	
SI ± SE	min					5.29 ± 1.18	
SI (95% CI)	min					2.69-7.82	
δ ± SE	min		1.46 ± 0.37		1.79 ± 0.28		7.51 ± 0.93
δ (95% CI)	min		0.78-2.37		1.17-2.28		5.69-9.52
p ± SE	-		1.18 ± 0.18		1.34±0.15		1.51 ± 0.14
p (95%CI)	-		0.85-1.65		0.99-1.54		1.25-1.84
4D	min	4.43	4.80	4.62	5.04	18.42	18.97
R^2 (adjusted)	-	0.923	0.924	0.935	0.950	0.941	0.947
RMSE	-	0.722	0.719	0.579	0.510	0.580	0.553

N_0: the initial population, Kmax: inactivation constant of the linear model, δ: time to achieve the first Log-reduction, SI: duration of shoulder phase, p: the shape of the inactivation curve, 4D: time to achieve a 4-log reduction, RMSE: Root Mean Squared Error.SE: standard error; 95 % CI: 95% confidence interval.

6.3.1.4 DISCUSSION AND CONCLUSIONS

Spore formers*: B. atrophaeus* and *G. stearothermophilus*

Historically, the hydrogen peroxide technology has been associated to vapor processes (VHP from American Amsco patented technology), where no condensing phase is promoted nor a truly gas is obtained. The reference microorganism of heat (water vapor) sterilization processes, *Geobacillus stearothermophilus*, has been commonly used for validation of these hydrogen peroxide vapor-based processes (Drinkwater et al., 2009). Later, other technologies with a different principle, such as HPV or ionHP+, have inherited the same reference, no matter the phase status of the hydrogen peroxide.

Nevertheless, it has already been observed that both the *G. stearothermophilus* and the *B. atropheaus* showed different inactivation mechanisms depending on the hydrogen peroxide technology in use. The gas or liquid-phase hydrogen peroxide status had a different impact on the lethality of the spore forming bacteria (Linley et al., 2012).

The hydrogen peroxide atomization technology is a wet, condensing technology, that relies mainly, but not only, on the capability of the liquid phase (a water-based solution) to transfer the oxidation potential of the primary active substance to the contaminated surface. Therefore, the hydrophobicity/hydrophilicity characteristics of the microorganism to be inactivated are critical in the understanding of the inactivation kinetics of this type of technology. According to Wiencek et al., (1990), the *Bacillus atrophaeus* demonstrated a higher hydrophobicity than *Geobacillus stearothermophilus*, making the hydrogen peroxide liquid solution initially repelled when surrounding the microorganism. The lower wettability of the outer membrane limits the penetration process, delaying the damage of the inner part of the microorganism by the liquid phase.

As discussed, the *G. stearothermophilus* microorganism showed an overall lower resistance, with a lower 4D value (21.60 min) than the *B. atropheaus* (24.75 min). Complete lethality was achieved in less time. However, it was slightly more resistant at the beginning of the process, with a δ of 7.15 ± 0.93 min compared to 5.74 ± 0.80 min of *B. atropheaus*. This phenomenon could be related to the faster impact of the gas phase of hydrogen peroxide in the *B. atropheaus*, since the gas phase was readily available into the system from the beginning of the injection and it was homogeneously distributed (Kirchner et al., 2013). It is important to recall, that even if the process is a wet or condensing technology, the vapor pressure in equilibrium with this liquid, delivers a gas phase of hydrogen peroxide that would also be in contact with the microorganism.

After the gas effect, the liquid phase would reach the specific point by the effect of the gravity, or the forces generated by the air streamlines. Once the liquid phase reached the spores, the faster penetration of *G. stearothemophilus* membrane enhanced the inactivation compared to *B. atropheaus*. Similar results were obtained by Pruß et al. (2012), who found that spores with low wettability had higher resistance to liquid-phase hydrogen peroxide. There have been investigations and open debate on the choice of microorganism as an appropriate biological indicator. In previous studies, *Bacillus atrophaeus* showed greater resistance to lethal stresses when exposed to aqueous sterilant applications, whereas *Geobacillus stearothermophilus* showed higher resistance to vapor-based approaches (Hultman et al., 2007).

Vegetative microorganisms, *L. monocytogenes* and MRSA

While *L. monocytogenes* was rapidly eliminated in all assays, the MRSA was posing a great resistance.

To understand the response of the MRSA in these experiments, it is important to understand its evolution in the last decade. The *Staphylococcus aureus*, a Gram-positive bacterium, was characterized by the production of an enzyme (β-lactamase) capable of minimizing the effect of the β-lactam antibiotics (penicillin among others) (Stapleton and Taylor, 2002). This type of antibiotics was the principal defense that healthcare professionals had to contend most of the infections. However, the *Staphylococcus aureus* microorganism showed resistance to the mentioned antibiotics. As soon as the scientific community developed a new antibiotic, the *Staphylococcus aureus*, now already so-called MRSA, expressed an additional penicillin-binding protein, protecting it more against the expected inactivation (Panchal et al., 2020). Nowadays, due to the use of different antibiotics against the strain, it is considered a multi-resistant microorganism with no specific treatment.

Thus, it is clear its historical ability to adapt to harsh environments, including to some biocides. Its adaptation capability when low hydrogen peroxide (sub-lethal) concentrations are applied has been demonstrated (Painter et al., 2015). This adaptation observed by these authors via mutagenic DNA repair was due to a higher catalase enzyme production that made the small-colony variants (SCV) more resistant to the hydrogen peroxide action. Interestingly, this adaptation occurred during the experiment, observing that the number of SCV colonies per mL continuously increased during the exposure to low concentrations of the biocide. Its ability to mutate make the microorganism more unpredictable.

The present experiment results showed that the mechanisms of protection of the MRSA are the reason for the required long expositions to obtain a complete inactivation. Even when compared to spore formers, such as *Geobacillus stearothermophilus*, its resistance was similar, with a 4D value of 18.97 min. Spore formers have protection mechanisms such as coatings that wrap the dormant vital macromolecules, or reparation processes of damaged elements during germination that enhance their resistance (Nicholson et al., 2002). Considering the present results, the generation of the catalase enzyme by the SCV posed an increasing resistance of the MRSA till levels similar to the ones obtained with the spore formers mechanisms.

The model obtained in the present investigation showed a significant difference between the first 10 minutes of exposition and the last phase of the process. The resistance mechanism appears to be effective till the wetting is achieved. Then, the subsequent peroxide of hydrogen concentration increase overpasses the production of the protective enzyme (Mishra and Imlay, 2012). As soon as the number of hydrogen peroxide molecules reaching the planktonic cells is higher than the catalase enzyme production, the inactivation would occur. This balance is noticeably better when the wetting and penetration is total, and therefore the behavior observed in the later phase of the process is explained.

On the other hand, both strains of *L. monocytogenes* showed very low resistance against the atomization technology. The 4D values were 5.04 and 4.80 minutes for both strains, RO15 and Scott A, respectively. This microorganism is also a catalase-positive microorganism, and its catalase enzyme production is regulated by the catalase gene (kat). A relevant factor in the expression of this gen is the aerobic or anaerobic conditions that are used in the growth of the *L. monocytogenes*. Møretrø et al., (2019), demonstrated that the larger amount of oxygen present during the growth process, the larger the production of kat. Therefore, it is expected that the resistance against the hydrogen peroxide biocide would vary depending on the growth conditions.

In this assay, two different strains, both grown following the same aerobic method, showed resistance in any case, very low compared with the other microorganisms. Yun et al., (2012) showed that planktonic *L. monocytogenes* strains exhibited significantly different susceptibility to 1 % (w/w) H_2O_2, classifying the strain Scott A as a tolerable microorganism to this biocide. At higher concentrations (6 and 10 % (w/w)), the resistances between strains of *L. monocytogenes* were not significantly different. Furthermore, other studies confirmed the low resistance to this biocide, even in biofilm forms (Robbins et al., 2005).

Robbins et al. (2005) did also observe that concentrations of 5 and 6 %(w/w) of hydrogen peroxide reached a complete inactivation in 15 min approximately. The same study showed that in planktonic cells, the exposure times were reduced to up to 10 min using even lower concentrations, 3 and 4% w/w.

In the present study, with an 8 %(w/w) hydrogen peroxide solution, the complete inactivation was, as expected, even faster. Both strains were inactivated in less than 8 minutes, starting from a population higher than 10^6 in both cases.

Conclusions

There are different conclusions to be gathered from these experiments. The very first one, related to resistances, as the spore formers appear to be the most resistant, following the next sequence (from less to more resistant): *L. monocytogenes* Scott A ≤ *L. monocytogenes* RO15 < MRSA < *G. stearothermophilus* < *B. atrophaeus*.

Additionally, despite the overall lower resistance, the MRSA and *G. stearothermophilus* strains showed an initial higher resistance than the *B. atrophaeus*. This fact reflects the importance of hydrogen peroxide's gas and liquid phase in the inactivation mechanism depending on the microorganism. While one type of process, gas phase-based technology, would favor the initial inactivation of one type of spore (*B. atrophaeus*), a condensing promoter technology, would be better in the second phase. Still, many published reports argued the need to reach a certain condensation level to optimize the inactivation times (Choi et al., 2012; Møretrø et al., 2019; Pruß et al., 2012).

The gas or liquid state is promoted or diminished throughout the variation of temperature and relative humidity. Measuring the condensation level and controlling the temperature will assist in the characterization of the microorganism inactivation mechanisms depending on the hydrogen peroxide phases.

On the other hand, the MRSA's ability to mutate instantaneously (Painter et al., 2015) makes this microorganism a real threat that should be considered in all contamination control programs of the Healthcare industry. Contrary to the results of Pottage et al. (2012b), the MRSA strain showed a lower resistance than the *G. stearothermophilus* spore. However, considering its high resistance and its evolution over history is necessary to evaluate its presence even when treated with potent biocides such as hydrogen peroxide. It is particularly relevant to consider this microorganism's capacity to resist at the beginning of the exposure time, even higher than the spore formers. It appears that the catalase production defense mechanism is greater than the spore protecting layers, but only when a lower concentration of hydrogen peroxide is readily available (gas phase). If the disinfecting programs do not apply enough contact time between the biocide and the surface to be decontaminated, no complete inactivation will be achieved. Also, if the contact microorganism-biocide is not enough, the exposure to the active compound might be reduced, leading to a minimization of the effect. Thus, a thorough risk assessment should be made before implementing such a disinfecting technology in a place with the potential growth of MRSA.

The results regarding the resistance of *L. monocytogenes*, together with the type of surface or place where this microorganism could be, leads to the conclusion that even more critical than the disinfection technology itself, the sanitation program should include a thorough cleaning before disinfecting (Chen et al., 2015; Fan et al., 2019; Reis-Teixeira et al., 2017). Also, considering the ability of this microorganism to create biofilms reported in many studies, the process of exposing the microorganism to the biocide becomes more critical than the compound itself (Chen et al., 2015; Kocot and Olszewska, 2017; Reis-Teixeira et al., 2017; Robbins et al., 2005). That means that when discussing the atomization technology, achieving a uniform distribution, and reaching hidden areas becomes especially important. If the hydrogen peroxide can penetrate till the microorganism, the inactivation achieved can be total even in low concentrations and low exposure times.

6.3.2 GAS-LIQUID PHASE INACTIVATION KINETICS ASSESSMENT

6.3.2.1 INTRODUCTION

Many published reports argue about the microbial inactivation mechanism when different hydrogen peroxide technologies are applied. As demonstrated, and discussed during the previous experiment, the non-consensus mainly lies in the dichotomy between the most active physical status, gas, or liquid phase, of the hydrogen peroxide when it acts over the microorganisms.

Authors supporting the condensed phase as the most important form claim that as per the physic laws (thermodynamic principles discussed in chapter 4), the hydrogen peroxide even if injected in the gas phase, whenever the molecules will touch the cooler surfaces, condensation of the flash distilled hydrogen peroxide will appear (Agalloco, James, Akers, 2013; Davies et al., 2011; Drinkwater et al., 2009; Fu et al., 2012; Holmdahl et al., 2011; Jildeh et al., 2020; Richter, 2016). This condensation is unavoidable, and therefore, should be controlled to avoid material damage. They claim a controlled micro-condensed layer that enhances the inactivation properties. This process was patented by Bioquell, GB9523717 (Watling, 1995).

On the other hand, authors supporting the gas phase mechanism (dry) claim that no condensation appears as the system is not in equilibrium. Only the gas phase is inactivating the potential bioburden of the surface, being the base of the patent of Steris in US416912 (Moore and Perkinson, 1979). The environmental conditions are maintained to avoid condensation at all times, avoiding this way, material damage (Chan et al., 2011; Chung et al., 2012.; Falagas et al., 2011; Kaer et al., 2012; Kirchner et al., 2013; Sandle, 2013).

The atomization technology is a liquid-phase process, but as in equilibrium, the gas phase (vapor) is also available in the system. Not in the levels of the previous methods (500 to 1000 ppm), but concentrations higher than 100 ppm are usually obtained when working at temperatures above 20 ºC. To assess the action of each phase in a technology based in atomization, a study separating the two phases would be required. However, at least with the means available at the thesis development time, it is difficult to separate both states. Therefore, two different variables, micro-condensation, and temperature will be monitored and related to one or the other matter status and eventually conclude how the inactivation kinetics are affected.

The CFD software previously used allowed the identification of areas of a specific volume with less particle density, and therefore, with a lower probability to be decontaminated with hydrogen peroxide in the liquid phase. In previous studies, such as the one published by Ito et al. (2016), CFD tools had been already used to model vaporized hydrogen peroxide distribution across a cleanroom. They proved that differences could be expected depending not only on the injection system position itself but also on the surfaces' temperature, type of material, and even the natural catalysts that the chemical might interfere with. Also, other studies focused on the distribution by assessing, empirically, microbial reduction in different points of a single volume and monitoring the reaching of the hydrogen peroxide particles using a condensing sensor (Chen and Chen, 2010; Hayrapetyan et al., 2020; Unger-Bimczok et al., 2008). Still, none of these studies created a CFD model that was afterwards validated with empirical data. Consequently,

this experiment aimed to obtain a model that allowed to predict the system's final answer associated with the microbial lethality depending on the time and the condensation factors.

On the other hand, temperature, as discussed in previous experiments, have a key effect, not just in the behavior of the hydrogen peroxide from the physical perspective but also in the decomposition rate of the hydrogen peroxide. Physically, the most important factors to be considered are the gas phase availability as well as the intrinsic higher kinetic energy the molecules have in this matter status (Soroush and Bahadori, 2017). Regarding the chemical perspective, it is worth reminding that one of the main resistance mechanisms, like catalase enzyme acting as a catalyst of the decomposition reaction discussed in chapter 4, relies on the ability to decompose faster than the arrival and penetration of the hydrogen peroxide into the vital components of the microorganisms. Thus, the lower the temperature, the slower this reaction would also be, and therefore, from this perspective, a faster inactivation would occur.

In previous chapters of this PhD dissertation, it was already observed that microbial inactivation was not complete when higher temperatures were present. That led to the assumption that, in those cases, the concentration of hydrogen peroxide would remain in the sub-lethal range. So that, the higher the temperature, lesser condensed or wet phase of hydrogen peroxide could reach the biological indicators. The microbiocidal efficacy would depend on the hydrogen peroxide concentration in gas-phase, which would be 200-300 times lower than in the wet phase.

Therefore, this experiment aimed to obtain a model that allow to predict the system's final answer associated with the microbial lethality depending on time, condensation and temperature.

6.3.2.2 MATERIAL AND METHOD

Three aspects should be considered to design the experiment. Particle reach or micro-condensation characterization, temperature assessment and microbial inactivation.

1) Micro-condensation

The particle reach (micro-condensation of the generated atomized hydrogen peroxide) characterization was done by means of a sensor developed by CiS Research Institute (CiS Forschungsinstitut für Mikrosensorik GmbH, Erfurt, Germany). The sensor BTF11356A (Figure 69) detects the condensed phase in a surface due to a change in the resistance in the electronic circuit. A multimeter to measure the voltage difference (output signal of the sensor) was used. The output signal was then corrected to nanograms of liquid hydrogen peroxide per mm^2, following equation 25:

$$M = 15 \times (V - b)$$

Equation 25 Quantification of hydrogen peroxide liquid per mm^2

Where M refers to the hydrogen peroxide in nanogram per mm^2, V refers to the measured voltage in mV, and b to the background measurement.

Figure 69 Microcondensation sensor BTF11356A

All six surfaces of the isolator were monitored in at least 2 points of measurement (Figure 70). Moreover, the output value for every surface and point was measured every 30 seconds until the first air pulse and then every minute. Three levels of condensation were defined: High, Medium, and Low. During the process of atomization with the ionHP+ technology, the relative humidity was not controlled, although it was registered with a RH monitoring sensor (Sensor Push, New York, USA)

The recipe for this charcterization was optimized, reducing the dwell time and with the next parameters: a) Airflow: 80 L/min, b) Liquid flow: 8 mL/min, c) Exposition time: 15 min, d) Air pulses: 3 with a duration of 2 seconds each at 6.5, 11 and 15 min, e) Total injection of water: 12 mL (20 mL/m^3).

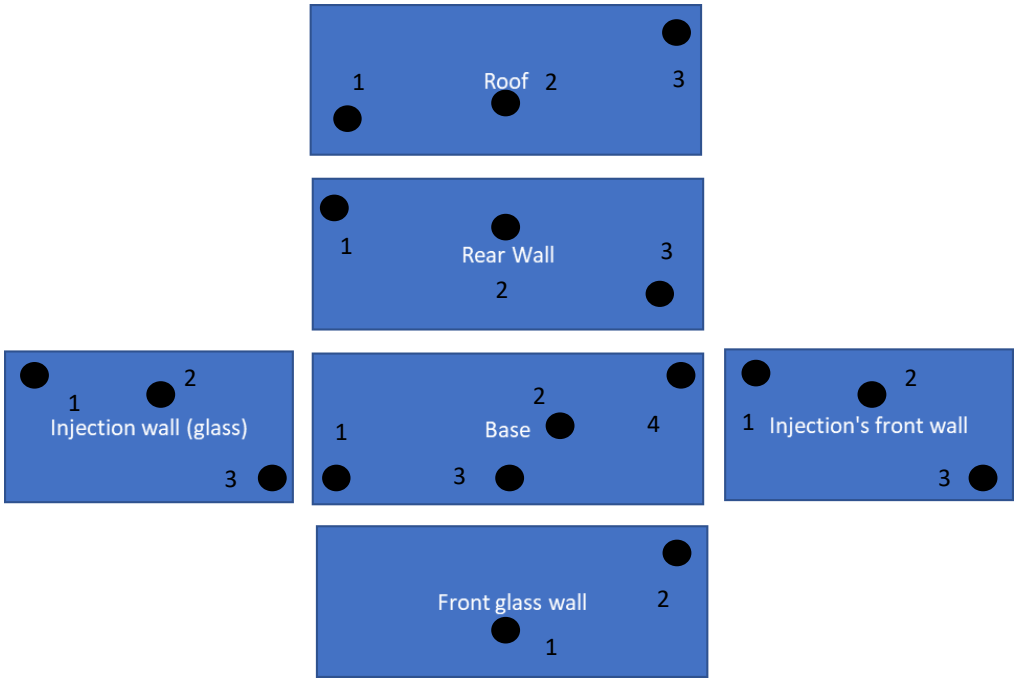

Figure 70 Volume surface micro-condensation characterization

2) Temperature

No control of temperature was fitted into the testing isolator. Therefore, no specific testing was performed for this variable characterization as it could not be directly modified or controlled.

All assays were done at room temperature and were classified into two levels of temperature. One group of assays (T1) was performed at a temperature of 21.60 ± 0.15 ºC and the other (T2) at 25.80 ºC ± 0.4 ºC. The temperature measurement was done by the installed Temperature and RH monitoring sensor (Sensor Push). The position of the

bioindicators was the same as the experiment 1. Both spore formers, *Bacillus atrophaeus* and *G. stearothermophilus* were analyzed at both temperature levels using commercial biological indicators (Mesalab).

3) Microbial inactivation

As in previous experiments, once the treatment time had elapsed at different times, the bioindicators were removed from the isolator. Then, again, the method suggested by Chen et al. (2015) for recovering the microorganisms from the bioindicators in these surfaces was followed. The commercial biological indicators were placed in a 5 mL solution of DENB (Dey-Engley neutralizing broth, Sigma-Aldrich. St Louis, USA) in a 10 mL tube with 0.5 g of sterile glass beads of 2 mm in diameter (Vidra Foc).

4) Data analysis and modelling

In the micro-condensation assessment, a minimum set of three experiments, with triplicate bioindicator per position was done. One of each experiment was related to a level of micro-condensation, High, Medium, and Low.

On the other hand, the temperature assessment counted with two, and five experiments, at T2 and T1 respectively.

The GInaFIT computer tool (Geeraerd et al., 2005) was used to determine the bacterial inactivation curve and 4D value. The best fit indicators to the determine the accuracy of the model were the adjusted coefficient of determination ($R^2_{adjusted}$) and the minimum Root Mean square deviation (RMSE). The prediction bands of the graphs, the standard error (SE), and the confidence intervals (CI) of the different parameters and statistical measures were obtained using the GraphPad Prism computer tool (GraphPad Software Inc., San Diego, CA, USA).

Minitab (Minitab Inc. State College, Pennsylvania, US) was used to aid in the surface characterization, identifying the significant differences in between the levels.

6.3.2.3 RESULTS

1) Micro-condensation

A mapping of the isolator was done, showing the densest areas of the isolator in terms of particle accumulation. Table 16 shows three points remarkably differentiated from the others, Base 3, Glass Front Wall 1 (G Front Wall 1) and Glass Front Wall 2 (G Front Wall 2), not just having the highest values in Maximum and Average ng/mm^2 but also in the standard deviation. The higher standard deviation was related to the actual exposure to the injection jet.

The points placed close to the glass wall showed a high particle reach, with maximum values beyond the sensor limit (>14,080 ng/mm^2) (data not shown). In addition, as expected, the Base 3 position showed a significantly higher value. While the standard deviation in high particle reach positions is above 4,000 ng/mm^2, in the rest of the positions, it remained below 500 ng/mm^2.

On the other hand, the Injection front wall, Injection wall, and the Base 1 points showed the lowest values of particle reach with lower than 500 ng/mm^2.

Throughout this mapping study, it appeared that even if some of the points replicated the CFD results in terms of particle reach, others were significantly different. It was evident

after this experiment that the CFD model should consider the same geometrical dimensions as well as thoroughly represent the air streamlines by positioning the air extraction in the correct area. Otherwise, the model will not serve as a prediction tool.

Table 16 Statistical data per isolator position (28 points in ng/mm^2)

Position	N	Mean	Standard deviation	Standard Error
Base 1	28	359	130	24
Base 2	28	814	272	51
Base 3	28	9,698	4,598	869
Base 4	28	1,134	577	109
I Front wall 1	28	281	41	8
I Front wall 2	28	579	89	16
I Front wall 3	28	250	77	14
Injection wall 1	28	306	156	29
Injection wall 2	28	476	206	39
Injection wall 3	28	428	206	39
Rear wall 1	28	246	141	27
Rear wall 2	28	237	131	25
Rear wall 3	28	243	145	28
G Front wall 1	28	12,237	5,356	1,012
G Front wall 2	28	11,904	5,279	998
Roof 1	28	1,887	859	162
Roof 2	28	2,138	1,044	197
Roof 3	28	2,530	1,200	227

In Figure 71, the signal in mV (output of the micro-condensation sensor) was transformed to ng/mm^2 (y-axis) showing how the liquid phase reached, depend on time (x-axis), each of the mapped points of the isolator. Significant differences ($p<0.05$) were observed in particle reach, between zones Base 3, G Front Wall 1 and G Front Wall 2 and the rest of the positions.

The relief valve (exhaust of air) was placed at the Rear wall 1. So that, although the air streamlines were directed towards that point, and the particles were eventually reaching to this place, due to the high convection factor that favors the gasification of the liquid phase, the condensation would be low.

The base 3 point showed an increasing trend of particle reach as consequence of the gravity. Even if, Base 1, 2 and 4 particle reach were stable over time, in the Base 4, a slight decrease was observed in the liquid phase content.

The roof, in every position, showed a good reach, with an average of 2,185 ng/mm^2 in the three screened positions.

In Figure 72, a zoom of the lower particle reach values is presented. Four events can be seen in the whole process: injection, pulse 1, pulse 2, pulse 3 and start of the aeration that are identified in the graph.

In point 1, the pulse of 6.5 minutes, shows in most of places of the isolator, an increase of the particle reaches in this instant. It was a sudden increase, but that, in less than a minute, the previous value is recovered. In the second pulse (point 2) a certain effect

was observed close to the injection nozzle, but it was insignificant when measuring far from the air inlet, front wall, or Base 4 points. Finally, in point 3, the start of the aeration, clearly impacts in the liquid phase present in the isolator. All points reached the lowest value after three minutes from the start of the aeration. There were no significant differences in between the different points. The points starting from a higher value such as the Glass Front wall points, took longer to be dry.

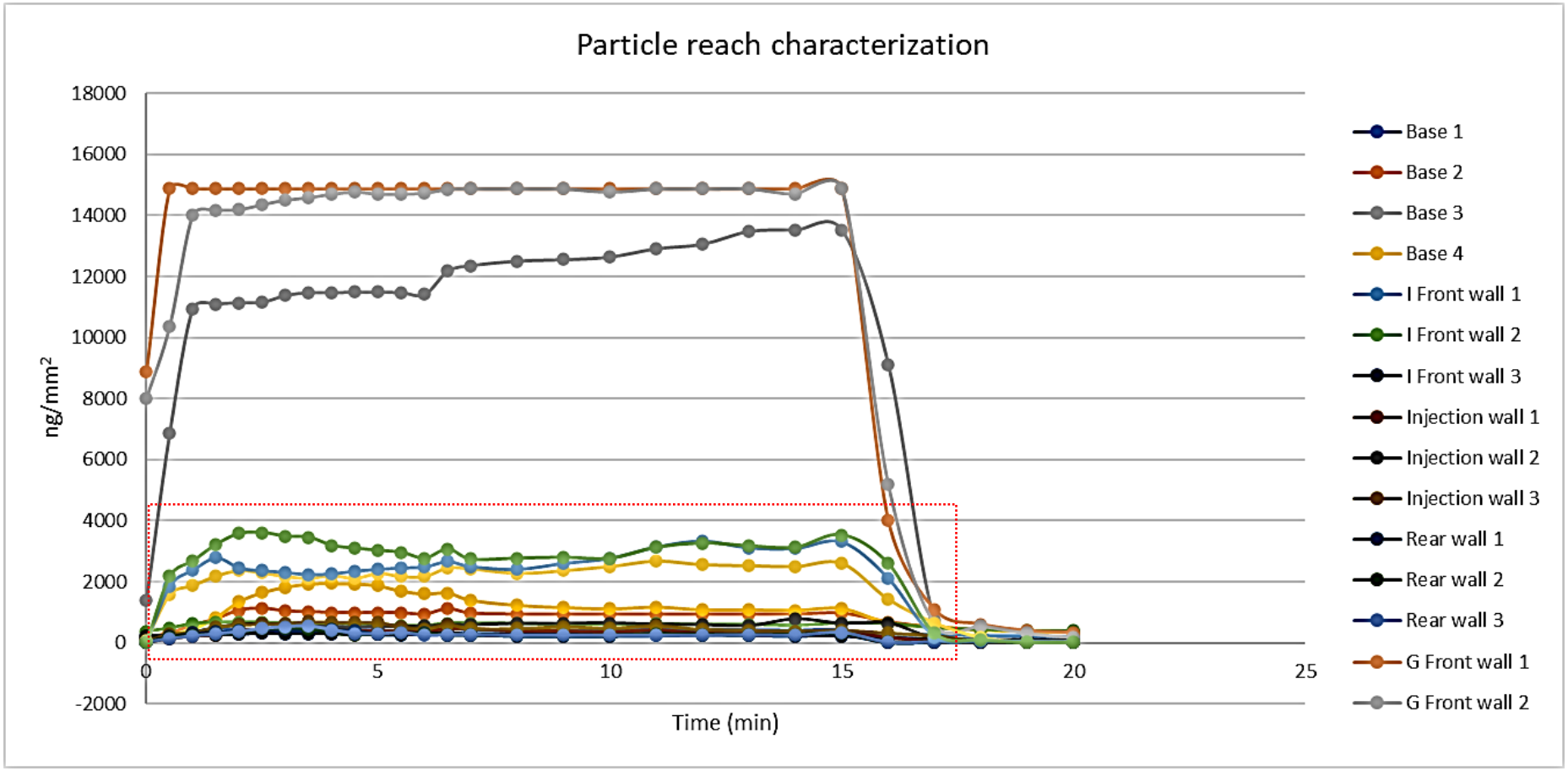

Figure 71 Particle reach distribution for each position of the isolator in function of time. The red square shows the lowest particle reach (see Figure 72 zoom)

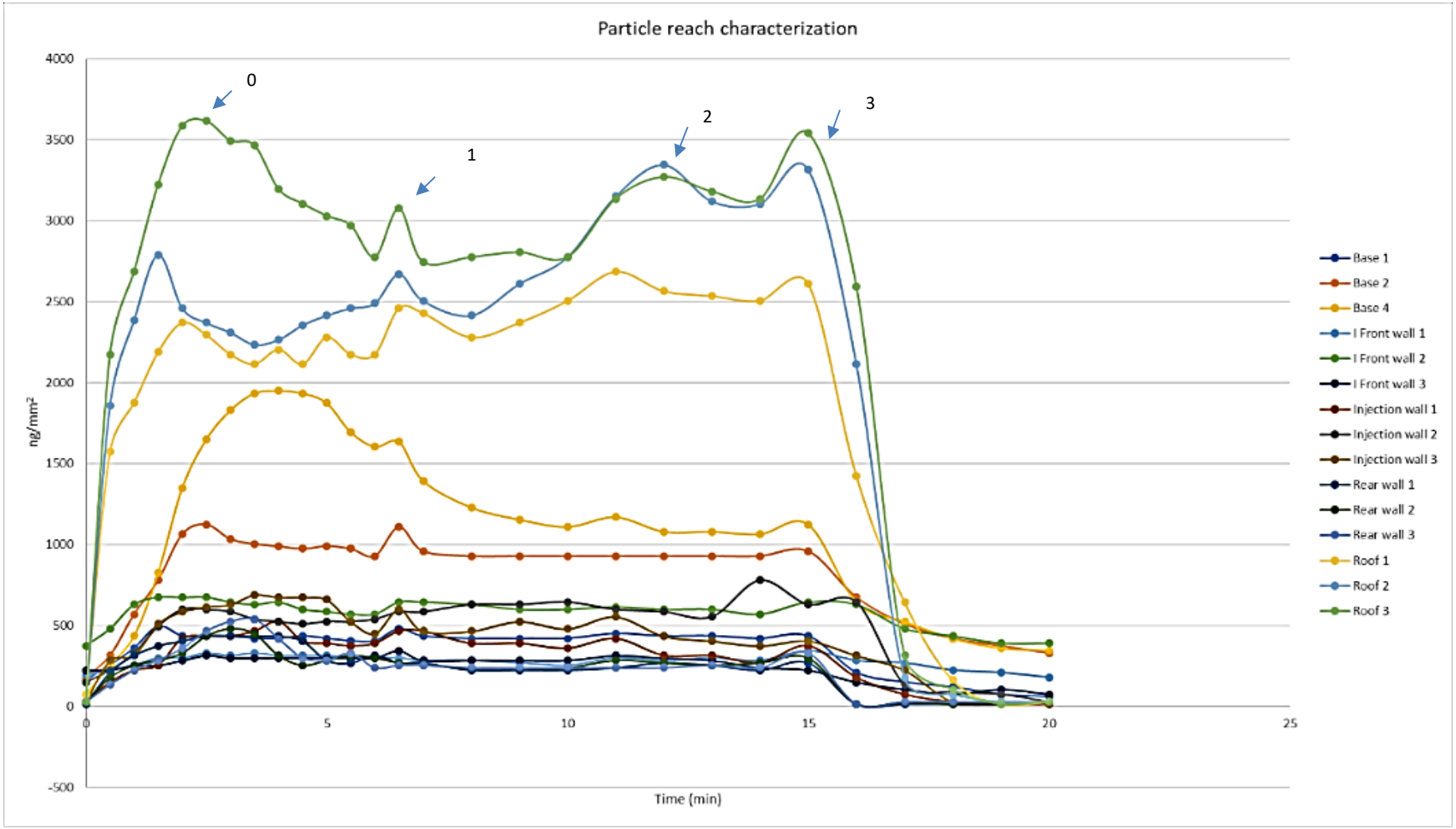

Figure 72 Red squared location (zoom) of Figure 71. Arrow 0 represents the end of injection and Arrows 1 to 3 represents when the pulses of air take place; after pulse 3 the aeration starts

After this analysis, three positions with significant differences between them ($p<0.05$) were defined to perform the microbial inactivation experiment. The High position assays corresponded to the Base 3 position, where previous experiments of *G. stearothermophilus* inactivation were performed. Then, due to constraints of the isolator design, the Medium and Low positions selected were the Base 4 and Injection wall 2 positions, respectively. Figure 73 shows the real micro-condensation data gathered during the microbial inactivation experiment.

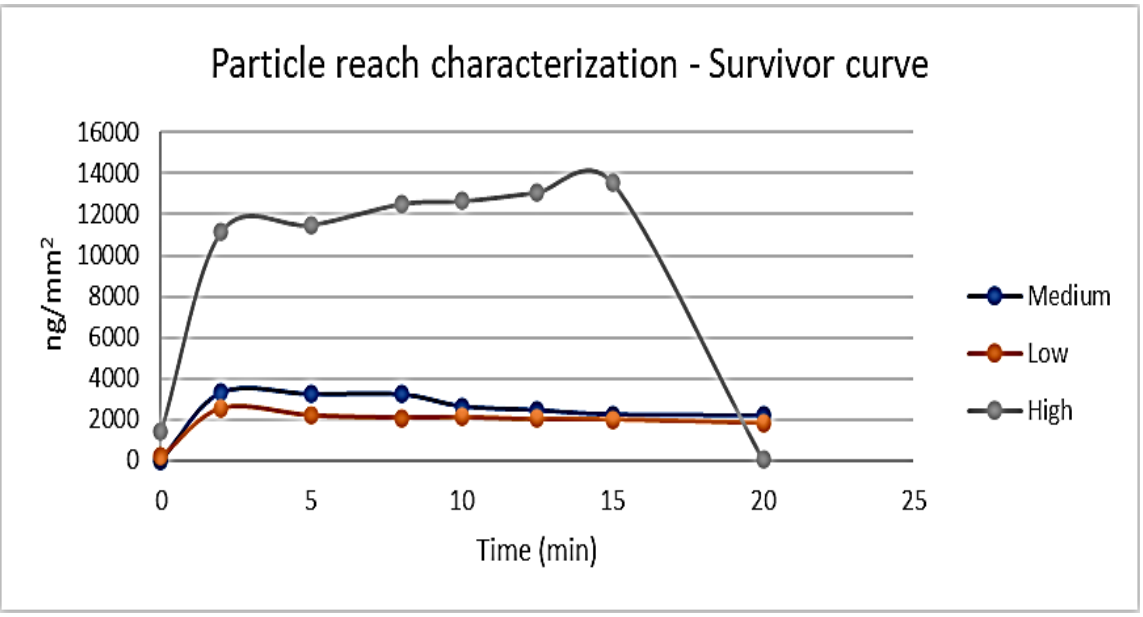

Figure 73 High, medium and low particle reach levels.

During this experiment, the mean value obtained in the Injection wall 2 was 1.883 ng/mm^2 (compared with 675 ng/mm^2 registered during the isolator mapping). In case of the Base 4, the mean value was 2.418 ng/mm2 (compared 1950 ng/mm^2), 28.4% higher than in the experiment of the isolator mapping.

The temperature and hydrogen peroxide concentration (ppm) levels followed the same trend as in Experiment 1, but the absolute values in temperature and ppm levels were different in experiments with Low and Medium particle reach compared to the High level. As the environmental temperature was not controlled in the isolator or the room, these differences were part of the experiment. Table 17 shows the mean and standard deviation for each of the experiments. As expected, the higher the temperature, the more available gas phase (higher ppm level).

Table 17 Temperature and ppm levels for High, Medium and Low Reach experiments

Position	Temperature (ºC)	Gas phase (ppm level)
High	21.6 ± 0.5	105.9 ± 20
Medium	22.6 ± 0.3	118.3 ± 25
Low	24.9 ± 0.3	171.6 ± 36

Additionally, in the current experiment, even though the Relative Humidity was not controlled, continuous monitoring of the %RH variation over time was performed. A similar trend was obtained in this parameter in all assays (Figure 74). At the start of the

injection (a), at 2 min, 55.0 %RH was measured. During the injection (b, 4 min), the relative humidity reached 65.0 %RH, and just at the end of it (c, 6 min), the value was in the range of 80.0 %RH. Then, the relative humidity continues increasing till almost the start of the aeration.

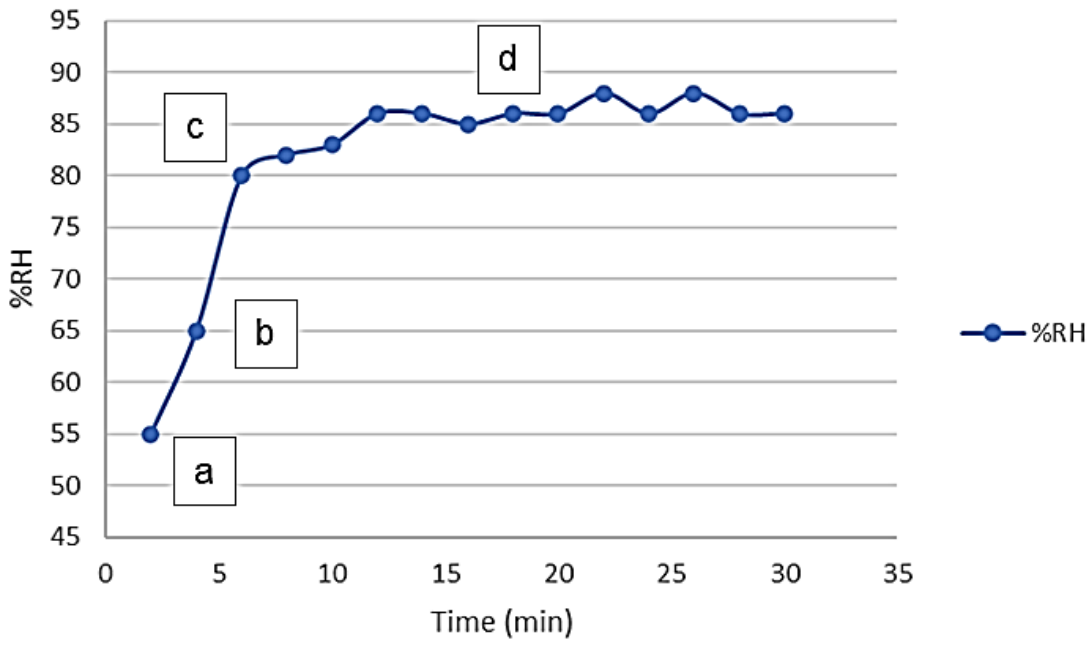

Figure 74 Relative humidity trend during a representative cycle. a-d represents 4 different points in time a) injection start, b, injection on-ongoing, c) end of injection and d) maximum % RH achieved

The microbiological experimental data was adjusted to Weibull inactivation models proposed by Marfart et al. (2002). All the three levels of micro-condensation were adjusted to the same model (Figure 75 and Table 18).

The results showed a faster inactivation in Low than in Medium and High micro-condensation. The 4D value for the High and Medium levels was 8.5 min, while for Low micro-condensation was 7.25 min. While to reach complete inactivation for High and Medium particle reach, 15 min of exposure were required, for Low particle reach 10 min were needed. The shape parameter (p) was slightly concave ($p<1$) in Medium and High micro-condensation levels, and in Low micro-condensation level was slightly convex ($p>1$). This fact was also reflected in the delta parameter (δ), following the order (from higher to lower: Low > High > Medium. In any case, high variability was obtained in the different kinetics parameters (Table 18), being necessary more experiments to confirm these results.

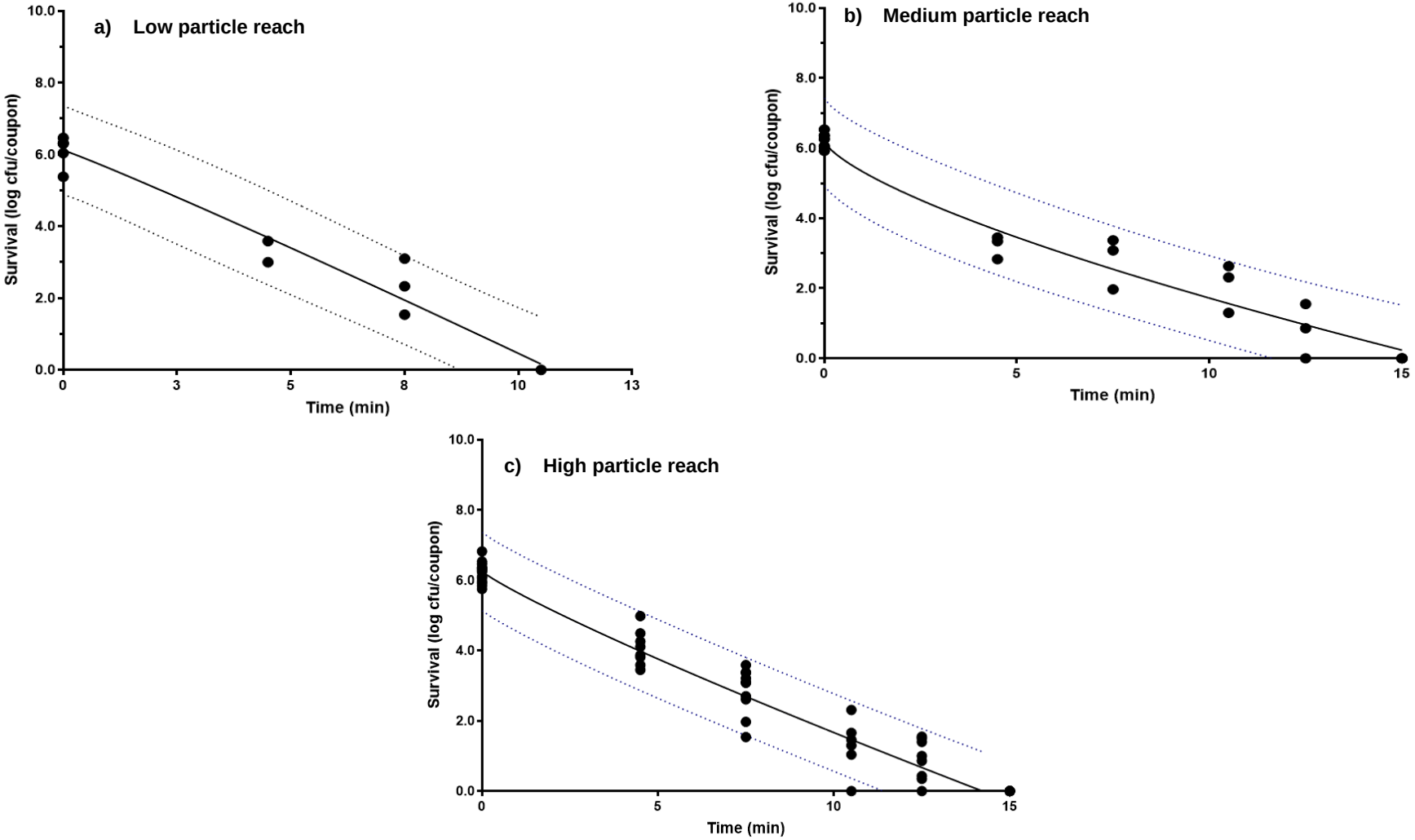

Figure 75 Inactivation models of G. stearothermophilus at High c), Medium b) and Low particle a) reach

Table 18 Statistical indexes and parameter estimation (mean, standard deviations and 95% confidence intervals) of the inactivation model used for G. stearothermophilus at High, Medium and Low particle reach during the atomization technology ionHP+.

Parameter	Unit	High	Medium	Low
Log (N_0) ± SE	log cfu/coupon	6.26 ± 0.12	6.22 ± 0.23	6.12 ± 0.21
Log (N_0) (95 % CI)	log cfu/coupon	6.01-6.51	5.74-6.70	5.65-6.59
δ ± SE	min	1.76 ± 0.27	1.18 ± 0.43	1.94 ± 0.53
δ (95 % CI)	min	1.27-2.33	0.42-2.32	0.83-3.22
p ± SE	-	0.88 ± 0.06	0.70 ± 0.10	1.06 ± 0.17
p (95 % CI)	-	0.76-1.01	0.49-0.96	0.69-1.51
4D	min	8.55	8.55	7.25
R^2 (adjusted)	-	0.954	0.944	0.958
RMSE	-	0.545	0.556	0.521

N_0: the initial population, Kmax: inactivation constant of the linear model, δ: time to achieve the first Log-reduction, p: the shape of the inactivation curve, 4D: time to achieve a 4-log reduction, RMSE: Root Mean Squared Error.SE: standard error; 95% CI 95% confidence interval.

2) Temperature

Microbial inactivation of both spore forms was analyzed at two levels of temperature T1 (21.6 ± 0.15 ºC) and T2 (25.8 ºC ± 0.4 ºC). In this case, the models that better fit the experimental data were the Weibull proposed by Marfart et al. (2002) and the Log-linear proposed by Bigelow and Esty (1920), the Geeraerd-tail model proposed by Geeraerd et al. (2000) and Double Weibull proposed by Coroller et al. (2006). The equations for the Geeraerd-tail and Double Weibull model were (Equation 26 and 27):

$$Log\ (N) = Log\ [(10^{N0} - 10^{Nres}) \times e^{-Kmax\ t} \times +10^{Nres}]$$

Equation 26 Geeraerd-tail model (Geeraerd et al., 2000)

Where the N_0 refers to the initial population, N_{res} refers to the residual population after stabilization, $Kmax$ parameter refers to the inactivation constant of the linear model, and t the time of treatment.

$$Log\ (N) = Log\ (10^{N0}) - Log\left(10^{(1+10^{\alpha})} \times 10^{\left(-\frac{t}{\delta 1}\right)^{p+\alpha}} \times (10^{\left(-\frac{t}{\delta 2}\right)^{p}}\right)$$

Equation 27 Double Weibull inactivation model (*Coroller et al., 2006)*

Where the N_0 refers to the initial population, the α parameter refers to the fraction of the first subpopulation remaining in the total population, the δ_1 and δ_2 refer to the time to first Log-reduction for the double curve, p to the shape of the inactivation curve, and *t* and t the treatment time.

The parameters and the statistical data for each model is summarized in Table 19.

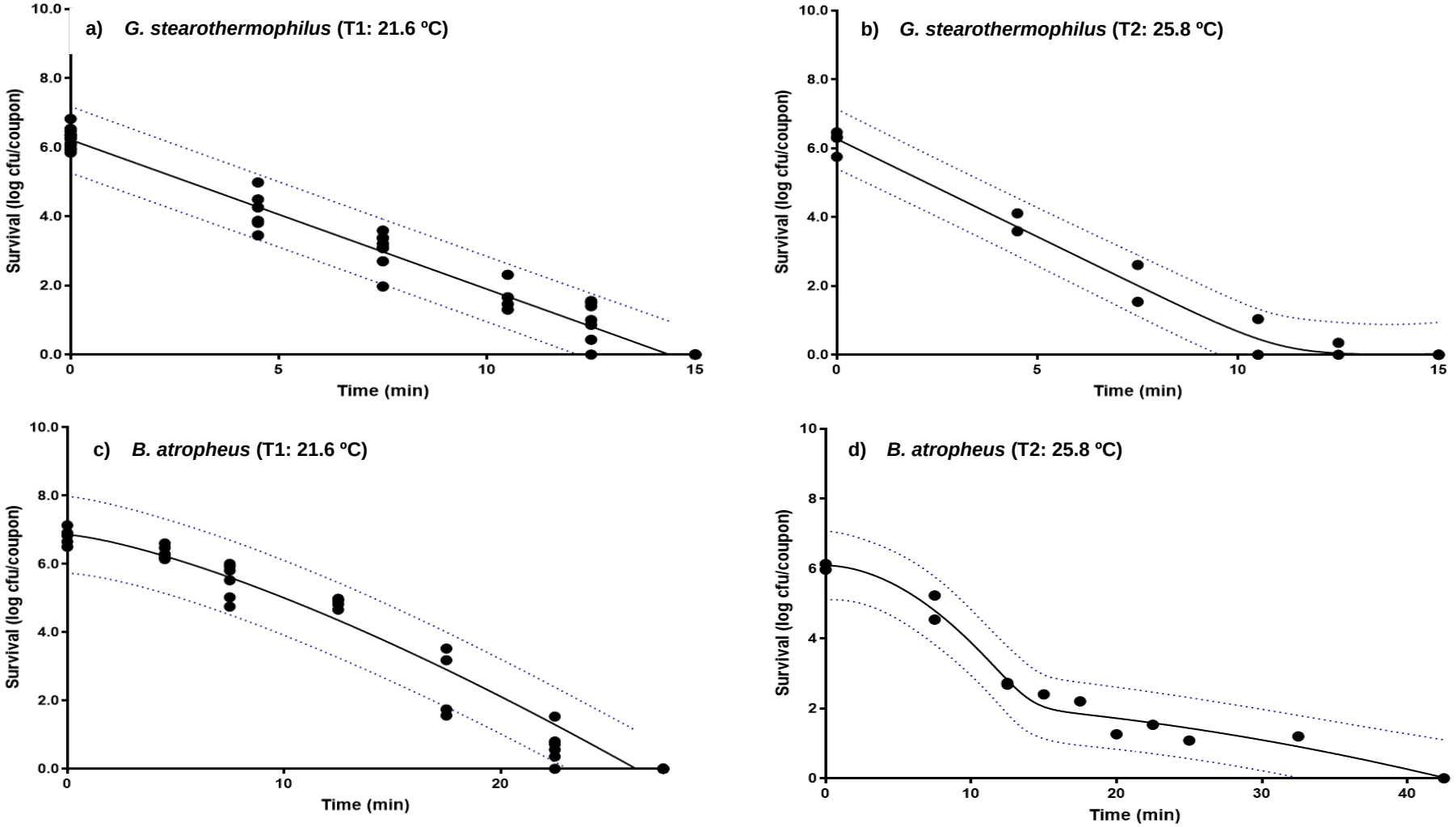

Figure 76 Inactivation models of G. stearothemophilus and B. atropheaus depending on environmental tempèrature: a) G. stearothermophilus (log-linear) at 21.6 ºC (T1), b) G, stearothermophilus (Geeraerd-tail) at 25.8 º C (T2), c) B. atrophaeus (Weibull) at 21.6 º C (T1) and d) B. atropheaus (Double Weibull) at 25.8 º C (T2) during throughout the ionHP+ hydrogen peroxide technology

Table 19 Statistical indexes and parameter estimation (mean, standard deviations and 95% confidence intervals) of the inactivation model used for G. stearothermophilus ans B atropheaus at T1 (21.6 ºC) and T2 (25.8ºC) during the atomization technology ionHP+.

		G. stearothemophilus		***B. atrophaeus***	
Parameter	**Unit**	**T1[a]**	**T2[b]**	**T1[c]**	**T2[d]**
Log (N_0) ± SE	log cfu/coupon	6.22 ± 0.11	6.27± 0.15	6.85 ± 0.17	6.09 ± 0.24
Log (N_0) (95% CI)	log cfu/ coupon	5.60-6.44	5.95-6.60	6.54-7.18	5.54-6.65
Log (N_{res}) ± SE	log cfu/coupon		0.0043 ±0.16		
Log (N_{res}) (95% CI)	log cfu/coupon		-0.348-0-0.317		
K_{max} ± SE	log cfu/min	1.00 ± 0.03	1.31 ± 0.07		
K_{max} (95% CI)	log cfu/min	0.94-1.05	1.18-1.46		
α ± SE	log cfu/coupon		5.75 ± 1.93		3.82 ± 0.33
α (95% CI)	log cfu/coupon				2.95-4.59
δ_1 ± SE	min			6.37 ± 0.74	6.54 ± 1.09
δ_1 (95% CI)	min			5.05-7.81	3.84-9.00
δ_2 ± SE	min				27.55 ± 4.82
δ_2 (95% CI)					14.91-42.19
p ± SE	-			1.36 ± 0.10	1.87±0.42
p (95% CI)	-			1.18-1.57	1.03-3.42
4D	min	9.3	7.05	17.88	14.88
R^2 (adjusted)	-	0.963	0.982	0.957	0.973
RMSE	-	0.463	0.337	0.533	0.330

N_0: the initial population, N_{res}: residual cell concentration after stabilisation at the end of the decrease, Kmax: inactivation constant of the linear model, α: fraction of the first subpopulation remaining in the total population, δ_1 and δ_2: the time to first Log-reduction for the double curve, p: the shape of the inactivation curve, 4D: time to achieve a 4-log reduction, RMSE: Root Mean Squared Error, SE: standard error; 95% CI: 95% confidence interval.a) Log-lineal inactivation model, b) Geeraerd tail inactivation model, c) Weibull inactivation model, and d) Double Weibull inactivation model.

The results showed that, at a higher temperature, the inactivation of both sporulated microorganisms was faster.

The *Geobacillus stearothermophilus* kinetic constant*, Kmax*, was approximately 30% higher at T2 level than at T1. The 4D value changed from 9.30 min to 7.05 min when the temperature was increased. To achieve total inactivation, at least 15 min were required in both cases.

In case of the *B. atropheaus,* the impact of temperature was even more significant. While this spore showed a similar 4D value reduction, the shape of the curve changed from a Weibull model with a remarkable linearity at T1, to a curve, where two different resistances were identified. At T2 level, a steep reduction was identified at the beginning of the exposure, at the first 15 min. However, afterwards, the lethality was notably reduced, showing a δ_2 of 27.55 min. The total inactivation at T2 was enlarged to more than 40 min of exposure.

The α refers to the fraction of the first subpopulation in the total population. While the *Geobacillus stearothermophilus* spore was close to be fully inactivated at the turning point (5.75 ± 1.93 versus the initial 6.06 ± 0.18), the second spore former, still has a high remaining population when the behaviour changed.

6.3.2.4 DISCUSSION AND CONCLUSIONS

1) Micro-condensation

A slightly faster inactivation of the *G. stearothermophilus* was obtained in Low particle reach conditions compared to Medium and High particle reach. Achieving complete lethality for High and Medium particle reach required at least 15 min of exposure. On the other hand, in Low particle reach, the exposure time was reduced to 10 min.

It was already demonstrated by Hayrapetyan et al., (2020) that in an atomization system where both phases (liquid and gas) are present, areas of more wettability did show lower inactivation rates than the ones subjected (initially) only to the gas phase. In this study, the wettability was also related to the particle reach, so analogously, the slower inactivation was found to be, the one with better particle reach. It was assumed that when both phases were present, the effective concentration that reached the spore required a first hydration step to enter into the inner components and damage the DNA of the *G. stearothemophilus* spore. This hydration step was the limiting step in the overall inactivation process.

On the other hand, in positions of lower wettability the hydration step was not occurring or occurring after the gas phase already started the inactivation process. The gas phase molecules, with higher kinetic energy, would directly enter into the spore's membrane and start damaging, throughout the Fenton's reaction, the DNA (Hayrapetyan et al., 2020b; Tachiev et al., 2000).

Another study performed by Unger-Bimczok et al., (2008), also discussed about the impact of the condensation over the inactivation of the same spore. They demonstrated that micro-condensation, above 2,900 ng/mm^2, did not improve the inactivation capability of the hydrogen peroxide. According to this study, there is a balance, at this particular moment (what they called subvisible condensation), where an increase in hydrogen peroxide solution would only generate a thicker layer of the solution, but with no extra biocidal activity.

All assays performed under this investigation created an atmosphere that was over the visible spectrum. The slight difference between particle reach levels was again the gas phase activity. In the Low particle reach assay, the liquid phase took longer to arrive to the position, and during that time only the gas phase started the inactivation.

The environmental conditions, Temperature and Relative Humidity were monitored. As described in Table 17, while the Medium and Low particle reach experiments were performed at 22.6 ± 0.3 and 24.9 ± 0.3 ºC, the High particle reach experiment was performed at 21.6 ± 0.5 ºC. The higher the temperature, the higher available gas phase in the system. In addition, the gas phase tops during the injection phase.

The Relative Humidity variable followed the trend showed in Figure 74. At the start of the injection (a), at 2 min, 55,0 %RH was measured. During the injection (b, 4 min) the relative humidity reached 65 %RH, and just at the end of it (c, 6 min), the value was in the range of 80 %RH. Then, the relative humidity continued increasing till the start of the aeration.

The same study performed by Unger-Bimczok et al., (2008), discussed the correlation between temperature, relative humidity, and inactivation time. The results showed that in low humidity levels (HL1, < 64,5% RH), the gas phase played a very significant role in

the process. In Low Humidity levels, changing the gas phase from 400 to 600 ppm remarkably increased the inactivation speed. While at 400 ppm, full inactivation required more than 15 min, at 600 ppm less than 6 min were required. On the other hand, at higher humidity levels (HL2, 95% RH), the inactivation rates were the same no matter the gas phase available in the system.

Discussing the current assays data, two facts should be discussed. The experiments counted with a different available gas phase quantity, and the difference was higher during the first 5 minutes (when the ppm level tops) of the experiment. In addition, the relative humidity trend showed that while point *a* and *b* (2 and 4 min since the start of the injection) are in the HL1 level of the Unger-Bimczok et al., (2008) experiment, the point *c* is already in HL4 values. Therefore, at the beginning of the inactivation, during the injection phase, and few minutes after, where the relative humidity is still in low values (*a* and *b)*, the gas phase plays a very important role. The microorganisms' membrane, at low relative humidity values, would be better penetrated by hydrogen peroxide with higher kinetic energy (Kimura, 2012).

In conclusion, the higher the gas phase and the lower the particle reach, appears to be the best combination for a faster log reduction in the first minutes of the process. It is important to highlight the importance of the initial relative humidity over this combination, as if this parameter is already high, the wetting would still take place and the impact of the higher or lower temperature, hence gas phase, would be lower.

It is also significant that even if lower particle reach would favour the initial log reduction, if no liquid or condense phase reaches the spore location, the available hydrogen peroxide concentration would not be enough to reach a complete inactivation. It is the hypothesis of this author, that a minimum particle reach would be required to ensure a reliable process and ensure a 6-log reduction of such microorganisms.

2) Temperature

In addition to the particle reach characterization, two temperature levels (T1 and T2) were analyzed from the microbial inactivation perspective. These two levels were studied for both spore formers bacteria, *G. stearothermophilus* and *B. atropheaus*. The results confirmed the previous assays, showing that higher temperatures during the decontamination process led to a faster inactivation. Despite the similarities and previous arguments related to the impact of the relative humidity, temperature, and gas-phase form over the microbial inactivation, it is worth discussing the differences between the identified models for both microorganisms and temperature levels.

When the temperature was increased, a different resistance behavior was observed. The models of microbial inactivation were non-log-linear in both microorganisms, but differences in models with better fit were obtained. While the *G. stearothermophilus* showed a slight tailing at the end of the exposure time, the *B. atrophaeus* showed an inactivation model with two different resistances, at the initial and final part of the treatments (Double Weibull). Pruß et al. (2012) already identified a non-log-linear model in the *B. atrophaeus* spores. In their experiment, the temperature of a specific surface, already with condensed hydrogen peroxide, was heated up. These authors observed that the inactivation rate dramatically increased when the dew point of the hydrogen peroxide solution was overpassed, and the re-evaporation occurred (gas phase quantity increase).

In the current research, a similar effect was observed. At 25.8 ºC (T2), when a higher gas phase was available, a much higher reduction rate was obtained during the first 5 to 10 minutes (δ1 of 6.54 ± 1.09). However, when the particle reached the microorganisms, and both phases (liquid and gas) were present, the reduction rate changed, showing a δ2 of 27.55 ± 4.82.

Regarding the *G. stearothermophilus*, the only effect to be considered is that, as the wettability influence is lower (lower hydrophobicity), the model of microbial inactivation was essentially log-linear. The tailing at the end of the exposure time that appeared at T2 might be related to the available concentration of hydrogen peroxide. Nevertheless, with the low data of this particular experiment, no definitive conclusions can be made.

Finally, and according to Pruß et al. (2012), it is crucial not only the environmental temperature but also the temperature of the biological indicator itself at the time of the experiment. The colder, the easier it is to get the condensed phase and act as a nucleus where the higher composition of the hydrogen peroxide would concentrate.

6.3.3 TYPE OF BIOINDICATORS LETHALITY ASSESSMENT

6.3.3.1 INTRODUCTION

Biological indicators are the main tool to ensure the efficiency of a decontamination process and validate it. Bacterial spores are commonly the microorganisms of use due to their proved high resistance to chemical and physical methods of sterilization (Raguse et al., 2016).

The manufacturing and commercialization of BIs is well regulated, and standards such as the ISO 11138, set the basis to reduce as much as possible the variability of the microorganism's population. However, even with certain standards in place, the extrinsic and intrinsic variations of the same reference microorganism, make that the development of sterilization, or disinfection cycles, is also dependent on the BI to be used (Castro et al., 2011). These variations can be very different, from alteration of the sporulation conditions, to the choose of the carrier material, or the spores' deposition technique.

Although it was not the initial purpose of the present investigation, the absolute results in the total time to reach complete lethality, led the author to further look into the type of bioindicators used during the previous studies. Two types of bioindicators were used, own-manufactured following the method proposed by Wells-Bennick et al., (2019) and commercial BIs depending on the study. During the comparison between the different spore formers and vegetative bacteria, own manufactured BIs were used and the *G. stearothermophilus* spore showed a 4D value of 21.5 min. However, when the same spore was used for the gas-liquid phase lethality assessment, and commercial BIs were used, the 4D value, at similar environmental conditions and position, was reduced to 8.55 min.

Therefore, the objective of this assessment is to evaluate the impact of the manufacturing process over the resistance of the same microorganism. Both spore forms, *G. stearothermophilus* and *B. atropheaus* have been analyzed at both manufacturing methods, Well-Benick et al., (2019) and ISO 11138.

6.3.3.2 MATERIAL AND METHOD

1) Type of bioindicators

The position of the bioindicators commercial and own manufactured was constant, being the same than in experiment 1, for both spore formers, *Bacillus atrophaeus* and *G stearothermophilus*. The ISO 11138 and the Wells-Bennick et al., (2019) manufacturing process are considered. The second is described alongside the current dissertation and the first one is not described as the ISO only sets the standards, but the procedure is confidential of each manufacturer.

2) Data analysis

A minimum set of 5 tests were analyzed for each type of bioindicator. As in previous experiments, once the treatment time had elapsed at different times, the bioindicators were removed from the isolator.

The GInaFIT computer tool (Geeraerd et al., 2005) was used to determine the bacterial inactivation curve and 4D value. The best fit indicators to the determine the accuracy of the model were the adjusted coefficient of determination ($R^2_{adjusted}$) and the minimum Root Mean square deviation (RMSE). The prediction bands of the graphs, the standard

error (SE), and the confidence intervals (CI) of the different parameters and statistical measures were obtained using the GraphPad Prism computer tool (GraphPad Software Inc., San Diego, CA, USA).

6.3.3.3 RESULTS

Microbial inactivation at two levels, own manufactured and commercial bioindicators, was analyzed for both spore forms. In this case, the models that better fit the experimental data were the Weibull proposed by Marfart et al. (2002), the Log-linear proposed by Bigelow and Esty (1920) and Weibull-tail model proposed by Albert and Mafart (2005). The equation for this last model is (Equation 28):

$$Log\ (N) = Log\left[\left(10^{log\ (N0)} - 10^{log\ (Nres)}\right) \times 10^{(-\frac{t}{\rho})^{p}}\ X\ 10^{\log(Nres)}\right]$$

Equation 28 Weibull-tail inactivation model (Albert and Mafart, 2005)

The results showed differences in the obtained lethality depending on the type of bioindicator (Figure 77 and Table 20). This lethality was faster in the commercial bioindicators of both spore formers.

In case of the own-manufactured BIs of *G. stearothermophilus*, greater resistance to the inactivation was observed, already in the initial phases, presenting a concave curve shape (p>1). However, the commercial BIs inactivation rate was initially slightly convexe. That fact was also reflected in a larger δ and 4D value in the own-manufactured BI. To achieve complete lethality in the own manufactured BI, 30 min were required. On the other hand, the commercial BIs only needed 15 min to achieve complete inactivation.

In case of *B. atropheaus*, results were quite similar, although the differences in the 4D value and the complete lethality were not so remarkable. The 4D value and time to reach complete inactivation in the own manufactured bioindicators were 25.6 and 45 minutes, respectively. On the other hand, the commercial BIs required time for reducing 4-log and complete inactivation were 17 and less than 35 min. In the commercial BI was observed a greater resistance (p> 1) in the initial phases. Later, its lethality kinetics increased, but in the final phases of treatment, a small fraction of the bacterial population showed resistance to the biocide action, observing a tailing effect. However, the own-manufactured BIs, with a slow inactivation kinetic (*Kmax*), showed a log-linear inactivation model.

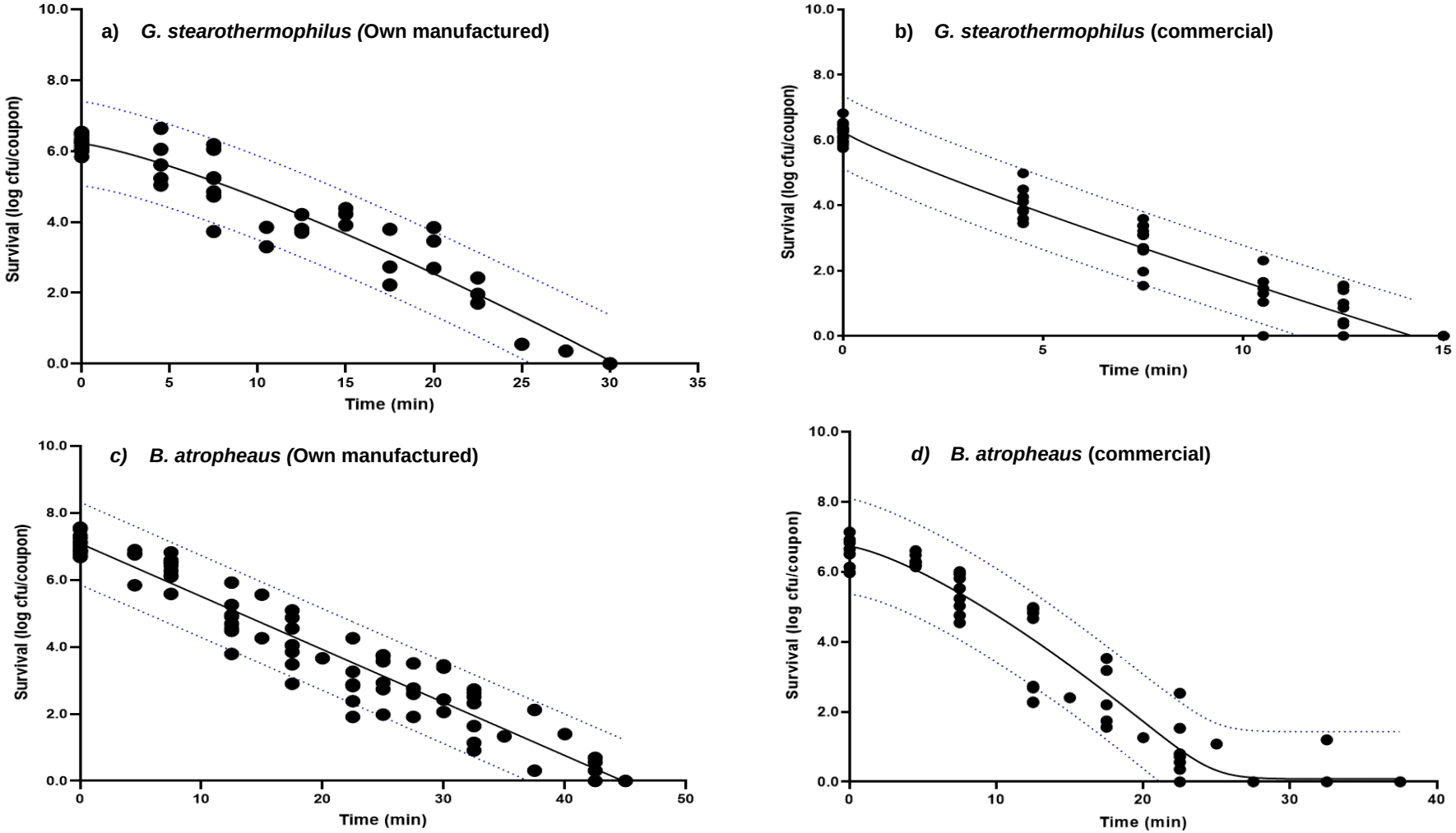

Figure 77 Inactivation models of G. stearothemophilus and B. atropheaus depending on the type of biological indicator: a) G. stearothermophilus own manufactured (Weibull), b) G. stearothermophilus commercial (Weibull), c) B. atrophaeus own manufactured (log-linear) and d) B. atropheaus commercial (Weibull+tail) throughout the ionHP+ hydrogen peroxide technology.

Table 20 Statistical indexes and parameter estimation (mean, standard deviations and 95% confidence intervals) of the inactivation model used for G. stearothermophilus *and* B atropheaus *using own-manufactured and commercial biological bioindicators during the atomization technology ionHP*

		G. stearothemophilus		***B. atropheaus***	
Parameter	**Unit**	**Own[a]**	**Commercial[a]**	**Own[b]**	**Commercial[c]**
Log (N_0) ± SE	log CFU/coupon	6.21 ± 0.14	6.26 ± 0.12	7.09 ± 0.11	6.71 ± 0.016
Log (N_0) (95% CI)	log CFU/coupon	5.92-6.50	6.01-6.51	6.87-7.30	6.32-7.09
Log (N_0) ± SE	log CFU/coupon				0.08 ± 0.16
Log (N_{res}) (95% CI)	log CFU/coupon				-025-0.40
K_{max} ± SE	log CFU/min			0.36 ± 0.01	
K_{max} (95% CI)	log CFU/min			0.34-0.39	
δ ± SE	min	7.15 ± 0.93	1.76 ± 0.27		6.06 ± 0.87
δ (95% CI)	min	5.32-9.19	1.27-2.33		4.53-7.78
p ± SE	-	1.26±0.12	0.88 ± 0.06		1.35± 0.14
p (95% CI)	-	1.03-1.55	0.76-1.01		1.15-1.65
4D	min	21.60	8.55	25.65	17.25
R^2 (adjusted)	-	0.909	0.954	0.924	0.937
RMSE	-	0.575	0.545	0.610	0.636

N_0: the initial population, N_{res}: residual cell concentration after stabilization at the end of the decrease, Kmax: inactivation constant of the linear model, α: fraction of the first subpopulation remaining in the total population, δ: time to achieve the first Log-reduction, p: the shape of the inactivation curve, 4D: time to achieve a 4-log reduction, RMSE: Root Mean Squared Error.SE: standard error; 95% CI 95% confidence interval.

a) Weibull inactivation model, b) Log-lineal inactivation model, c) Weibull-tail Geeraerd tail

6.3.3.4 DISCUSSION AND CONCLUSIONS

The type of bioindicators' manufacturing process plays an essential role in the generation of several layers, clustering, or high density of spores in the bioindicator (Raguse et al., 2016; Sigwarth and Stärk, 2003). One of the factors that allow the creation of multilayers is the reduced space where >10^6 spores are inoculated. It has already been documented that larger densities can create a protective layer, either actively, due to the manufacturing process, or passively throughout the accumulation of debris after a certain time of hydrogen peroxide exposition that increases the required exposure for complete inactivation (Drinkwater et al., 2009).

In the present investigation, microbial inactivation was faster in commercial bioindicators of both spore formers bacteria and especially for *G. stearothemophilus.* The commercial bioindicators had a concave shape, and the own manufactured ones were flat. This concave shape might undoubtedly influence the deposition of the biocide and its resident time, favoring the inactivation kinetics. Raguse et al., (2016) and Drinkwater et al., (2009) already demonstrated that sharp edges or different forms might interfere in the deposition process of the spores or even in the biocide activity.

Another factor that could affect the spore resistance is the method to produce spores. Own-manufactured BIs were obtained using the method of Wells-Bennik et al. (2019), and the commercial BIs manufacturing process followed the ISO11138-1 (ISO, 2017).

Wells-Bennik et al. (2019) found that the variability in spore heat-resistance could largely be attributed to strain variability and the conditions used during sporulation (especially the sporulation medium).

In conclusion, the manufacturing method of the reference bioindicator is, according to the present study and the previous experiments results, a variable with a remarkable impact over the overall resistance of the analyzed spore forms. Thus, if other factors are studied, the same BIs manufacturing process should be used.

Further studies would be required to better understand the justification for such a large difference.

7 CONCLUSIONS

A process where thermodynamic, engineering, chemical and microbiological variables are involved, is an extremely complex process to be modelled and eventually automated. Throughout this research, and under the Industrial Phd Program in collaboration with Azbil Telstar Technologies, an automated hydrogen peroxide decontamination method has been developed and partially modelled.

All the mentioned variables were present, both during the technology development and the microbial modelling, delivering conclusions, that would eventually ease the complete modelling process.

The main conclusions are summarized as follows:

1) The distribution can only be modelled if both the atomization process, and the geometrical patterns, are considered within the same system. The load, the air-streamlines, or the injection position will directly impact the final reach of the liquid phase hydrogen peroxide. The CFD simulation showed areas (bottom quadrants below the nozzle) of a BioSAS where less particle reach was present due to the modelled geometry and nozzle and exhaust position.
2) The particle reach or level of condensation is directly related with the inactivation. According to the results, there is a turning point (2,000 ng/mm^2 approximately), where more condensation does not directly imply a faster inactivation. However, for a complete inactivation, a minimum condensation is required. The gas level in an atomization process will never be larger the equilibrium vapor pressure of the hydrogen peroxide solution. Therefore, if no condensation is present, only 100-200 ppm will be inactivating the biological contaminant.
3) In an atomization process, the temperature has demonstrated to play a more important role than expected. Minor temperature differences (2-4ºC) can lead to different inactivation models, even when the same microorganism is treated. It could be concluded that when temperatures are below 30ºC, the larger the temperature, the faster the inactivation would be. On the other hand, when temperature is above 30ºC, the inactivation of a >10^6 population (cfu/coupon) of *Geobacillus stearothermophilus* was not always possible. Finally, the behavior of the spore formers was different at higher or lower temperatures. While the *Geobacillus stearothermophilus* maintained a Log-linearity at higher temperatures, the *B. atropheaus* showed two different resistances when the temperature was increased. These resistances are related to the higher hydrophobicity of the membrane, adding a wetting process that could eventually limit the overall inactivation process.
4) During an atomization process, the relative humidity was not controlled. Even if initially no effect was expected or encountered, this variable has proved to be important at the beginning of the process. In lower humidity conditions, the gas phase of the hydrogen peroxide level becomes even more critical. The penetration is better at higher kinetic energies. However, at higher initial humidity levels, the gas phase becomes less critical, as the microorganism' outer layers are already wet.

5) The more significant microbiological contaminants are diverse and depend on the activity of the industry. Furthermore, each of them behave differently, not just to the same decontamination technology but also to the different environmental conditions or manufacturing method of the BI. In this research, representative bioburden of each industry was selected (pharmaceutical, medical and food industry), like *Listeria monocytogenes*, methicillin-resistant *Staphylococcus aureus* (MRSA), *G. stearothermophilus* and *B. atropheaus*. Both the inactivation models and the resistances were different for each of the microorganisms. Higher resistance was obtained in spore formers, being the *B. atropheaus* the one to have the higher 4D value, 24.75 min. The sequence from less to more resistant was *L. monocytogenes* Scott A ≤ *L. monocytogenes* RO15 < MRSA < *G. stearothermophilus* < *B. atrophaeus*. In addition, an assessment of the lethality depending on the type of BI was done, concluding that the commercial BIs showed a remarkable lower resistance to the ionHP+ technology, compared to the own-manufactured ones. The manufacturing method or the differences in geometry or roughness of the BI carrier are likely to be the main reasons for such a large difference.

A multidisciplinary development process, involving engineering, chemical and microbiology expertise should lead any automated decontamination method to be placed in the market. Without any of the three disciplines, the technology could end in false negatives with high risk to the public health, and very likely, with worse results than the traditional manual decontamination methods. This research has demonstrated that differences in the inactivation process can appear even with small changes in the environmental conditions or in the engineering design.

8 NEXT STEPS

Even though the current research has well-appointed certain conclusions regarding the bio-decontamination application, it has still left points for further research. These open points will help in the reliability and optimization of a hydrogen peroxide technology, with an increasing interest in targeted industries of this dissertation, and other areas, such as large public spaces. Schools, theatres, or even public transport facilities could be better decontaminated by an automated technology that ensures a homogeneous biocide distribution and clarifies the inactivation models.

For achieving so, the main areas of research could be summarized in the following points:

1) Distribution: it has been demonstrated that the distribution, either in the gas or liquid phase, is likely to be the most important research area. Together with the microbiological inactivation modelling, a proper distribution characterization could lead to a reliable decontamination method. Therefore, to carry on with the hydrogen peroxide homogeneous distribution, in addition to the already described Computer Fluid Dynamics (CFD) simulation, the following areas of investigation are identified:
    a. Actual measurement of the particle generation process: During the current research, the specifications of the nozzle manufacturer were used to estimate the particle diameter. Throughout the use of Laser Diffraction Methods, a particle distribution can be calculated, and a real pattern can be obtained (Cornillault, 1972). This pattern will be specific to a certain air to liquid ratio.
    b. Digital twin throughout the improvement of the CFD model (Computer Fluid Dynamics): To create a simplified model where the user of a decontamination method could insert the main process variables and obtain with a calculated level of assurance, the exposure time and concentration to be added in the particular modelled volume. Different loads and geometries could be simulated.
    c. Process Analytical tool integration. The integration of a continuous measurement of the condensation level at different points of the volume to be decontaminated. The relationship between the mentioned continuous measurement and the inactivation models could lead to a reduced cycle time and risk of contamination.
    d. Ultrasonic nozzle. The particle generation process could be improved by using ultrasonic atomization (Dalmoro et al., 2013). The high turbulences generated by a high-speed air jet at a specific point of the volume lead to unpredictable particle tracking.
    e. Pressure. Vacuum pulses to enhance the distribution. As per other technologies, such as thermal sterilization, vacuum pulses help in the homogeneous vapor reach.

2) Cycle time optimization: several phases and variables influence the total cycle time of the decontamination process. Injection, exposure, and aeration time could be improved by a better understanding and optimization of the following processes:
    a. Nozzle injection process. Either modifying the working flows or the nozzle technology, the injection time could be minimized.
    b. Microbial modelling. The characterization of the inactivation kinetics and the main variables impacting the model would lead to a minimized exposure time. The bioburden of the specific application should be periodically assessed, and the decontamination recipe would be adjusted to the specific bioburden of the volume.
    c. Aeration minimization. Temperature, absorption/desorption mechanisms modelling for different pharmaceutical materials or higher air exchange ratios are just some of the variables to be tested. Catalysts or air conditioners could lead to reduced aeration processes.
3) Hydrogen Peroxide formulation: the solution of hydrogen peroxide should also ensure homogeneity over time. As discussed in chapter 5, different active ingredients are added to the formula to do so.
    a. Stabilizers. even if important in the homogeneity of inactivation over time, the residues usually generated by this sort of stabilizers can lead to technological issues (filters clogging, pumps damaging, etc.) to cross contamination of pharmaceutical or food products. Reducing this sort of stabilizers without losing excessive activity over time is a key area of research that is already ongoing within the Azbil Telstar SLU activities.
    b. Enhancers. Other enhancers than isopropyl alcohol can be tested. Metals or enzymes appear to increase the biocidal activity and, therefore, help in reducing the total inactivation time.
4) Microbial modelling: physical-chemical variables influence over different inactivation models. In this research, temperature, and particle reach (condensation) variables were studied for two particular spore formers. Further testing not just in the same variables but in others such as the following will help in a reliable decontamination method implementation:
    a. Material. Inoculation of the microbial load into different materials. The impact of the material over the gas hydrogen peroxide system (Sigwarth and Stärk, 2003). It is expected that an atomization process would be more robust in this sense.
    b. Temperature and relative humidity. Even though the current research has already shown trends, larger experimental activities should be carried out to confirm behaviors

c. Type of microorganisms. Another bioburden could be tested to create a library where the user would just have to pick a preselected recipe to deactivate the volume.

9 BIBLIOGRAPHY

Abreu, A.C., Tavares, R.R., Borges, A., Mergulhão, F., Simões, M., 2013. Current and emergent strategies for disinfection of hospital environments. Journal of Antimicrobial Chemotherapy 68, 2718–2732. https://doi.org/10.1093/jac/dkt281

AFNOR, 2014. NF T72 281:2014, Procédés de désinfection des surfaces par voie aérienne – Détermination de l'activité bactéricide, fongicide, levuricide, mycobactericide, tuberculocide, sporicide et virucide incluant les bactériophages.

Agalloco, J., Akers, J., 2016. Advanced Aseptic Processing Technology. CRC Press LLC. ISBN 1439825440.

Agalloco, J., Akers, J., 2013. Overcoming limitations of vaporized hydrogen peroxide: Hydrogen peroxide is highly potent and highly problematic. Pharm. Technol. 37, 46–56.

Akers, J.E., Agalloco, J.P., Kennedy, C.M., 1995. Experience in the Design and Use of Isolator Systems for Sterility Testing. PDA Journal of Pharmaceutical Science and Technology 49, 140 LP – 144.

Albert, I., Mafart, P., 2005. A modified Weibull model for bacterial inactivation. Int. J. Food Microbiol. 100, 197–211. https://doi.org/10.1016/j.ijfoodmicro.2004.10.016

Ali, S., Muzslay, M., Bruce, M., Jeanes, A., Moore, G., Wilson, A.P.R., 2016. Efficacy of two hydrogen peroxide vapour aerial decontamination systems for enhanced disinfection of meticillin-resistant Staphylococcus aureus, Klebsiella pneumoniae and Clostridium difficile in single isolation rooms. Journal of Hospital Infection 93, 70–77. https://doi.org/10.1016/j.jhin.2016.01.016

Ashgriz, N., 2011. Handbook of Atomization and Sprays, Theory and Applications. Springer, New York. https://doi.org/10.1007/978-1-4419-7264-4

Atkinson, J., Chartier, Y., Lúcia Pessoa-Silva, C., Jensen, P., Li, Y., Seto, H., 2009. Natural Ventilation for Infection Control in Health-Care Settings. WHO Guidelines. ISBN 97892415478/57.

Attri, P., Kim, Y.H., Park, D.H., Park, J.H., Hong, Y.J., Uhm, H.S., Kim, K.N., Fridman, A., Choi, E.H., 2015. Generation mechanism of hydroxyl radical species and its lifetime prediction during the plasma-initiated ultraviolet (UV) photolysis. Scientific Reports 5, 1–8. https://doi.org/10.1038/srep09332

Back, K.-H., Ha, J.-W., Kang, D.-H., 2014. Effect of hydrogen peroxide vapor treatment for inactivating Salmonella Typhimurium, Escherichia coli O157:H7 and Listeria monocytogenes on organic fresh lettuce. Food Control 44, 78–85. https://doi.org/10.1016/j.foodcont.2014.03.046

Bigelow, W.D., Etsy, J.R., 1920. The thermal death point in relation to time of typical thermophilic organisms. J. Infect. Dis. 27, 602–617.

Biology dictionary, 2021. Biology dictionary, Gram-Positive vs. Gram-Negative | Biology Dictionary (accessed 3.12.20)

Boyce, J.M., 2016. Modern technologies for improving cleaning and disinfection of environmental surfaces in hospitals. Antimicrobial Resistance & Infection Control. https://doi.org/10.1186/s13756-016-0111-x

Buchanan, R.L., Golden, M.H., Whiting, R.C., 1993. Differentiation of the Effects of pH and Lactic or Acetic Acid Concentration on the Kinetics of Listeria Monocytogenes Inactivation. Journal of food protection 56, 474–478. https://doi.org/10.4315/0362-028X-56.6.474

Castro, L.C.M., Lourenço, F.R., Pinto, T.J.A., 2011. Assessment of biological indicators in the validation of isolator decontamination with hydrogen peroxide. Rev. Ciencias Farm. Basica e Apl.

CDC, 2019. Las infecciones mortales por estafilococo siguen siendo una amenaza en los EE. UU [WWW Document]. URL https://www.cdc.gov/spanish/mediosdecomunicacion/comunicados/p_vs_estafilococo_030519.html (accessed 4.16.21).

Cerf, O., 1977. A REVIEW Tailing of Survival Curves of Bacterial Spores. J. Appl. Bacteriol. 42, 1–19. https://doi.org/10.1111/j.1365-2672.1977.tb00665

Chan, H.-T., White, P., Sheorey, H., Cocks, J., Waters, M.-J., 2011. Evaluation of the biological efficacy of hydrogen peroxide vapour decontamination in wards of an Australian hospital. Journal of Hospital Infection 79, 125–128. https://doi.org/10.1016/j.jhin.2011.06.009

Chen, D., Zhao, T., Doyle, M.P., 2015. Control of pathogens in biofilms on the surface of stainless steel by levulinic acid plus sodium dodecyl sulfate. International Journal of Food Microbiology. https://doi.org/10.1016/j.ijfoodmicro.2015.04.026

Chen, X., Chan, Q., 2010. Comparison of different decontaminant delivery methods for sterilizing unoccupied commercial airliner cabins. Building and Environment. https://doi.org/10.1016/j.buildenv.2010.01.013

Choi, N.Y., Baek, S.Y., Yoon, J.H., Choi, M.R., Kang, D.H., Lee, S.Y., 2012. Efficacy of aerosolized hydrogen peroxide-based sanitizer on the reduction of pathogenic bacteria on a stainless steel surface. Food Control. https://doi.org/10.1016/j.foodcont.2012.02.027

Chung, S.Y., Kern, R.G., Koukol, R.C., Barengoltz, J.B., Cash, H.A., 2008. Vapor Hydrogen Peroxide as Alternative to Dry Heat Microbial Reduction. Biotechnology and Planetary Protection Group, Jet Propulsion Laboratory, California Institute of Technology, Pasadena, California, USA.

Coroller, L., Leguerinel, I., Mettler, E., Savy, N., Mafart, P., 2006. General model, based on two mixed weibull distributions of bacterial resistance, for describing various shapes of inactivation curves. Applied and Environmental Microbiology 72, 6493–6502. https://doi.org/10.1128/AEM.00876-06

Cornillault, J., 1972. Particle Size Analyzer. Appl. Opt. 11, 265–268. https://doi.org/10.1364/AO.11.000265

Council of Europe, 2021. Biological indicators and related microbial preparations, in: European Pharmacopoeia (Ph. Eur.). pp. 622–625.

Cui, J., Li, F., Shi, Z.-L., 2019. Origin and evolution of pathogenic coronaviruses. Nature Reviews Microbiology 17, 181–192. https://doi.org/10.1038/s41579-018-0118-9

Cutting, S.M., Hong, H.A., Baccigalupi, L., Ricca, E., 2009. Oral vaccine delivery by recombinant spore probiotics. International Reviews of Immunology 28, 487–505. https://doi.org/10.3109/08830180903215605

Dalmoro, A., Barba, A.A., d'Amore, M., 2013. Analysis of Size Correlations for Microdroplets Produced by Ultrasonic Atomization. Sci. World J. 2013, 482910. https://doi.org/10.1155/2013/482910

Davies, A., Pottage, T., Bennett, A., Walker, J., 2011. Gaseous and air decontamination technologies for Clostridium difficile in the healthcare environment. Journal of Hospital Infection 77, 199–203. https://doi.org/10.1016/j.jhin.2010.08.012

de la Torre, B.G., Albericio, F., 2020. The pharmaceutical industry in 2019. An analysis of FDA drug approvals from the perspective of molecules. Molecules 25. https://doi.org/10.3390/molecules25030745

Denyer, S.P., Stewart, G.S., 1998. Mechanisms of action of disinfectants. International Biodeterioration and Biodegradation 41, 261–8.

Deshmukh, S.P., Patil, S.M., Mullani, S.B., Delekar, S.D., 2019. Silver nanoparticles as an effective disinfectant: A review, Materials Science and Engineering: C. Elsevier Ltd. https://doi.org/10.1016/j.msec.2018.12.102

Doletski, B.G., Dunn, T.M., Arnold, E.V., Mueller, E.P., Raulli, R.E., Benedek, K.R. Murville, M., 2014. Sterilization system and device. US 8808622.

Doll, M., Morgan, D.J., Anderson, D., Bearman, G., 2015. Touchless Technologies for Decontamination in the Hospital: A Review of Hydrogen Peroxide and UV Devices. https://doi.org/10.1007/s11908-015-0498-1

Drinkwater, J., Chewins, J., Steele, G., 2009. The biological challenge of spores and kill mechanism of hydrogen peroxide vapor. European Journal of Parenteral & Pharmaceutical Sciences 14, 5–10.

Edwards, A., 1967. HYDROGEN PEROXIDE HANDBOOK - Technical Report AFRPL-TR-67-144. Chemical and Material Sciences Department, Research Division, Rocketdyne, Division of North American Aviation, Inc. Canoga Park, California.

EFSA, 2010. Analysis of the baseline survey on the prevalence of methicillin-resistant Staphylococcus aureus (MRSA) in holdings with breeding pigs, in the EU, 2008 -

Part B: factors associated with MRSA contamination of holdings. EFSA Journal 8. https://doi.org/10.2903/j.efsa.2010.1597

El Azab, W., 2019. A justified process for cleaning and disinfection. Cleanroom Technology, March (25–26). A justified process for cleaning and disinfection (cleanroomtechnology.com) (accessed 5.20.2021)

EMA, 2019. Guideline on the sterilization of the medicinal product, active substance, excipient, and primary container.

EMA, 2017. EMA Manufacture of Sterile Medicinal Products Annex I Draft 1–50.

Eschlbeck, E., Seeburger, C., Kulozik, U., 2018. Influence of spore and carrier material surface hydrophobicity on decontamination efficacy with condensing hydrogen peroxide vapour. J. Appl. Microbiol. 124, 1071–1081. https://doi.org/10.1111/jam.13695

European Commission, 2005. Commission Regulation (EC) No 2073/2005 of 15th November 2005 on microbiological criteria for foodstuffs.

European Chemicals Bureau European Union, 2003. Risk Assessment Report hydrogen peroxide.

Falagas, M.E., Thomaidis, P.C., Kotsantis, I.K., Sgouros, K., Samonis, G., Karageorgopoulos, D.E., 2011. Airborne hydrogen peroxide for disinfection of the hospital environment and infection control: a systematic review. Journal of Hospital Infection 78, 171–177. https://doi.org/10.1016/J.JHIN.2010.12.006

Fan, Z., Xie, J., Li, Y., Wang, H., 2019. Listeriosis in mainland China: A systematic review. International Journal of Infectious Diseases 81, 17–24.

Favero, M.S., Bond, W.W., 2001. Chemical disinfection of medical and surgical materials, in: Block, S.S. (Ed.), Disinfection, Sterilization, and Preservation. Lippincott Williams & Wilkins, Philadelphia, pp. 881–917.

FDA, 2020a. Ethylene Oxide Sterilization for Medical Devices | FDA [WWW Document]. URL https://www.fda.gov/medical-devices/general-hospital-devices-and-supplies/ethylene-oxide-sterilization-medical-devices (accessed 1.26.21).

FDA, 2020b. Investigating Decontamination and Reuse of Respirators in Public Health Emergencies | FDA [WWW Document]. URL https://www.fda.gov/emergency-preparedness-and-response/mcm-regulatory-science/investigating-decontamination-and-reuse-respirators-public-health-emergencies (accessed 5.15.21).

FDA, 2018. Hazard Analysis and Risk-Based Preventive Controls for Human Food: Guidance for Industry.

FDA, 2016. Guidance for Industry and FDA Staff Submission and Review of Sterility Information in Premarket Notification (510 (k)) Submissions for Devices Labeled as Sterile 510, 11.

FDA, 2004. Guidance for Industry, Sterile Drug Products Produced by Aseptic Processing — Current Good Manufacturing Practice.

Finnegan, M., Linley, E., Denyer, S.P., McDonnell, G., Simons, C., Maillard, J.-Y., 2010. Mode of action of hydrogen peroxide and other oxidizing agents: differences between liquid and gas forms. Journal of Antimicrobial Chemotherapy 65, 2108–2115. https://doi.org/10.1093/jac/dkq308

Freeman, D.E., Auer, J.A., 2012. Instrument Preparation, Sterilization, and Antiseptics. Equine Surgery 98–111. https://doi.org/10.1016/B978-1-4377-0867-7.00009-0

French, G.L., Otter, J.A., Shannon, K.P., Adams, N.M.T., Watling, D., Parks, M.J., 2004. Tackling contamination of the hospital environment by methicillin-resistant Staphylococcus aureus (MRSA): a comparison between conventional terminal cleaning and hydrogen peroxide vapour decontamination. Journal of Hospital Infection 57, 31–37. https://doi.org/10.1016/j.jhin.2004.03.006

Fu, T.Y., Gent, P., Kumar, V., 2012. Efficacy, efficiency and safety aspects of hydrogen peroxide vapour and aerosolized hydrogen peroxide room disinfection systems. Journal of Hospital Infection 80, 199–205. https://doi.org/10.1016/J.JHIN.2011.11.019

Gad, S.C., 2014. Peracetic Acid, in: Encyclopedia of Toxicology: Third Edition. Elsevier, pp. 788–790. https://doi.org/10.1016/B978-0-12-386454-3.01197-0

Garrett, T.R., Bhakoo, M., Zhang, Z., 2008. Bacterial adhesion and biofilms on surfaces. Progress in Natural Science 18, 1049–1056. https://doi.org/10.1016/J.PNSC.2008.04.001

Geeraerd, A.H., Herremans, C.H., Van Impe, J.F., 2000. Structural model requirements to describe microbial inactivation during a mild heat treatment. Int. J. Food Microbiol. 59, 185–209. https://doi.org/10.1016/S0168-1605(00)00362-7

Geeraerd, A.H., Valdramidis, V.P., Van Impe, J.F., 2005. GInaFiT, a freeware tool to assess non-log-linear microbial survivor curves. Int. J. Food Microbiol. 102, 95–105. https://doi.org/10.1016/j.ijfoodmicro.2004.11.038

Gómez Lopez, V., 2014. Chlorine Dioxide. CBAS-CSIC 1. https://doi.org/10.1016/B978-0-12-386454-3.00278-5

Gradini, R., Chen, F., Tan, R., Newlin, L., 2019. A summary on cutting edge advancements in sterilization and cleaning technologies in medical, food, and drug industries, and its applicability to spacecraft hardware. Life Sciences in Space Research 23, 31–49. https://doi.org/10.1016/j.lssr.2019.05.002

Halvorson, H.O., Ziegler, N.R., 1933a. Application of Statistics to Problems in Bacteriology. Journal of Bacteriology 26, 559–567. https://doi.org/10.1128/jb.26.6.559-567.1933

Handlos, V., 1980. Kinetics of the aeration of ethylene-oxide sterilized plastics. Biomaterials 1, 149–157. https://doi.org/10.1016/0142-9612(80)90038-1

Hatanaka, K., Shibauchi, Y., 1989. Sterilization method and apparatus. US 4797255.

Hayrapetyan, H., Nederhoff, L., Vollebregt, M., Mastwijk, H., Nierop Groot, M., 2020. Inactivation kinetics of Geobacillus stearothermophilus spores by a peracetic acid or hydrogen peroxide fog in comparison to the liquid form. International Journal of Food Microbiology 316, 108418. https://doi.org/10.1016/j.ijfoodmicro.2019.108418

Holmdahl, T., Lanbeck, P., Wullt, M., Walder, M.H., 2011. A Head-to-Head Comparison of Hydrogen Peroxide Vapor and Aerosol Room Decontamination Systems. infection control and hospital epidemiology 32. https://doi.org/10.1086/661104

Howard, A., McMeekin, E., 2020. Coronavirus research: Detailed 3D model of SARS-CoV-2 revealed [WWW Document]. University of Glasgow - University news. URL https://www.gla.ac.uk/news/coronavirus/headline_723737_en.html (accessed 2.14.21).

Huang, L., 2013. Determination of thermal inactivation kinetics of Listeria monocytogenes in chicken meats by isothermal and dynamic methods. https://doi.org/10.1016/j.foodcont.2013.03.049

Hultman, C., Hill, A., McDonnell, G., 2007. The physical chemistry of decontamination with gaseous hydrogen peroxide. Pharmaceutical Engineering 27, 22.

ISO, 2017. EN ISO 11138:2017 Sterilization of health care products - Biological indicators - Part 1: General requirements.

ISO, 2014. ISO 11135:2014 Sterilization of health-care products — Ethylene oxide — Requirements for the development, validation, and routine control of a sterilization process for medical devices.

Ito, K., Yoo, S.-J., Horata, H., 2016. Identification of Model Parameters of Vaporized Hydrogen Peroxide Decomposition Flux on Building Materials for Computational Fluid Dynamics. Journal of Environmental Protection 7, 212–229. https://doi.org/10.4236/jep.2016.72019

Jildeh, Z.B., Kirchner, P., Oberländer, J., Vahidpour, F., Wagner, P.H., Schöning, M.J., 2020. Development of a package-sterilization process for aseptic filling machines: A numerical approach and validation for surface treatment with hydrogen peroxide. Sensors and Actuators, A: Physical 303. https://doi.org/10.1016/j.sna.2019.111691

Kaer, P., vrek, J., Syslov, K., Vclavk, J., Pavlk, D., erven, J., Kuzm, M., 2012. Vapor Phase Hydrogen Peroxide – Method for Decontamination of Surfaces and Working Areas from Organic Pollutants, in: Organic Pollutants Ten Years After the Stockholm Convention - Environmental and Analytical Update. InTech. https://doi.org/10.5772/33451

Keyes, F.G., 1947. The Thermodynamic Properties of Water Substance 0° to 150°C PART VI. The Journal of Chemical Physics 15, 602–612. https://doi.org/10.1063/1.1746606

Khoumeri, B., Balbi, N., Leoni, E., Chiaramonti, N., Balbi, J.H., 2000. Decomposition of hydrogen peroxide a non-linear dynamic model. Journal of Thermal Analysis and Calorimetry 59, 901–911. https://doi.org/10.1023/A:1010130510308

Kimura, T., 2012. Effective decontamination of laboratory animal rooms with vapour-phase ("vaporized") hydrogen peroxide and peracetic acid. Scandinavian Journal of Laboratory Animal Science 39, 17–23.

Kirchner, P., Oberländer, J., Suso, H.-P., Rysstad, G., Keusgen, M., Schöning, M.J., 2013. Monitoring the microbicidal effectiveness of gaseous hydrogen peroxide in sterilisation processes by means of a calorimetric gas sensor. https://doi.org/10.1016/j.foodcont.2012.11.048

Kocot, A.M., Olszewska, M.A., 2017. Biofilm formation and microscopic analysis of biofilms formed by Listeria monocytogenes in a food processing context. LWT 84, 47–57. https://doi.org/10.1016/J.LWT.2017.05.042

Ling, M.L., Apisarnthanarak, A., Thu, L.T.A., Villanueva, V., Pandjaitan, C., Yusof, M.Y., 2015. APSIC Guidelines for environmental cleaning and decontamination. Antimicrobial Resistance and Infection Control. https://doi.org/10.1186/s13756-015-0099-7

Linley, E., Denyer, S.P., McDonnell, G., Simons, C., Maillard, J.-Y., 2012. Use of hydrogen peroxide as a biocide: new consideration of its mechanisms of biocidal action. Journal of Antimicrobial Chemotherapy 67, 1589–1596. https://doi.org/10.1093/jac/dks129

Liu, C., Geng, L., Yu, Y., Zhang, Y., Zhao, B., Zhao, Q., 2018. Mechanisms of the enhanced antibacterial effect of Ag-TiO 2 coatings. Biofouling 1–10. https://doi.org/10.1080/08927014.2017.1423287

Ma, J.W., Huang, B.S., Hsu, C.W., Peng, C.W., Cheng, M.L., Kao, J.Y., Way, T.D., Yin, H.C., Wang, S.S., 2017. Efficacy and Safety Evaluation of a Chlorine Dioxide Solution. https://doi.org/10.3390/ijerph14030329

Mafart, P., Couvert, O., Gaillard, S., Leguerinel, I., 2002. On calculating sterility in thermal preservation methods : Application of the Weibull frequency distribution model. Int. J. Food Microbiol. 72, 107–114. https://doi.org/10.1016/S0168-1605(01)00624-9

Maiti, Bidinger, 1981. The expanded application of most probable number to the quantitative evaluation of extremely low microbial count. J. Chem. Inf. Model. 53, 1689–1699.

Martinus, A., Van Boekel, S., 2002. On the use of the Weibull model to describe thermal inactivation of microbial vegetative cells. International journal of food microbiology 74, 139–159. https://doi.org/10.1016/S0168-1605(01)00742-5

Mattila, K., 2002. Biofilms on stainless steels exposed to process waters. ISSN 1239-9469. University of Helsinki, Finland.

McMurtrie, R.L., Keyes, F.G., 1948. A Measurement of the Diffusion Coefficient of Hydrogen Peroxide Vapor into Air. Journal of the American Chemical Society 70, 3755–3758. https://doi.org/10.1021/ja01191a063

Mei, X., Gong, G., 2017. Influence of Indoor Air Stability on Suspended Particle Dispersion and Deposition, in: Energy Procedia. Elsevier Ltd, pp. 4229–4235. https://doi.org/10.1016/j.egypro.2017.03.908

Meireles, A., Simões, M., 2017. Sanitation of equipment, in: Food Preservation. Elsevier, pp. 167–195. https://doi.org/10.1016/b978-0-12-804303-5.00005-5

Mishra, S., Imlay, J., 2012. Why do bacteria use so many enzymes to scavenge hydrogen peroxide? Archives of biochemistry and biophysics 525, 145. https://doi.org/10.1016/J.ABB.2012.04.014

Moerman, F., Mager, K., 2016. Cleaning and Disinfection in Dry Food Processing Facilities. Handbook of Hygiene Control in the Food Industry: Second Edition 521–554. https://doi.org/10.1016/B978-0-08-100155-4.00035-2

Monger, J.M., 1966. Storable Concentrated Hydrogen Peroxide. Technical report AFRPL-TR-66-353. Air Force Rocket Propulsion Laboratory, Research and Technology Division, Edwards, California.

Montgomery, D.C., Runger, G.C., 2010. Applied Statistics and Probability for Engineers. John Wiley & Sons.

Moore, F.C., Perkinson, L.R., 1979. Hydrogen Peroxide Vapor Sterilization method. United States Patent US 4169123.

Møretrø, T., Fanebust, H., Fagerlund, A., Langsrud, S., 2019. Whole room disinfection with hydrogen peroxide mist to control Listeria monocytogenes in food industry related environments. International Journal of Food Microbiology 292, 118–125. https://doi.org/10.1016/j.ijfoodmicro.2018.12.015

Nicholson, W.L., Fajardo-Cavazos, P., Rebeil, R., Slieman, T.A., Riesenman, P.J., Law, J.F., Xue, Y., 2002. Bacterial endospores and their significance in stress resistance. Antonie van Leeuwenhoek, International Journal of General and Molecular Microbiology 81, 27–32. https://doi.org/10.1023/A:1020561122764

Ogata, S., Matsui, Y., 2000. Photocatalytic body and method for making same. US 6107241.

Painter, K.L., Strange, E., Parkhill, J., Bamford, K.B., Armstrong-James, D., Edwards, A.M., 2015. Staphylococcus aureus adapts to oxidative stress by producing H2O2-resistant small-colony variants via the SOS response. Infection and Immunity 83, 1830–1844. https://doi.org/10.1128/IAI.03016-14

Panchal, V. V., Griffiths, C., Mosaei, H., Bilyk, B., Sutton, J.A.F., Carnell, O.T., Hornby, D.P., Green, J., Hobbs, J.K., Kelley, W.L., Zenkin, N., Foster, S.J., 2020. Evolving MRSA: High-level β-lactam resistance in Staphylococcus aureus is associated with RNA polymerase alterations and fine tuning of gene expression. Plos Pathogens 16. https://doi.org/10.1371/journal.ppat.1008672

Peiris, J.S.M., Guan, Y., Yuen, K.Y., 2004. Severe acute respiratory syndrome. Nature Medicine 10, S88–S97. https://doi.org/10.1038/NM1143

Pereira, C.G., 2019. Vapor À Liquid Equilibrium in Food Processes, Thermodynamics of Phase Equilibria in Food Engineering. Elsevier Inc. https://doi.org/10.1016/B978-0-12-811556-5.00006-5

Pérez-Rodríguez, F., Valero, A., 2013. Predictive Microbiology in Foods. Springer. ISBN 9781461455202.

Pottage, T., Macken, S., Giri, K., Walker, J.T., Bennett, A.M., 2012a. Low-temperature decontamination with hydrogen peroxide or chlorine dioxide for space applications. Applied and Environmental Microbiology. https://doi.org/10.1128/AEM.07948-11

Pottage, T., Macken, S., Walker, J.T., Bennett, A.M., 2012b. Meticillin-resistant Staphylococcus aureus is more resistant to vaporized hydrogen peroxide than commercial Geobacillus stearothermophilus biological indicators. Journal of Hospital Infection 80, 41–45. https://doi.org/10.1016/j.jhin.2011.11.001

Pruß, K., Stirtzel, S., Kulozik, U., 2012. Influence of the surface temperature of packaging specimens on the inactivation of Bacillus spores by means of gaseous H2O2. Journal of Applied Microbiology. https://doi.org/10.1111/j.1365-2672.2011.05223

Radl, S., Larisegger, S., Suzzi, D., Khinast, J., 2011a. Quantifying Absorption Effects during Hydrogen Peroxide Decontamination. Journal of Pharmaceutical Innovation 6, 202–216. https://doi.org/10.1007/s12247-011-9114-6

Raguse, M., Fiebrandt, M., Stapelmann, K., Madela, K., Laue, M., Lackmann, J.-W., Thwaite, J.E., Setlow, P., Awakowicz, P., Moeller, R., 2016. Improvement of Biological Indicators by Uniformly Distributing Bacillus subtilis Spores in Monolayers To Evaluate Enhanced Spore Decontamination Technologies. Applied and Environmental Microbiology 82, 2031–2038. https://doi.org/10.1128/AEM.03934-15

Ratkowsky, D.A., 2004. Model Fitting and Uncertainty, in: McKellar, R.C., Lu, X. (Eds.), Modelling Microbial Responses in Food. CRC Press LLC., pp. 151–196.

Reis-Teixeira, F.B. dos, Alves, V.F., de Martinis, E.C.P., 2017a. Growth, viability and architecture of biofilms of Listeria monocytogenes formed on abiotic surfaces. Brazilian Journal of Microbiology 48, 587–591. https://doi.org/10.1016/J.BJM.2017.01.004

Richard, Amy.W., Dennis, F., Cutler Lynn, Teel, S.J., 2007. Enhanced stability of hydrogen peroxide in the presence of subsurface solids. Journal of Contaminant Hydrology 91, 312–326.

Richter, W., 2016. Final Report for the Bioquell Hydrogen Peroxide Vapor (HPV) Decontamination for Reuse of N95 Respirators. Columbia, Ohio.

Richter, W.R., Wood, J.P., Wendling, M.Q.S., Rogers, J. V., 2018. Inactivation of Bacillus anthracis spores to decontaminate subway railcar and related materials

via the fogging of peracetic acid and hydrogen peroxide sporicidal liquids. Journal of Environmental Management 206, 800–806. https://doi.org/10.1016/J.JENVMAN.2017.11.027

Robbins, J.B., Fisher, C.W., Moltz, A.G., Martin, S.E., 2005. Elimination of Listeria monocytogenes biofilms by ozone, chlorine, and hydrogen peroxide. Journal of Food Protection 68, 494–498. https://doi.org/10.4315/0362-028X-68.3.494

Rodgers, R.C., Hill, G.E., 1978. Equations for vapour pressure versus temperature: derivation and use of the antoine equation on a hand-held programmable calculator. Br. J. Anaesth. 50, 415–424. https://doi.org/10.1093/BJA/50.5.415

Ross, T., 1996. Indices for performance evaluation of predictive models in food microbiology. J. Appl. Bacteriol. 81, 501–508. https://doi.org/10.1111/j.1365-2672.1996.tb03539

Rutala, W.A., Weber, D.J., 2019. State of the Science Review Disinfection, sterilization, and antisepsis: An overview. AJIC: American Journal of Infection Control 47, A3–A9. https://doi.org/10.1016/j.ajic.2019.01.018

Rutala, W.A., Weber, D.J., 2013. Disinfectants used for environmental disinfection and new room decontamination technology. American Journal of Infection Control 41, S36–S41. https://doi.org/10.1016/j.ajic.2012.11.006

Saleh, R., Robinson, E.S., Ahern, A.T., Donahue, N.M., 2017. Evaporation rate of particles in the vaporizer of the Aerodyne aerosol mass spectrometer. Aerosol Science and Technology 51, 501–508. https://doi.org/10.1080/02786826.2016.1271109

Salem, I.A., El-Maazawi, M., Zaki, A.B., 2000. Kinetics and mechanisms of decomposition reaction of hydrogen peroxide in presence of metal complexes. International Journal of Chemical Kinetics 32, 643–666. https://doi.org/10.1002/1097-4601(2000)32:11<643::AID-KIN1>3.0.CO;2-C

Sandle, T., 2016. Biological indicators, in: Pharmaceutical Microbiology. Elsevier, pp. 161–169. https://doi.org/10.1016/b978-0-08-100022-9.00013-x

Sandle, T., 2013. Sterility, Sterilisation and Sterility Assurance for Pharmaceuticals: Technology, Validation and Current Regulations., 1st Editio. ed. Woodhead Publishing Ltd, Sawston.

Scatchard, G., Kavanagh, G.M., Ticknor, L.B., 1952. Vapor-Liquid Equilibrium. VIII. Hydrogen Peroxide—Water Mixtures 1. Journal of the American Chemical Society 74, 3715–3720. https://doi.org/10.1021/ja01135a001

Schmidt, M.G., von Dessauer, B., Benavente, C., Benadof, D., Cifuentes, P., Elgueta, A., Duran, C., Navarrete, M.S., 2016. Copper surfaces are associated with significantly lower concentrations of bacteria on selected surfaces within a pediatric intensive care unit. American Journal of Infection Control 44, 203–209. https://doi.org/10.1016/j.ajic.2015.09.008

Schumb, W.C., Satterfield, C.N., Wentworth, R.L., 1955. Hydrogen Peroxide. Reinhold Pub. Corp, New York.

Scientific Committee on Occupational Exposure Limits, 2014. Recommendation from the Scientific Committee on Occupational Exposure Limits for Nitrogen Dioxide. Brussels.

Seaver, L.C., Imlay, J.A., 2001. Alkyl hydroperoxide reductase is the primary scavenger of endogenous hydrogen peroxide in Escherichia coli. Journal of bacteriology 183, 7173–7181. https://doi.org/10.1128/JB.183.24.7173-7181.2001

Seinfeld, J.H., Pandis, S.N., 2016. Atmospheric Chemistry and Physics from Air Pollution to Climate Change, 3rd edition. ed. John Wiley & Sons Inc., New Jersey.

Shereen, M.A., Khan, S., Kazmi, A., Bashir, N., Siddique, R., 2020. COVID-19 infection: Emergence, transmission, and characteristics of human coronaviruses. Journal of Advanced Research 24, 91–98. https://doi.org/10.1016/J.JARE.2020.03.005

Sias, R.M., Sias, H.E., Diniz, S.J., Guerrero, F., Pierce, J.M., Louis Montulli, 2006. Decontamination apparatus and method using an activated cleaning fluid mist. US7008592 B2.

Sigwarth, V., Stärk, A., 2003. Effect of carrier materials on the resistance of spores of Bacillus stearothermophilus to gaseous hydrogen peroxide. PDA journal of pharmaceutical science and technology 57, 3–11.

Soroush, E., Bahadori, A., 2017. Vapor e Liquid Equilibrium (VLE) Calculations, Fluid Phase Behavior for Conventional and Unconventional Oil and Gas Reservoirs. Elsevier. https://doi.org/10.1016/B978-0-12-803437-8.00005-1

Spiegelman, J., Alvarez, D., 2015. Cheating Raoult's Law to Enable Delivery of Hydrogen Peroxide as a Stable Vapor. Cheating-Raoults-Law-to-Enable-Delivery-of-Hydrogen-Peroxide-as-a-Stable-Vapor.pdf (rasirc.com) (accessed 3.20.20)

Stapleton, P.D., Taylor, P.W., 2002. Methicillin resistance in Staphylococcus aureus: mechanisms and modulation. Science progress. https://doi.org/10.3184/003685002783238870

Tachiev, G., Roth, J.A., Bowers, A.R., 2000. Kinetics of hydrogen peroxide decomposition with complexed and "free" iron catalysts. International Journal of Chemical Kinetics 32, 24–35. https://doi.org/10.1002/(SICI)1097-4601(2000)32:1<24::AID-JCK4>3.0.CO;2-A

Taguchi, G., 1993. Taguchi on Robust Technology Development Methods. ASME Press: New York 1–40.

Toledo, R.T., Escher, F.E., Ayres, J.C., 1973. Sporicidal properties of hydrogen peroxide against food spoilage organisms. Appl. Microbiol. 26, 592–7.

Uhl, L., Gerstel, A., Chabalier, M., Dukan S., 2015. Hydrogen peroxide induced cell death: One or two modes of action? https://doi.org/10.1016/j.heliyon.2015.e00049

UNE, 2015. UNE-EN 13697:2015+A1, Antisépticos y desinfectantes químicos. Ensayo cuantitativo de superficie no porosa la evaluación de la actividad bactericida y/o fungicida de los desinfectantes químicos utilizados en productos alimenticios, en la industria, en el hogar y en colectividad.

UNE, 2019. UNE-EN 13704, Desinfectantes químicos. Ensayo cuantitativo de suspensión para la evaluación de la actividad esporicida de los desinfectantes químicos utilizados en productos alimenticios, en la industria, en el hogar y en colectividades.

Unger-Bimczok, B., Kottke, V., Hertel, C., Rauschnabel, J., 2008. The influence of humidity, hydrogen peroxide concentration, and condensation on the inactivation of geobacillus stearothermophilus spores with hydrogen peroxide vapor. Journal of Pharmaceutical Innovation 3, 123–133. https://doi.org/10.1007/s12247-008-9027-1

USP, 2011. Chapter 128: Validation Of Isolator Systems. Rockville, USA.

USP, 2020. USP 43-NF38, Chapter 55 Biological Indicators-Resistance Performance test.

Van der Velde, M., Van der Meulen, B., 2011. EU food hygiene law and implications for food factory design, Hygienic Design of Food Factories. Woodhead Publishing Limited. https://doi.org/10.1533/9780857094933.1.37

Verce, M.F., Jayaraman, B., Ford, T.D., Fisher, S.E., Gadgil, A.J., Carlsen, T.M., 2008. Minimizing decomposition of vaporized hydrogen peroxide for biological decontamination of galvanized steel ducting. Environmental Science and Technology. https://doi.org/10.1021/es702404g

Voss, A., Milatovic, D., Wallrauch-Schwarz, C., Rosdahl, V.T., Braveny, I., 1994. Methicillin-Resistant Staphylococcus aureus in Europe. European Journal of Clinical Microbiology & Infectious Diseases 13, 50–55. https://doi.org/10.1007/BF02026127

Watling, D., 1995. Method and apparatus for hydrogen peroxide vapor sterilization. EP0774263B1.

Watling, D., Ryle, C., Parks, M., Christopher, M., 2002. Theoretical analysis of the condensation of hydrogen peroxide gas and water vapour as used in surface decontamination. PDA journal of pharmaceutical science and technology 56, 291-299.

Wells-Bennik, M.H.J., Janssen, P.W.M., Klaus, V., Yang, C., Zwietering, M.H., Den Besten, H.M.W., 2019. Heat resistance of spores of 18 strains of Geobacillus stearothermophilus and impact of culturing conditions. Int. J. Food Microbiol. 291, 161–172. https://doi.org/10.1016/j.ijfoodmicro.2018.11.005

Wiencek, K.M., Klapes, N.A., Foegeding, P.M., 1990. Hydrophobicity of Bacillus and Clostridium spores. Applied and Environmental Microbiology 56, 2600–2605. https://doi.org/10.1128/aem.56.9.2600-2605.1990

Yang, C., Mao, Z.-S., 2014. Chapter 2 - Fluid flow and mass transfer on particle scale, in: Yang, C., Mao, Z.-S. (Eds.), Numerical Simulation of Multiphase Reactors with Continuous Liquid Phase. Academic Press, Oxford, pp. 5–73. https://doi.org/https://doi.org/10.1016/B978-0-08-099919-7.00002-0

Yoshino, D., Nakamuraya, K., Nakajima, T., Sato, T., 2015. Development of low-temperature sterilization device using atmospheric pressure air plasma with circulating flow. Mechanical Engineering Journal 2, 15-00187-15–00187. https://doi.org/10.1299/mej.15-00187

Yun, H.S., Younghoon, K., Oh, S., Jeon, W.M., Frank, J.F., Kim, S.H., 2012. Susceptibility of Listeria monocytogenes Biofilms and Planktonic Cultures to Hydrogen Peroxide in Food Processing Environments. Biosci. Biotechnol. Biochem. 76, 2008–2013. https://doi.org/10.1271/bbb.120238